A THESIS

FOR THE DEGREE OF DOCTOR OF PHILOSOPHY

Bioactive natural products from marine algae

and soft corals

I. P. Shanura Fernando

Department of Marine Life Sciences

GRADUATE SCHOOL

JEJU NATIONAL UNIVERSITY

August, 2017

Bioactive natural products from marine algae and soft corals
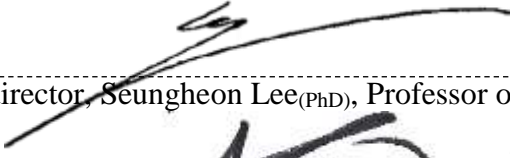
I. P. SHANURA FERNANDO

(Supervised by Professor You-Jin Jeon)

A thesis submitted in partial fulfillment of the requirement for the degree of

DOCTOR OF PHILOSOPHY

August 2017
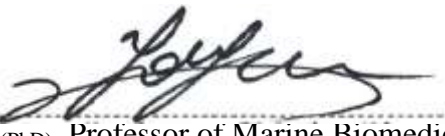
This thesis has been examined and approved by

Thesis director, Seungheon Lee(PhD), Professor of Aquatic Pharmacology

----

Soo-Jin Heo(PhD), Principal Senior Scientist, Korea Institute of Ocean Science and

Technology

WonWoo Lee(PhD), Associate Professor of Marine Biomedical Sciences

----

Ryu BoMi(PhD), Associate Professor, Molecular Bioscience

You-Jin Jeon(PhD), Professor of Marine Biomedical Sciences

08 / 2017
Date

Department of Marine Life Sciences

GRADUATE SCHOOL

JEJU NATIONAL UNIVERSITY

Contents

iv

SUMMARY

Natural products drug discovery from marine sources has received a remarkable attention in recent years given their potential biological activities. Second to none, natural products from marine origin exert a fascinating functionality owing to their wide range of structural diversity. Based on the literature, marine organisms including sponges, soft corals, cyanobacteria, microalgae, macroalgae, bryozoans, cnidaria, platyhelminthes, hoplonomertea, polychaetes, and hemichordate have extensively been studied for identifying numerous bioactive natural products those which are the secondary metabolites of these organisms. Some extensive reviews discuss the significance of marine natural products as bioactive agents [1, 2]. However, given the vast biological diversity of marine organisms widespread throughout the globe in different environmental habitats facing different physical and chemical environmental conditions, marine natural products remain under-explored. With recent developments which enable the exploration of marine habitats, the world has gone one foot forward in exploring fascinating marine organisms.

Current series of studies merely represent a hay in a haystack contributing to the vast knowledge base of natural product drug discovery. The source of these studies were seaweeds harvested from the coast of Sri Lanka and soft corals harvested from ocean bordering Jeju island of the Republic of Korea. Following a general methodology of natural product drug discovery, extraction methods were designed to obtain targetted compound categories. Regarding seaweeds, the studies were focused upon the purification of bioactive polysaccharides and polyphenolic compounds. In the case of soft corals, the objectives were set to purify bioactive terpenoids and their derivatives. All selected fractions and purified compounds indicated potential functionality towards tested bioactivities unraveling their potential to be used in manufacturing a wide variety of consumer products.

The studies incorporate the use of different chromatographic purification techniques, spectroscopic techniques, computational methods of molecular geometry optimization, spectroscopic analysis, and molecular docking and a variety of biological and chemical assays based on colorimetry, spectroscopy, western blot analysis and in vivo zebrafish model. The content of the thesis is divided into four parts to provide the reader a clear understanding of the workflow of current studies, which spread their branches to a variety of different areas.

The first part of this thesis is devoted for the extraction, screening of bioactivities and purification of natural products from Sri Lankan marine algae. This section provides a general introduction to the importance of exploring marine natural products of seaweed featuring green, brown, red and microalgae and their significance in facilitating physiological wellbeing of man. In the first study crude polysaccharides were obtained from eleven different seaweed species by hot water extraction and ethanol precipitation. Among the investigated algae, the brown algae *Chnoospora minima* were found to be having better alkyl and DPPH radical scavenging activities and better intracellular ROS scavenging potential against both H_2O_2 and AAPH induced ROS levels in "Chang" cells. FTIR analysis and monosaccharide composition of these crude polysaccharides were used to confirm its structural characteristics. During the interpretation of FTIR, a novel approach that combines the use of computational quantum chemical calculations in combination with predesignated structural information was followed. The calculations were done using density functional theory (DFT) calculations at RB3LYP/6-31G(d,p) level. Finally, the major constituent of the crude polysaccharides of *Chnoospora minima* was identified as fucoidan.

In the next study, the green extraction approach that combines the use of enzymes to obtain a better yield of bioactive constituents were utilized in obtaining the water-based algae extracts. Ten different commercial food grade enzymes consisting of 5 carbohydrases (Viscozyme, Celluclast, AMG, Termamyl, and Ultraflo) and five proteases (Protamex, Kojizyme,

Flavozyme, Alcalase, and Neutrase) were utilized in obtaining the extracts provided their optimum extraction conditions. Celluclast extracts gave the highest yield for all the algae samples with higher amounts of polyphenolic contents. The antioxidant and anti-inflammatory properties of the Celluclast extracts of *Sargassum polycystum* and *Chnoospora minima* were identified superior compared to other extracts using both *in-vivo* and *in-vitro* analysis. As for the third study, the polysaccharides rich in fucoidans were precipitated out from the Celluclast extract of *C. minima* using ethanol and further purification was done via a DEAE-Sepharose fast flow column. Four fractions were collected from the column purification. One of the purified fraction demonstrated excellent anti-inflammatory effects compared to other three fractions *in-vivo* and *in-vitro*. The selected fraction was found to be a fucoidan with a higher fucose content and degree of sulfation via FTIR characterization and monosaccharide analysis. The results further demonstrated the variation of anti-inflammatory properties with the degree of sulfation of the polysaccharide backbone. In the next study, we optimized a method to obtain fucoidan-rich polysaccharides from *S. polycystum* and *C. minima* following depigmentation, phenol polymerization, enzyme-assisted extraction, removal of alginate impurities by $CaCl_2$ addition and ethanol precipitation. The obtained polysaccharides demonstrated the characteristics of fucoidan evidenced via both FTIR analysis and monosaccharide composition analysis. Further, they demonstrated superior antioxidant properties for DPPH and Alkyl radical scavenging activities. Also, the fucoidan-rich polysaccharides demonstrated desirable bioactive properties such as anti-inflammatory, tyrosinase inhibition, skin whitening, elastase and collagenase inhibition abilities making them much desirable natural ingredients to be used in the formulation of cosmeceutical products.

Apart from studying about the fascinating bioactive polysaccharides of algae, 70% ethanol extracts of some selected algae were evaluated for their bioactive properties. The algae (*Ahnfeltiopsis pygmaea*, *Gracilaria corticata var. ramalinoides*, *Chnoospora minima*, and

Caulerpa racemosa) extracts obtained in such manner was found to composed of a higher level of polyphenolic content when compared to their water based extracts described previously. Among the extracts, *C. minima*, and *C. racemose* demonstrated superior antioxidant and anti-inflammatory effects. Also, the *C. minima* indicated potential anti-cancer activities against HL-60 cell line. The crude of selected *C. minima* and *C. racemose* extracts were dissolved in water and fractionated between inert organic solvents in order of increasing their polarity following hexane, Chloroform, and ethyl acetate. The ethyl acetate fraction of *C. minima* and *C. racemose* demonstrated strong antioxidant and anti-inflammatory properties whereas the hexane fraction indicated anti-inflammatory activity. Chloroform fractions of *C. racemose* indicated potential anti-cancer properties against HL-60 (human leukemia) and MCF-7 (human breast cancer) cells. Further purification of the hexane fraction guided by bioassays (anti-inflammatory activity) resulted in the isolation of Squalene, which was confirmed based on its molecular weight, and NMR data. The purified compound indicated a desirable anti-inflammatory effect on LPS-induced RAW 264.7 murine macrophages by the reduction in NO production and down-regulation of pro-inflammatory cytokines and inflammatory regulators. Further, the anti-inflammatory implications of the isolated compound were confirmed in the LPS-induced *in vivo* zebrafish embryo model.

Investigation of soft corals harvested from Jeju describes the next part of the study. Soft corals are species belongs to the order of Alcyonacea, which defines corals that do not produce a calcium carbonate skeleton. They primary inhabit nutrition rich tropical or subtropical waters favoring habitats with less light and warm seawaters. Based on the estimates from 2010 to 2011, 22% of the total new marine natural products have been discovered from soft corals [3]. Natural products from soft corals are considered as a primary source of a new array of therapeutics. Surprisingly, most of the natural products identified from soft corals have reported demonstrating a spectrum of biological activities including antitumor, antiviral, antifouling and

anti-inflammatory effects [4]. Given their evolutionary perspectives, these compounds many of which are toxic to other organisms assist the soft corals in protecting themselves from predators [5]. The soft corals belong to the genus *Dendronephthya* that was central to current studies encompasses nearly 248 species and are highly prolific and widely distributed throughout the Indian Ocean, the Red Sea, Pacific Ocean and Southeast Asia [6]. Especially the sterols isolated from soft corals have shown promising bio functionalities. A review about marine sterols published in 1993 report the discoveries been done on more than 200 different types of mono hydroxy sterols from marine organisms [7]. Discovery of these various metabolites will shape the future of natural product drug development with a broad perspective of counteracting a broad range of disease conditions.

Ten different soft coral species including *Dendronephthya gigantea*, *Dendronephthya spinulosa*, *Dendronephthya puetteri*, *Dendronephthya castanea*, *Dendronephthya aurea*, *Dendronephthya suensoni*, *Scleronephthya gracillimum*, *Chromonephthea hirotai* and two unknown *Dendronephthya* species designated *Dendronephthya sp1* and *Dendronephthya sp2* were extracted using 70% ethanol for the initial evaluation of its bioactive properties. The 70% ethanol extracts of *Dendronephthya gigantea*, *Dendronephthya aurea*, *Dendronephthya puetteri*, *Chromonephthea hirotai*, and *Scleronephthya gracillimum* indicated promising anti-inflammatory effects against LPS-induced NO production, down-regulation of pro-inflammatory cytokines and inflammatory mediators. Among the screened soft corals *Dendronephthya gigantea* was selected for further studies to purify bioactive principals responsible for the observed anti-inflammatory and anti-cancer effects. The solvent/solvent fractionation of the 70% ethanol extract obtained by 6.00 Kg of the *Dendronephthya gigantea* dry powder indicated the accumulation of the anti-inflammatory and anti-cancer effects in the hexane fraction. Following the bioassays, the hexane fraction was further purified by two consecutive silica open columns to obtain a subfraction with highest potential bioactive

properties. The selected fraction indicated a remarkable anti-inflammatory activity towards LPS-induced RAW 264.7 macrophages evidenced via the reduced NO production, down-regulation of pro-inflammatory cytokines and inflammatory mediators. Effects were also displayed in LPS-induced *in vivo* zebrafish model. The active principals in the purified fraction were identified as a mixture of eight 3β-hydroxy-Δ5-steroidal congeners via GC-MS/MS analysis. Following the impressive biological functionality of the purified fraction, attempts were taken to isolate the individual compounds in the sterol mixture. The separation of sterols is a tricky task that needs both accuracy and precision. For the further separation, a long silica column was used with gradually increasing amounts of ethyl acetate in hexane mixture. Column eluates were collected into 130 test tubes and grouped into five fractions. Based on its TLC analysis patterns, the selected test tubes were mixed with each other and further developed on a preparative TLC plate. The separated bands were collected from the TLC plates and analyzed via GC-MS/MS and NMR. The isolated sterols are remaining to be screened for some possible bioactivities including anti-inflammatory, anti-cancer, and anti-diabetic. Hence, the progressions in marine bioresource technology would provide a new scope and a platform for the developments in natural product chemistry, functional food, cosmeceutical, and pharmaceutical industry.

LIST OF FIGURES

LIST OF TABLES

PART I;

NATURAL PRODUCTS FROM SRI LANKAN MARINE ALGAE

PART I;

NATURAL PRODUCTS FROM SRI LANKAN MARINE ALGAE

SECTION 1;

HOT WATER EXTRACTION OF BIOACTIVE POLYSACCHARIDES SCREENING OF BIOACTIVITIES AND CHARACTERISATION.

ABSTRACT

Sri Lanka is a tropical island located in the Indian Ocean with an average temperature of 29°C in its coastal areas. Coastal areas of Sri Lanka provide the habitat for a large number of algae estimated about 896 species based on a study done in 1999 (Illangasinghe et al. 1999). However, except for several taxonomical studies and few number of studies based on natural products chemistry, many of these algae and their metabolites remains under-explored for their potential biofunctional properties. Among them are the algae polysaccharides that have shown potential biofunctional properties. Unlike polysaccharides found in terrestrial plants, some of the polysaccharide types found in algae show interesting biological functionality, chemical properties and physical characteristics that enable them to be used in multiple applications. The aim of the current investigation was to identify the biofunctional properties of hot water soluble polysaccharides of several selected algae species to explore their potential as antioxidants. The functional properties were investigated via radical scavenging activities and intracellular ROS scavenging properties. The polysaccharides were characterized by FTIR spectroscopy and by the analysis of monosaccharide content. Computational chemistry based calculations of vibrational spectra for the constructed dimeric units of polysaccharides were taken in aid to resolve the observed spectra simultaneously with an extensive literature review.

2

Based on the results, crude polysaccharides of *Chnoospora minima* indicated the best DPPH and alkyl radical scavenging activities with potential intracellular ROS scavenging effects. The major polysaccharide constituent coming to the hot water extract of *C. minima* was found to be a fucoidan-based on its FTIR spectrum and monosaccharide content as well as comparatively higher sulfate content. These observations highlight the importance of exploring marine algae such as *C. minima* for identifying potential bioactive substituents that could be beneficial for the development of functional materials in industries.

1. INTRODUCTION

Natural products of marine bioresources have immensely contributed to the development of the knowledge base of natural product chemistry, medicinal chemistry, and related areas. Over the past few years, a wide range of extensive studies has been conducted using marine bioresources to understand their chemistry, the numerous types of compounds with the most unusual chemical structures that exhibit a broad range of biofunctional properties which would be of use to effectively counteract some disease conditions. Still, the vastness and mysteries of the ocean, the largest ecosystem of the world extending more than 70% of the earth's surface, remain underexplored.

1.1. A historical overview

The history of natural product drug discovery dates back to 2600 B.C. when Mesopotamians were tabulating the use of oils from *Commiphora species* (myrrh) and *Cupressus sempervirens* (Cypress) which are still used as remedies for coughs, colds, and inflammation. When a distinguished Egyptian pharmaceutical record "Ebers Papyrus" in 2900 B.C. record many 700 plant-based drugs consisting disinfectants, pills, ointments, and infusions. When comes to

Chinese Materia Medica, "Wu Shi Er Bing Fang" in 1100 B.C. reports 52 natural drug prescriptions, Shennong Herbal around 100 B.C., keep a record of 365 drugs and the Tang Herbal during 659 A.D. records 850 drugs of natural products. The Greek physician, Dioscorides, (100 A.D.) and scientist, Theophrastus (~300 B.C.) have reported to use and store herbs and herbal extracts. The knowledge about natural product drugs developed in the West was preserved during the Dark and Middle Ages (6th to 14th centuries) in monasteries of England, Germany, Ireland, and France. Arabs were the first to own private pharmacies (8th century) whereas a Persian pharmacist, philosopher, and a physician, "Avicenna" has done an immense contribution to medicinal chemistry, pharmacy, and medicine [8].

1.2. Natural products of marine algae

Natural products in a broad sense define the primary and secondary metabolites of organisms which have a specific biological function. Given organic chemistry, natural products are mainly defined as purified organic compounds isolated from organisms that are products of primary or secondary metabolism. However, the secondary metabolites which are unique to an organism or group of organisms receive much attention in medicinal chemistry given their biofunctional properties compared to the primary metabolites which are common to all organisms [8]. Natural products have played a central role in drug discovery due to their relatively robust properties and effectiveness. These compounds represent a wide variety of structural features and sometimes most unlikely structures with highly efficient biological functionalities. Natural products chemistry is one of the central fields of Organic Chemistry bringing up puzzling structures providing challenging targets for structural characterization and investigating synthetic pathways urging scientists to develop novel technologies [9].

Algae are primarily aquatic organisms ranging from flagellated unicellular organisms which are few microns in diameter to multicellular organisms 80 m long. Algae represent a large informal grouping of a heterogeneous, polyphyletic or paraphyletic group of organisms belonging to many different evolutionary lineages [10]. Due to this genetic diversity, algae are different, regarding morphological, ultrastructural, ecological, biochemical, and physiological traits. Marine algae are a source of biologically active metabolites having diverse chemical structures originated from their different secondary metabolic pathways. Many of these compounds possess desirable biological functionalities and therefore are of vital importance in drug development, functional food, and related industries. Marine algae have yielded thousands of novel metabolites within the past fifty years. Among the natural products derived from seaweed, special attention is directed towards polyphenols, which are mainly of brown algae origin [11]. Moreover, sulfated polysaccharides of brown algae are of vital importance due to their numerous bioactive properties and biocompatibility [12]. Apart of above, significant attention has paid towards the identification and evaluation of terpenoids (steroids), mycosporine-like amino acids, fatty acids, and peptides [3, 13]. The bioactive properties of these natural products are widespread and may include antioxidant, anti-inflammatory, anticancer, antimicrobial, anti-hypertensions, anti-diabetics, anti-obesity, immunomodulatory, and a host of other functionalities. Many of these phytochemicals offer robust properties compared to most of the synthetic derivatives. Hence, the continued search for bioactive natural products receives a superior attention in medicinal chemistry.

1.2.1. Polyphenolic compounds of marine algae

Polyphenols of algae have been given a greater attention among all other algae-derived natural products owing to their strong antioxidant functionality and a broad range of other bioactive properties. Polyphenols represent a diverse class of secondary metabolites with over 8000

5

naturally occurring compounds discovered so far. These compounds contain the phenol group as the common structural feature. Polyphenols could be further divided into several subclasses as phenolic acids, coumarins, lignins, tannins, lignans, flavonoids, stilbenes, and other types [14]. The biosynthesis of polyphenols proceeds through the involvement of shikimic acid and acetate–malonate pathways [11]. The occurrence of antioxidant activity in polyphenols which is central to their biofunctional properties is described in detail by Fernando et al. [14]. Some of the other reported bioactivities of polyphenols are anti-inflammatory activity, inhibition of enzymes such as α-Glucosidase, α-amylase, acetylcholinesterase, butylcholinesterase, angiotensin-I-converting enzyme, matrix metalloproteinases, hyaluronidase, and tyrosinase, anti-bacterial activity, anti-cancer, antiallergic and a variety of other bioactivities [11]. In fact, the analysis of the polyphenolic content of algae extracts has become a common routine before evaluating its bioactivity. Fig. 1 represent structures of some of the polyphenolic compounds isolated from marine algae [14].
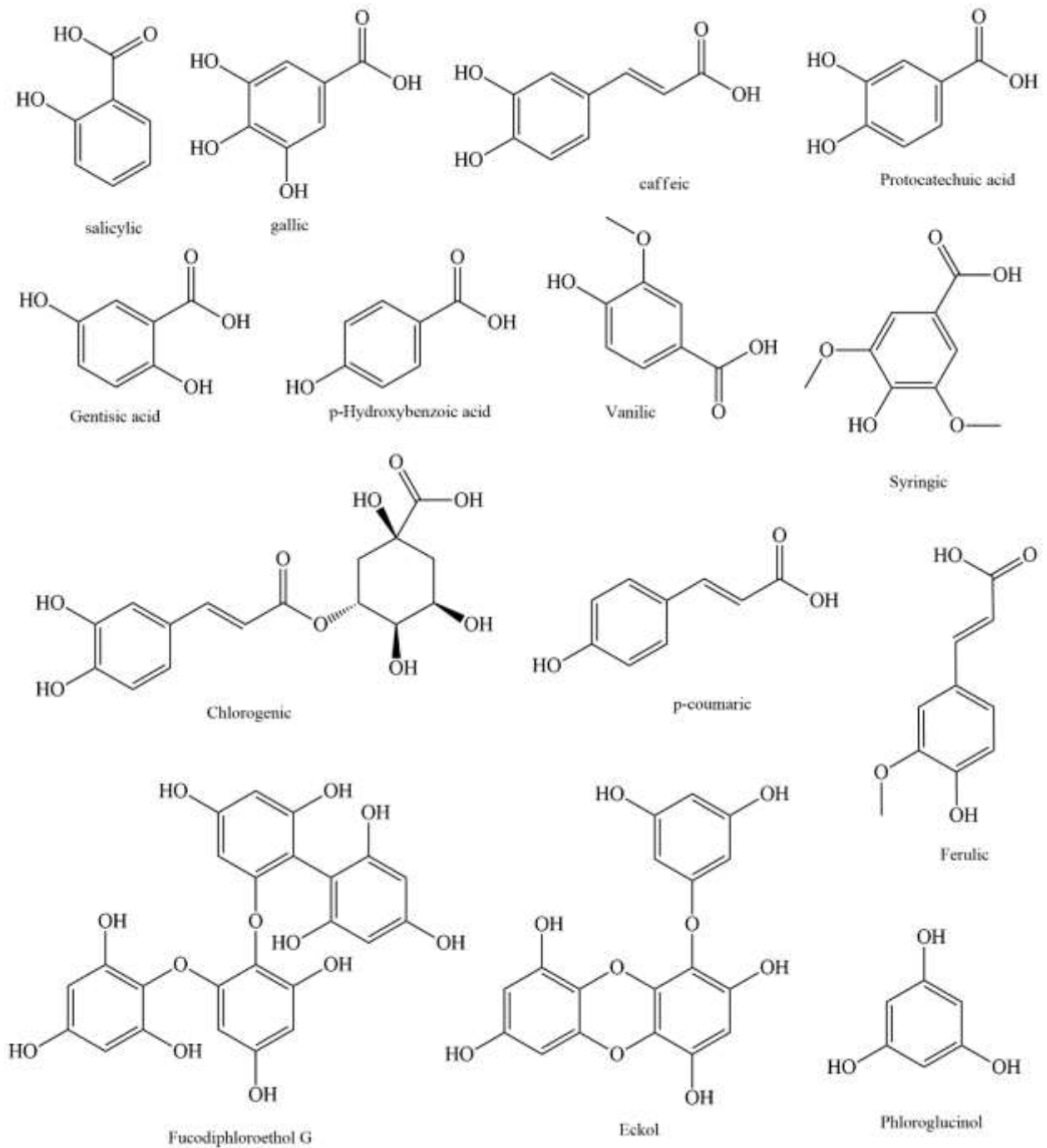
Fig. 1 Structures of some of the polyphenolic compounds found in marine algae

1.2.2. Bioactive polysaccharides of marine algae

Algae are a renounced source of some biologically active polysaccharides with a wide variety

of bioactive properties. Many of these bioactive polysaccharides are biological markers unique

to the type of algae exhibiting the polyphyletic evolutionary characters. Brown algae mainly contains anionic polysaccharides including alginates, fucans which include fucoidan (a glycan-rich in sulfated fucose) laminarin and mannitol. Red algae contains galactans including carrageenans, agars, xylans, porphyrin, mannans, and floridean starch whereas green algae contains starch, sulphated galactans, ulvan, xylans, and mannans [15]. Fig. 2 exhibit the structures of the bioactive polysaccharides derived from algae, which are of interest.
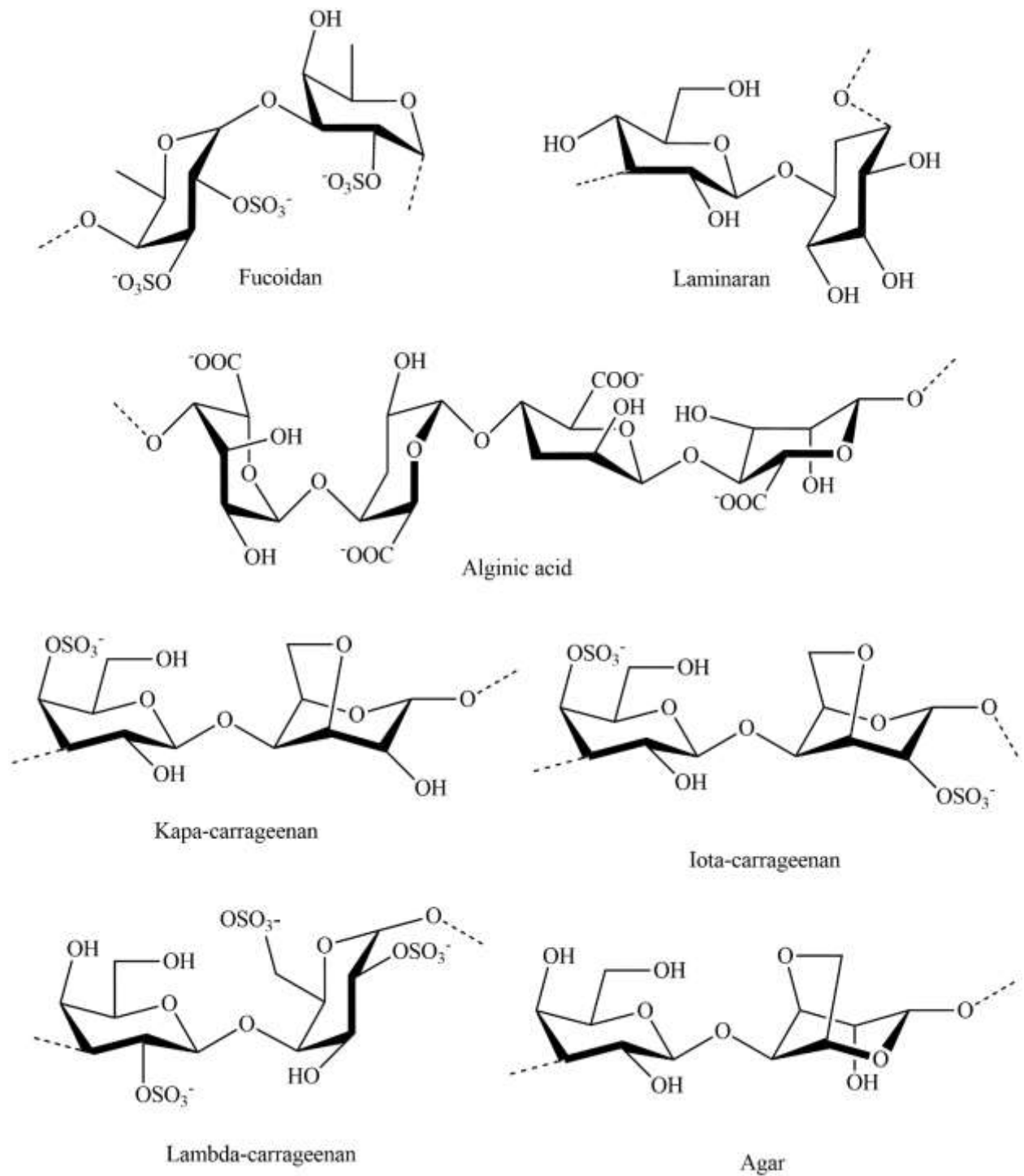
Fig. 2 Structures of some polysaccharides found in marine algae.

Apart from their bioactive properties, certain polysaccharides have physical properties desirable for many types of applications as stabilizers, gelling agents, emulsifiers, and

9

thickeners [16]. Hence, they could be used in a variety of different applications to manufacturing consumables including cosmeceuticals and functional food products. Among these polysaccharides fucans, carrageenans, agar, porphyrin, sulfated galactans and ulvans contain sulfate groups in the polysaccharide backbone. Many of these sulfated polysaccharides are effective as bioactive agents. The biological activity of these polysaccharides is a function of its characteristic structural properties which include the degree of sulfation the connectivity and the sequence of monosaccharides and attachment of other functional groups [17].

Among the bioactive polysaccharides of marine algae, fucoidans receive a particular interest as for their diverse bioactive properties and biocompatibility. Fucoidan is one of the extensively exploited polysaccharides of marine algae owing to their bioactive properties such as radical scavenging, antioxidant, anti-inflammatory, anticancer, anticoagulant, antiviral, antithrombotic and a host of other bioactivities [18]. Fucoidans from different brown algae exhibit different structural properties and hence different bioactives. Therefore, the investigation of fucoidans from various sources of brown algae are of interest.

1.3. Sri Lankan marine algae

Sri Lanka is a small country with an area size of 65,610 km² surrounded by the vast Indian Ocean filled with wonderful and untapped natural resources. The tropical environment of the country and the nutrition rich soil are desirable for the flourished growth of wide variety of flora. Sri Lankan coastline that spans for 1,340 km is home to numerous species of algae and host of other marine organisms. According to a study published in 1999, an estimate of approximately 896 algae species is recorded in Sri Lanka [19]. Also, seaweeds of Sri Lanka remain under-explored for their bioactive natural products thus could be a source of important untapped secondary metabolites with pharmaceutical potential. Literature indicates several

studies, once that focus on the biodiversity and distribution of algae through the coastline of Sri Lanka. A historical record of research related to marine algae in Sri Lanka is of considerable interest for these studies. The first collection of Sri Lankan algae had been done during 1646-1695 by Paul Hermann a Professor of Botany at Leiden (Netherlands). His collections have much contributed to the publication "Flora Zeylanica" of Linnaeus [20]. Another publication by G.G. Sigmond in 1841 describe the Ceylon moss a seaweed harvested from Jaffna and its extract that possess glue like adhesive character [21]. An extensive study done in 1961 profoundly describe the seaweed biodiversity of Sri Lanka by then [22]. Moreover, it provides detail guidelines to identify different algae species morphologically. Up to date that is the only publication which indicates a taxonomic key helpful to identify algae. A recent study by Coppejans et al. presents a pictorial guide to the different types of seaweeds inhabiting the coastal area of Sri Lanka. (Coppejans et al., 2009). It further maps the distribution of seaweed around the coastline, and that study has contributed much to the establishment of an algae herbarium section in the National Herbarium of Sri Lanka at Peradeniya Botanical Garden. However, after 2009 there haven't been any extensive surveys about algae species inhabiting Sri Lanka. At present naturalists including M.A.U. Mallikarachchi and Malik Fernando are carrying out small-scale studies based on their interests to identify the algal species inhabiting the island. Mahendran et al has described the first record of investigating natural products of Sri Lankan algae. whereas it describes the identification of sterols in 18 Sri Lankan marine algae species based on Gas Chromatography–Mass Spectrometry (GC-MS) [23].

Present studies involve the exploration of marine algae collected from different areas of the country targeting their natural products. The results of current investigations will benefit the locals to gain efficient use out from these untapped bioresources. This involves the development of seaweed aquaculture, refining of bioactives, manufacturing of functional food, cosmeceutical products, and certain drugs.

1.4. Commercial and industrial applications of marine algae

Natural products receive increased attention as ingredients in consumer products due to their bioactive properties and biocompatibility compare to most of the synthetic compounds available. Further, their nutraceutical properties make them suitable as a source of functional food. As stated in sections above algae-derived natural products possess a variety of different biological functionalities. Hence the utilization of these materials could assist in developing an infinite array of consumer goods including pharmaceuticals, various types of cosmeceuticals, and functional foods.

Algae polysaccharides in a special manner contain a host of desirable physical properties apart from their bioactive and biocompatible properties, which make them suitable for numerous applications. Given some examples, alginic acid from brown algae could form hydrogels which are used in numerous applications including the formulation of the nanocomposite material, biofilms, nano-aggregates, and nanofibers mainly for wound healing, tissue engineering, drug delivery, and a host of other applications [24]. Moreover alginic acid is extremely efficient as a heavy metal cheater which make it suitable for manufacturing sorbent material for removing heavy metal ions from contaminated water [25]. Further, many of these polysaccharides are highly desirable for the use of manufacturing cosmeceutical products to incorporate properties such as stabilizers, viscosity controlling agents, emulsification and gelling properties that aid in improving texture and consistency of a cosmetic product [16]. These polysaccharides are at the center of many outstanding types of research, which will aid to shape the future of science.

2. MATERIALS AND METHODS

Polysaccharide standards were purchased from Sigma, Aldrich, USA (Alginic acid from brown algae, A7003; Fucoidan from Fucus vesiculosus, F5631; ι-Carrageenan, C1138; Agar, 56763).

Heavy metal salts, KBr powder (FTIR grade), Hydrogen peroxide and nitric acid (≥99.999% trace metals basis) were purchased from Sigma-Aldrich, USA. Multi-element Calibration Standard 3 and calibration blank containing 1% HNO3 for ICP-OES was purchased from PerkinElmer Inc. USA. Ultrapure deionized water (Heavy metals: < 1 ppb) used as the blank and solvent was obtained from Instrument center of Jeju National University. Filtered through a Millipore Milli-Q Gradient A10 purifier. All the other chemicals were of highest purity grade.

2.1. Collection of algae samples

Algae samples were collected from several sampling sites (Fig. 3) of the coastline during 2013 – 2017 period with the assistance of research groups including the University of Colombo and Industrial Technology Institute in Sri Lanka. Necessary approval for the collection of the samples was obtained through the Department of Wild Life Conservation of Sri Lanka.

Expedition 1 (16-08-2013)

Sampling site – Hikkaduwa Beach 6°07'51.9"N 80°05'58.7"E

A list of collected algae (for screening bioactivity)

Padina commersonii, Sargassum crassifolium, Sargassum sp. A, Sargassum sp. B

Expedition 2 (23-12-2013)

Sampling site – Rathgama beach   6° 4'53.80"N 80° 8'51.89"E

A list of collected algae (for screening bioactivity)

Gracilaria corticata, Gracilaria corticata var. ramalinoides, Chnoospora minima, Halimeda gracilis Harvey , Padina commersonii, Laurencia natalensis, Sargassum crassifolium, Caulerpa racemose, Grateloupia lithophila

Expedition 3 (2014-07-14)

Sampling site – Rathgama beach   6° 4'53.80"N 80° 8'51.89"E

A list of collected algae (based on selection)

Padina commersonii, Caulerpa racemosa, Chnoospora minima

Expedition 4 (2015-01-23)

Sampling site – Kalpitiya coastal area

A list of collected algae

Gracilaria edulis, Chaetomorpha antennina, Jania adhaerens, Gracilaria corticata var. ramalinoides, *Halophila ovalis* (a seagrass)

Expedition 5 (2015-08-11)

Sampling site – Beruwala shore

A list of collected algae

Padina commersonii, Caulerpa racemosa, Chnoospora minima,

Expedition 6 (2016-01-13)

Sampling site – Hikaduwa shore   6° 7'50.24"N 80° 6'1.49"E and Pigeon Island, Nilaweli 8°43'21.57"N 81°12'18.47"E

A list of collected algae

Sargassum polycystum, Caulerpa parvula, Padina commersonii, Caulerpa racemose, Gracilaria edulis, Jania intermedia, Cladophoropsis sundanensis, Caulerpa racemose, Ahnfeltiopsis pygmaea, Halimeda discoidea, Gracilaria corticata, Chnoospora minima, Champia ceylanica, Sargassum polycystum, Caulerpa racemosa var. racemose, Caulerpa imbricate, Padina commersonii, Grateloupia lithophila, Grateloupia lithophila, Jania adhaerens, Chaetomorpha antennina

Expedition 7 (2016-06-28)

Sampling site – Jaffna   9°49'18.10"N 80° 6'50.25"E

A list of collected algae

Caulerpa racemose, Hypnea spinella, Dermonema virens, Sargassum sp., and Sargassum crassifolium

1.2.1. Sample collection

The selected algae samples based on their amount were dually washed with fresh water to remove salt, sand and attached debris. Algae samples were kept stored at -20°C until further processing. Part of the algae samples was sent for identification by experts in the field at the University of Colombo and Industrial Technology Institute, Colombo. Another part was used

제주대학교 중앙도서관
JEJU NATIONAL UNIVERSITY LIBRARY

for analyzing the proximate composition that includes moisture, ash, protein, lipid and polysaccharide content sequentially by drying at 100°C, ashing in a furnace at 600°C for 5 hours, using kjedhal digestion, Soxhlet method and by phenol-sulfuric acid method [26]. Aforementioned analytical techniques are the standard methods specified by AOAC 2005 [27]. Several of the selected algae was used for analyzing the mineral content using ICP-OES.

Fig. 3 Sampling sites of Sri Lanka

2.2. Extraction of hot water soluble crude polysaccharides

Each 5.0 g of acetone depigmented algae powder was extracted twice using distilled water at 90 – 95°C providing continuous agitation for 3h. Extracts were filtered, and the filtrates were concentrated to 1/4th of their original volume by applying vacuum using a rotary evaporator. Crude polysaccharides were precipitated by reducing the dielectric constant of the mixture by adding three volumes of 95% EtOH. After gentle mixing for 30 sec mixtures were kept undisturbed at 4°C for 8h facilitating the precipitation of polysaccharides. The polysaccharides were separated by centrifugation (12000 rpm) at 4°C. Henceforth the crude polysaccharide precipitates will be referred to as CP fractions.

2.3. Evaluation of chemical composition

Evaluation of chemical composition in each extract is an essential step before the analysis of its further biological and physical properties. This includes the assessment of polysaccharide, protein and polyphenol content. Accordingly, the levels of polysaccharide were evaluated according to the phenol-sulfuric method, protein content by BSA protein assay kit and polyphenol content by Folin-Ciocalteu assay.

2.3.1. Analysis of polysaccharide content using phenol-sulfuric acid colorimetric assay

The analysis was carried out according to the method described by DuBois et al. with minor modifications [26]. A calibration standard composed of increasing concentrations of glucose 0 – 0.1 mg/ml was prepared in triplicate in test tubes with a total volume of 1.00 ml. Samples were prepared to be 0.1 mg/ml. A 25 µl of 80% phenol was treated into each test tube. Then 2.50 ml of conc. Sulfuric acid was incorporated into each tube followed by vortex mixing. The tubes were kept in the dark at room temperature for 30 min. Then 200 µl of each test tube was transferred to a 96 well plate, and the absorbance was measured at 480 nm. Measurementa were taken with reference to the glucose.

2.3.2. Analysis of polyphenol content by Folin-Ciocalteu assay.

The analysis was carried out according to the method described by Chandler and Dodds with minor modifications [28]. A calibration standard composed of increasing concentrations of Gallic acid 0 – 0.1 mg/ml was prepared in triplicate in test tubes with a total volume of 1.00 ml. Samples were prepared to be 0.1 mg/ml. A 1.00 ml of 95% ethanol was introduced into each test tube followed by 5.00 ml of DW and 0.50 ml of 50% (1N) Folin-Ciocalteu reagent. Tubes were mixed by vortex and incubated for 1h in the dark. After 200 µl of each test tube

was transferred to a 96 well plate and the absorbance was measured at 700 nm. The amount of polyphenols were calculated with reference to Gallic acid.

2.4. Analysis of radical scavenging antioxidant activity of samples by electron spin resonance (ESR) spectroscopy.

DPPH, alkyl, and hydroxy free radical scavenging activities of the samples were measured respectively according to the methods described by Nanjo et al., Hiramoto et al. and Finkelstein et al. with some minor modifications [29-31]. Analysis was carried out using an electron spin resonance (ESR) spectrometer (JESFA200; Jeol, Tokyo, Japan) with the instrument configuration of; modulation frequency 100 kHz, central field 3475 G, modulation amplitude 2 G, gain 6.3×10^5, and temperature 298 K. Microwave power was changed based on the experiment as 5 mW, 1 mW, and 10 mW respectively for DPPH, hydroxyl, and alkyl radical assay.

2.5. Functional group analysis of crude polysaccharides using FTIR spectroscopy.

FTIR spectra were analyzed using the KBr method for solid sample analysis under a low humid atmosphere. A 5 g of KBr was mixed with 15 mg of polysaccharide and ground to a fine powder using a porcelain mortar and pestle. KBr pellets were cast by applying pressure (5000-10000 psi) to the mold. The pressed pellet was removed from the sample die and placed in the FTIR sample holder. The analysis was done using an FTIR spectrometer (Thermo Scientific Nicolet™ 6700, MA USA). Scans were collected as an average of 32 scans within 500-4000 cm^{-1} wavenumber region with a spectral resolution of 4 cm^{-1}. Background scans were collected every 30 min. Results were analyzed using "Origin pro-2015" software package.

제주대학교 중앙도서관
JEJU NATIONAL UNIVERSITY LIBRARY

2.5.1. Interpretation of FTIR spectra using computational calculations of constructed disaccharide models

Cartesian coordinates for the Gaussian calculations were developed by the Gaussian view molecular modeling software. Initial energy reduction and geometry optimization of the molecules were performed using PM6 semi-empirical calculations. Fine optimization of molecular geometry and calculation of harmonic vibrational frequencies were done using ab initio time-dependent density functional theory (DFT) calculations at RB3LYP level using the 6-31G(d,p) basis set with added p-type polarization functions (developed by J.A. Pople) to the hydrogens as described by Cardenas-Jiron et al. (2011). Scaling factors were applied to the calculated vibrational spectra as 0.9645, 0.9799, 0.9819, 0.8625, 0.8719, and 0.9319 respectively for alginic acid, fucoidan, sulfated galactan, mannan, agar, and lambda carrageenan.

2.6. Maintenance of cell lines

"Chang" liver cells, RAW 264.7 macrophages and MCF-7 human breast cancer cells were maintained in DMEM media supplemented with 10% FBS and 1% antibiotic (penicillin and streptomycin). "Vero" (kidney epithelial cells of an African green monkey) and HL-60 (human leukemia) cancer cells were maintained in RPMI media supplemented with 10% FBS and 1% antibiotic (penicillin and streptomycin). Cells were periodically subcultured and maintained at 37°C with 5% CO_2 under a humidified atmosphere. Cells under exponential growth (log phase) were seeded for experiments. Experiments were carried out using appropriate cell line seeded in culture plates. Cytotoxicity of the samples was evaluated as a measurement of cell viability by MTT assay [32]. Readings were obtained using a Synergy HT multi-detection microplate reader (BioTek Inc., Winooski, VT, USA).

2.6.1. Evaluation of intracellular ROS scavenging effects

Intracellular ROS levels were quantified using the 2′,7′-dichlorofluorescin diacetate (DCFH-DA) assay following the method described by Engelmann et al. (2005). "Chang" or "Vero" cells were pre-seeded in 24 well plates for 24h and treated with different concentrations of the samples. After 1h, the wells except the control were treated with H_2O_2 or AAPH respectively reaching a final concentration of 1mM and 10 mM. After incubating for a predesignated period (1 – 3h). DCFH-DA (25 µg mL-1) was incorporated into each well and incubated for 10 min. Fluorescence was measured using a 485 nm excitation and 530 nm emission wavelength using a Synergy HT multi-detection microplate reader (BioTek Inc., Winooski, VT, USA).

2.7. Statistical analysis

Results are represented as the mean ± standard deviation based on at least three independent experiments. Significant differences between the parameters were calculated using IBM SPSS Statistics 20 software using one-way ANOVA by Duncan's multiple range test (DMRT). P-values less than 0.05 ($P < 0.05$) and 0.001 ($P < 0.001$) were considered as significant.

3. RESULTS AND DISCUSSION

3.1. Proximate composition of algae material

Proximate composition of the algae material was determined according to the standard methods specified by AOAC 2005 (Table 1) [27]. Among the evaluated algae, *Jania adhaerens* indicated the highest amount of ash content with low amounts of proteins, lipids, and carbohydrates. Highest polysaccharide content was observed in brown algae except for the *P. commersonii* and next in the red algae. Among the investigated algae species, *Chnoospora*

21

minima indicated the highest polysaccharide content (67.71 ± 0.36%). *Ulva fasciata* indicated the highest protein content (22.68 ± 0.38%), and the lipid content was higher in *Gracilaria corticata var. ramalinoides* (2.27 ± 0.01%).

Table 1. Proximate composition of algae material

Sample name	Moisture	Ash	Protein	Lipid	Polysaccharide
Green algae					
Chaetomorpha antennina	2.11 ± 0.08	39.73 ± 0.71	13.56 ± 0.09	0.59 ± 0.07	42.21 ± 0.32
Halimeda discoidea	0.82 ± 0.08	65.72 ± 0.17	17.42 ± 0.47	0.83 ± 0.02	13.61 ± 0.21
Halimeda gracilis	0.41 ± 0.03	61.21 ± 1.00	20.08 ± 0.33	0.54 ± 0.01	15.11 ± 0.35
Ulva fasciata	0.53 ± 0.01	18.76 ± 0.65	22.68 ± 0.38	0.95 ± 0.04	40.38 ± 0.52
Cladophora herpestica	0.62 ± 0.02	50.88 ± 0.54	9.08 ± 0.15	0.34 ± 0.06	28.63 ± 0.43
Caulerpa racemosa var. racemosa f. remota	0.88 ± 0.05	60.67 ± 0.72	20.45 ± 1.10	0.64 ± 0.07	15.83 ± 0.23
Red algae					
Gracilaria corticata var. ramalinoides	1.53 ± 0.06	33.84 ± 0.52	16.74 ± 0.06	2.27 ± 0.01	43.31 ± 0.46
Gracilaria foliifera	1.64 ± 0.04	39.42 ± 0.38	10.54 ± 0.09	0.94 ± 0.06	45.12 ± 0.52
Ahnfeltiopsis pygmaea	0.56 ± 0.04	37.88 ± 0.14	16.25 ± 0.14	0.15 ± 0.06	43.61 ± 0.35
Gracilaria corticata	0.83 ± 0.06	34.3 ± 0.53	10.26 ± 0.27	1.16 ± 0.05	50.21 ± 0.09
Jania adhaerens	0.17 ± 0.03	73.45 ± 0.70	4.19 ± 0.18	0.01 ± 0.01	20.34 ± 0.42
Grateloupia lithophila	0.52 ± 0.06	18.58 ± 0.85	15.83 ± 0.28	1.25 ± .005	62.24 ± 0.27
Gracilaria edulis	2.61 ± 0.02	38.17 ± 0.49	7.56 ± 0.29	0.45 ± 0.07	49.15 ± 0.28
Brown algae					
Chnoospora minima	3.56 ± 0.04	14.54 ± 0.02	12.3 ± 0.20	0.25 ± 0.05	67.71 ± 0.36
Sargassum polycystum	1.02 ± 0.31	17.35 ± 0.18	12.76 ± 0.15	1.03 ± 0.05	57.32 ± 0.26
Sargassum natans	0.68 ± 0.12	24.15 ± 0.89	11.52 ± 0.40	0.96 ± 0.07	52.45 ± 0.63
Padina commersonii	0.05 ± 0.02	48.40 ± 0.85	14.36 ± 0.42	0.81 ± 0.04	34.00 ± 0.48

Results represent means ± standard deviation of at least triplicate determinations.

3.2. Yields of polysaccharide precipitates obtained by adding ethanol

Ethanol was incorporated into the extraction mixture to initiate the precipitation of polysaccharides. Ethanol reduces the dielectric constant of the medium facilitating the precipitation of polysaccharides. Table 2 indicate a detailed summary of the yields of polysaccharides obtained after the ethanol precipitation. Among the hot water extracted algae *G. edulis* gave a markedly high amount of polysaccharide precipitate upon the introduction of ethanol. In fact, the separation of this polysaccharide precipitate by centrifugation was challenging due to its high density.

Based on the chemical composition of the polysaccharide precipitates, precipitate by *G. edulis* contained the highest amount of polysaccharides. The precipitate of *C. minima* contained 3.16 $\pm$ 0.50 % of proteins. The highest reported polyphenol content (4.83 $\pm$ 0.16%) and the highest sulfate content (due to sulfated polysaccharides) were also reported from the precipitate of *C. minima*.

Table 2. Yields of polysaccharide precipitates

Sample source	Yield	Total soluble carbohydrate content		Total soluble Proteins	Total polyphenol content
		Polysaccharide	Sulfate		
C. antennina	**28.06 ± 0.51**	82.24 ± 1.02	9.21 ± 0.30	0.31 ± 0.28	2.60 ± 0.16
H. discoidea	**20.93 ± 0.52**	68.44 ± 0.30	5.20 ± 0.17	0.96 ± 0.21	4.04 ± 0.00
H. gracilis	**18.99 ± 0.82**	70.04 ± 0.48	5.20 ± 0.08	0.06 ± 0.07	3.93 ± 0.47
C. racemosa	**13.85 ± 0.71**	56.15 ± 0.69	10.51 ± 0.37	1.21 ± 0.56	4.38 ± 0.79
G. corticata	**21.42 ± 0.93**	74.99 ± 0.53	1.65 ± 0.29	0.41 ± 0.28	4.27 ± 0.00
G. foliifera	**14.63 ± 1.03**	74.22 ± 0.46	4.08 ± 0.33	1.21 ± 0.42	4.60 ± 0.15
A. pygmaea	**13.25 ± 0.82**	83.92 ± 0.72	4.55 ± 0.25	0.36 ± 0.35	4.04 ± 0.00
J. adhaerens	**18.68 ± 0.16**	64.37 ± 0.78	2.82 ± 0.54	0.31 ± 0.28	4.16 ± 0.16
G. edulis	**51.24 ± 0.92**	84.18 ± 1.07	9.65 ± 0.16	0.66 ± 0.21	3.93 ± 0.05
C. minima	**5.82 ± 0.37**	70.09 ± 0.21	11.80 ± 0.79	3.16 ± 0.50	4.83 ± 0.16

Results represent mean ± standard deviation of at least triplicate determinations.

3.3. Radical scavenging activities of the algae crude polysaccharides from hot water extracts of algae.

The free radical scavenging activity of the crude polysaccharides obtained from hot water extracts of algae was evaluated using ESR spectroscopic methods (Table 3). The best radical scavenging activities for DPPH and alkyl radical scavenging were evident from the polysaccharides of *C. minima* respectively accounting for IC_{50} values of 89.51 ± 17.00 and $106.80 \pm 0.66\,\mu g/ml$. The highest hydroxyl radical scavenging activity was evident by the green algae *C. antennina*. Compared to ascorbic acid polysaccharides of *C. antennina* had better hydroxyl radical scavenging properties. However, DPPH and alkyl radical scavenging activity of ascorbic acid were superior to any of the polysaccharides investigated. This result is acceptable because ascorbic acid is used as a standard antioxidant.

Table 3. Radical scavenging antioxidant activities of the hot water soluble algae crude polysaccharides

Source of crude polysaccharide samples	IC$_{50}$ values for radical scavenging activity (µg/ml)		
	DPPH	Alkyl	Hydroxyl
C. antennina	>2000	278.18 ± 0.75	102.68 ± 16.00
H. discoidea	>2000	110.06 ± 2.98	1008.65 ± 8.19
H. gracilis	>2000	116.60 ± 2.59	1006.90 ± 6.40
C. racemosa var. racemosa f. remota	>2000	359.48 ± 20.54	200.08 ± 8.17
G. corticata var. ramalinoides	>2000	367.43 ± 1.74	654.13 ± 9.14
G. foliifera	1654 ± 37.46	382.55 ± 1.23	582.465 ± 9.29
A. pygmaea	>2000	377.24 ± 6.10	768.92 ± 8.10
G. corticata	603.38 ± 40.3	332.33 ± 15.29	287.63 ± 13.68
J. adhaerens	>2000	114.59 ± 5.01	281.70 ± 4.96
G. edulis	>2000	113.09 ± 7.13	602.95 ± 12.26
C. minima	89.51 ± 17.00	106.80 ± 0.66	193.57 ± 3.38
Ascorbic acid	23.22 ± 0.52	35.62 ± 0.41	248.35 ± 0.52

Results represent mean ± standard deviation of at least triplicate determinations.

3.4. Sample toxicity of crude polysaccharides upon normal cells

As shown in Fig. 4 none of the algae samples indicated a significant toxicity under the used concentrations. Cell viability was over 80% for all the polysaccharide precipitates. Hence, concentrations up to 200 µg/ml could be considered safe for carrying out further experiments.

3.5. Intracellular ROS scavenging activity and cytoprotective effects

Intracellular ROS scavenging activities of the hot water extracted polysaccharides were evaluated using Chang cells. H_2O_2 and AAPH were introduced to the cells pre-treated with different concentrations of the polysaccharide samples. DCFH-DA assay was adopted for the determination of the intracellular ROS levels. As indicated in Fig. 5, the treatment of H_2O_2 or AAPH (alone) increased the intracellular ROS levels. Co-treatment of polysaccharide samples could reduce the intracellular ROS levels in a dose-dependent manner. The polysaccharide precipitate of C. minima indicated the highest efficient anti-oxidant effects compared to the others.
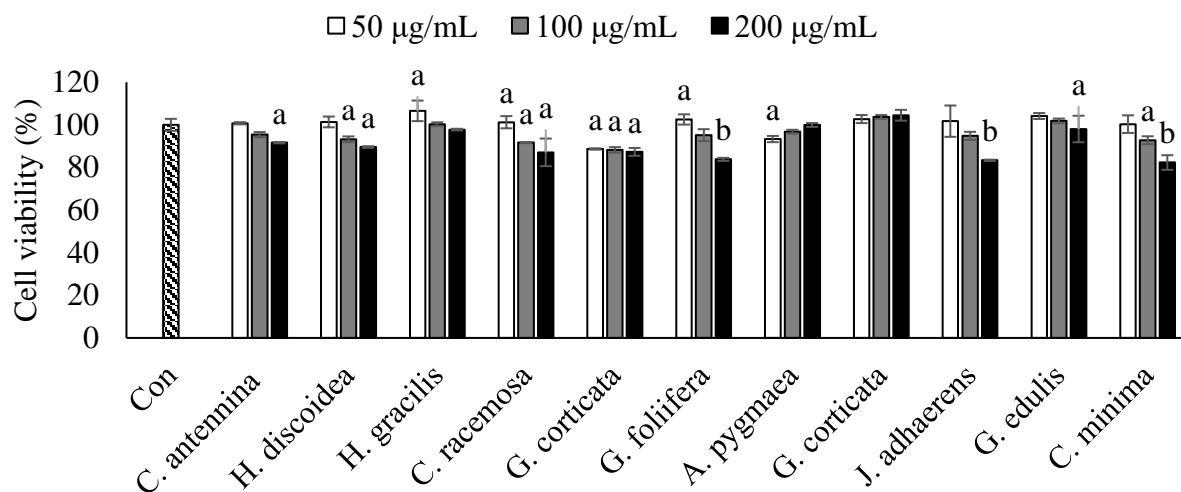
Fig. 4 Cytotoxicity of the crude polysaccharides. Vero cells were seeded in 96 well culture plates (1 x 10^5 cells/ml) and treated with different concentrations of the samples. Following a 24h incubation period, the cell viability was determined by MTT assay. Experiments were carried out in triplicate, and the results are represented as means ± SD. Values are significantly different from the control at *P < 0.05 and **P < 0.001.
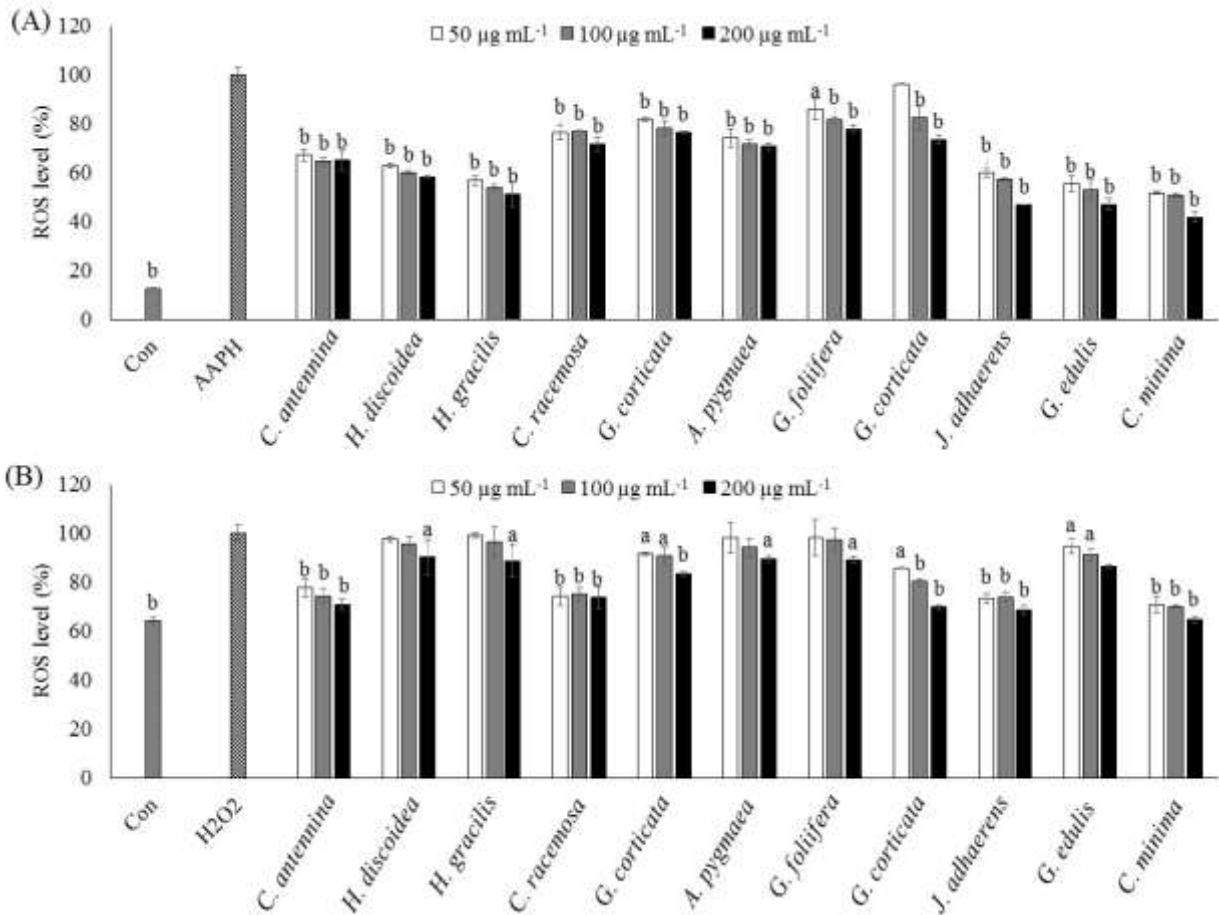
Fig. 5 Intracellular ROS scavenging activities of the samples. Vero cells were seeded in 96 well culture plates (1 x 10^5 cells/ml), treated with different concentrations of the samples and co-treated with AAPH or H_2O_2. Following a 3h incubation period, the intracellular ROS levels were determined by DCFH-DA assay. Experiments were carried out in triplicate, and the results are represented as means ± SD. Values are significantly different from the positive control (AAPH or H_2O_2 treated group) at *P < 0.05 and **P < 0.001.

3.6. Structural characterization of crude polysaccharides

3.6.1. FTIR analysis via computational calculations and predefined peak characteristics

The FTIR spectra are analyzed via referring to pre-defined spectral features. Nonetheless, it is the most convenient approach in analyzing FTIR data. However, with a large number of publications, there is certain discrimination as sometimes opposed interpretation are given in the literature. During the present study, we considered both information reported in the literature and compared with vibrational spectra obtained by computational quantum chemistry calculations based on the novel models. Initially, the disaccharides were constructed using Gaussian View to generate the Cartesian coordinates (input files for Gaussian calculations). The constructed dimers were initially optimized using the basic PM6 semi-empirical method calculations to obtain the most favorable geometry for DFT calculations. Further geometry optimization and harmonic vibrational modes were calculated using time-dependent density functional quantum-chemical (DFT) calculations at RB3LYP level using 6-31G(d,p) basis set as described by Jiron et al. [33]. Fig. 6 indicates the structures of the constructed dimers together with their free energy of formation.

(A) Fucoidan
$G_f^\theta = -7,925,239.74$ kJ mol^{-1}

(B) Alginic acid
$G_f^\theta = -3,795,743.52$ kJ mol^{-1}

(C) Sulfated galactan
$G_f^\theta = -6,682,436.09$ kJ mol^{-1}

(D) Mannan
$G_f^\theta = -3,406,932.07$ kJ mol^{-1}

(E) Agar
$G_f^\theta = -3,206,258.04$ kJ mol^{-1}

(F) Lambda carrageenan
$G_f^\theta = -8,320,184.72$ kJ mol^{-1}
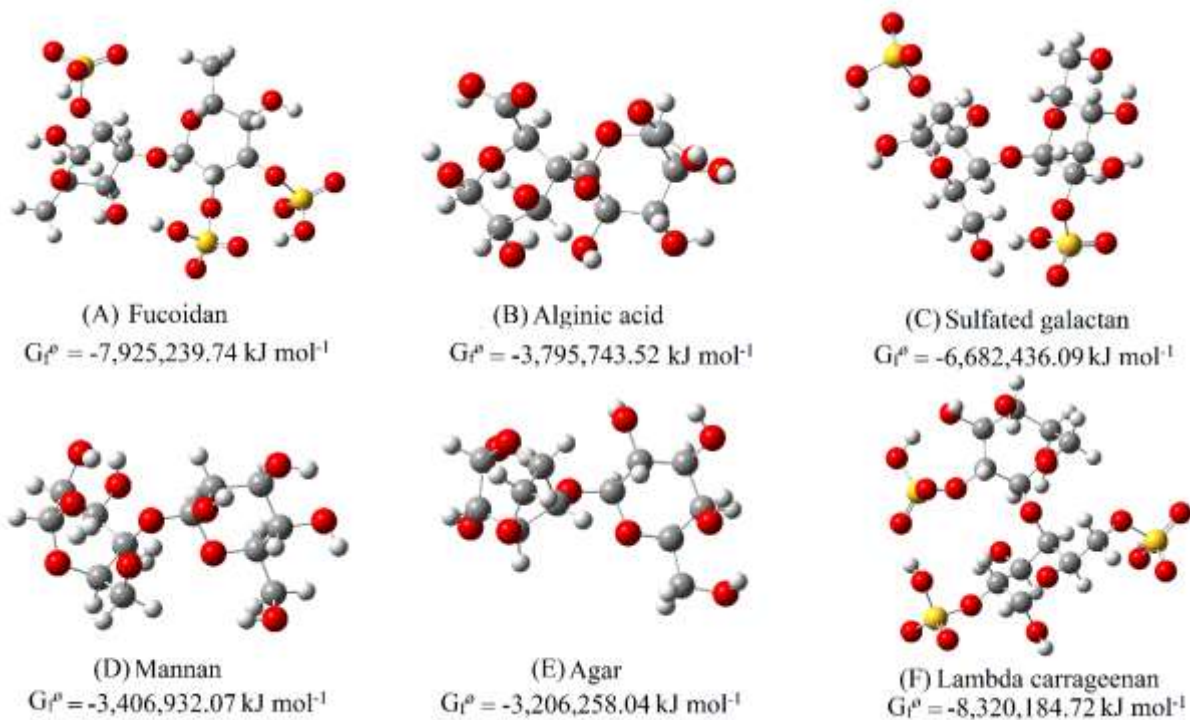
Fig. 6 Structures of the constructed dimeric units of the polysaccharides and their calculated standard free energy of formation.

Fig. 7 indicate the vibrational spectra of standard, calculated and sample polysaccharides found in algae. The vibrational spectra of calculated dimeric units were scaled by factors 0.9645, 0.9799, 0.9819, 0.8625, 0.8719 and 0.9319 respectively accounting alginic acid, fucoidan, sulfated galactan, mannan, agar, and lambda carrageenan. The Obtained vibrational spectra were arranged in the same figure along with the sample and standard spectra of the commercial reference material to easily discriminate between the structural characteristics. IR spectra within 500 cm^{-1} to 1500 cm^{-1} wavenumber region that represents the fingerprint region for polysaccharides were used during the structure interpretation. Table 4 indicate some of the defining vibrational spectral features of algae polysaccharides [34-37]. The peak centered 1035 cm^{-1} corresponds to the bond vibrations of the glycosidic linkages between the monomeric units which are a standard feature observed in all polysaccharides[36]. However, this peak appears broadened within 1010 – 1090 cm^{-1} region due to the overlapping of other peaks [38, 39].

Table 4. The general scheme for FTIR characterization

IR Transmittance wavenumber (cm^{-1})	Signal properties
3500 – 3200	The broadened peak indicate the stretching vibrations of OH group.
1650	Indicate the carbonyl group in carboxylic acid.
1135	Glycosidic stretching vibrations (C—O bond).
1315–1220 and 1140–1050	Stretching vibrations of RO—SO^{3-} bond of ester sulfate groups
1370	Sulfate groups
1250	Asymmetric stretching of S═O
930	The vibration of the C—O—C bridge of 3,6-anhydro-L-galactose and 3,6-anhydro-D-galactose (common to both agar and carrageenan)
890	Anomeric CH of β–galactopyranosyl residues.
840	Sulfation at C4 galactose
830	Sulfation at C2 galactose units
805	Sulfation at C2 of the 3,6anhydroLgalactose
740 and 716	C—O—C bending vibrations of glycosidic linkages
1210 - 1280	Sulphate Broadband represents the sulfate group
822	Mannuronic unit (characteristic band)
808	Guluronic unit (characteristic band)

Fig. 7,A indicate the FTIR spectra of polysaccharides found in brown algae. Except for the peak common to 1035 cm^{-1}, the peak at 1135 cm^{-1} represents the characteristic glycosidic bond vibration in fucoidans. Sulfated polysaccharide receives a major attention due to their bioactive properties and biocompatibility. The major sulfated polysaccharides found in brown algae includes fucoidans, laminaran and alginates. The intense and broadened peak between 1120 - 1270 cm^{-1} corresponds to S$=$O stretching vibrations. The peak observed at 845 cm^{-1}, represents C─O─S-bending vibration that further clarifies the presence of sulfate group. The peak at 1616 cm^{-1} represent the asymmetric stretching vibrations of carboxylate O─C─O bond in alginic acid. The intense peak 1710 cm^{-1} as seen in commercial alginic acid represents the stretching vibrations of C$=$O in carbonyl group. Considering the spectra of *C. minima* polysaccharides, the absence of an intense peak at 1710 cm^{-1} suggest the absence of alginic acid in the spectrum. The absence of other peaks that are corresponding to alginic acid further confirm this speculation.

About the polysaccharides of green algae, the abundant Galatians indicate IR peaks at 930, 845, 820 and 805 cm^{-1} (Fig. 7,B) that correspond to 3,6-anhydrogalactose and sulfation of C-4, C-6 of galactose units and C-2 of 3,6-anhydrogalactose [40]. The interested types of sulfated polysaccharides in green algae includes Galatians, mannans, and xylans. As seen all polysaccharide samples of green algae, the sharp and broadened peak between 1120 - 1270 cm^{-1} is indicative of the S-O stretching vibration of sulfate ester groups. Also, the peak at 1380 cm^{-1} also indicates the sulfate substitution [41]. The presence of mannans is signified by the peaks at 1146, 1390 cm^{-1} [42].

The red algae mainly contain interesting polysaccharide types including carrageenans and agar. The peak at 930 cm^{-1} (Fig. 7,C) signifies the C─O─C vibration of 3,6-anhydro-D-galactose and 3,6-anhydro-L-galactose residues in both agar and carrageenan. The peak at 1375 cm^{-1} is arising from the sulfate groups. Peaks at 716 cm^{-1} and 740 cm^{-1} indicates each separate C─O─C

bending vibrations in glycosidic linkages. The peak at 890 cm^{-1}, represents the stretching vibrations of the anomeric C-H of unsulfated β–galactopyranosyl residues. Carrageenans are categorized into several types based on their degree and connection of sulfates [43]. The peak within 1210 and 1270 cm^{-1} signifies the stretching vibration of S═O in sulfate groups a characteristic feature observable in all carrageenan types. As Fig. 7,C indicates, this feature was seen in the commercial standard of lambda-carrageenan and algae polysaccharide samples, *G. foliifera*, *A. pygmaea*, *G. corticata*, and *J. adhaerens* except for *G. edulis*. Different types of carrageenans have minor structural differences Roberts et al. describe the characteristic spectral features of these different types of carrageenans [43]: Briefly the peak at 840-850 cm^{-1} indicates D-galactose-4-sulfate, at 820-830 cm^{-1} - D-galactose-2sulfate and the peak between 800-805 cm^{-1} correspond to 3,6-anhydro-D-galactose-2-sulfate. The weak peak seen at 770 cm^{-1} represents the binding of galactose ring skeleton [38].
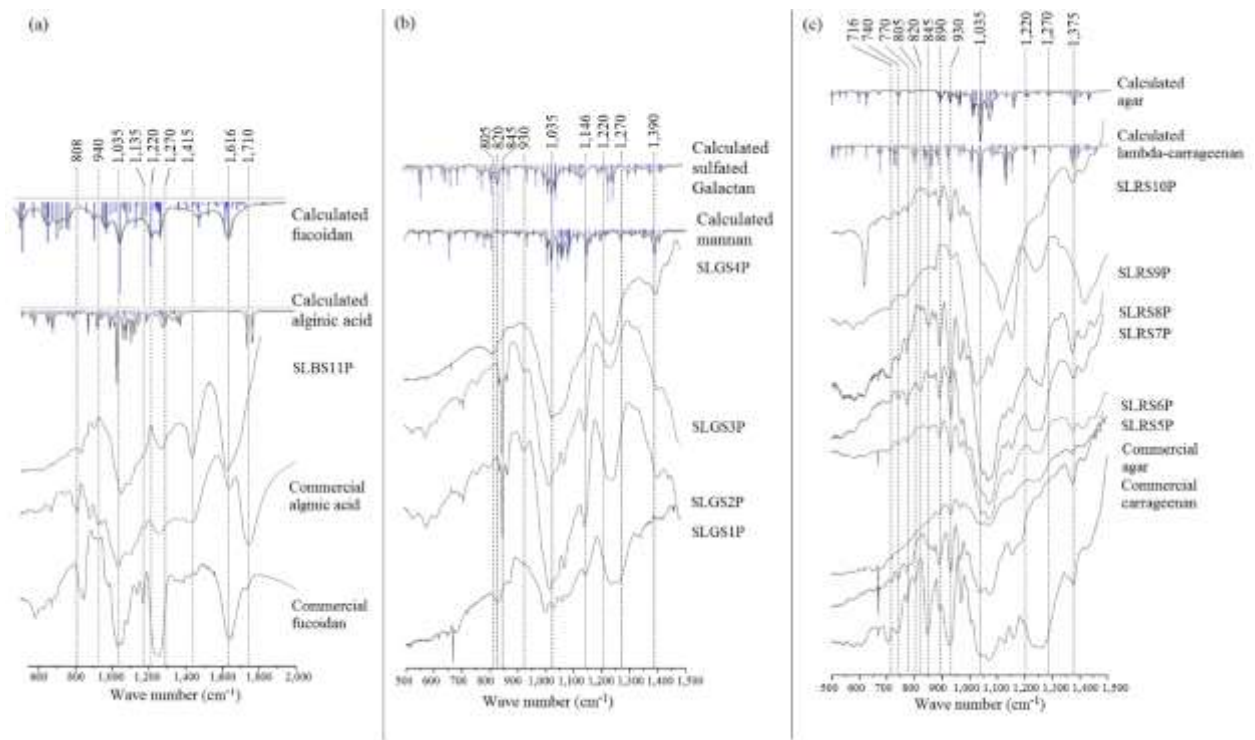
Fig. 7 FTIR spectra of algae polysaccharides. Spectral profile of the sample polysaccharides is indicated together with the vibrational spectra of standard polysaccharides and calculated spectra of constructed dimeric units. Polysaccharides encountered in; (a) brown algae, (b) green algae and (c) red algae.

37

3.6.2. Analysis of the monosaccharide composition

Analysis of the monosaccharide composition is another means of which can be used to obtain reliable information about the polysaccharides present in marine algae samples. Many of the monosaccharides found in algae polysaccharides indicate a heterogeneous composition. Although the composition could vary, certain monomeric units are specific only to particular types of polysaccharides. Table 5 lists the monosaccharide composition of the polysaccharides obtained by hot water extraction of algae. Accordingly, a higher glucose amount was recorded from green algae. Red algae were rich in galactose and glucose. All red and green algae indicated a negligible amount of fucose whereas the brown algae *C. minima* polysaccharides were rich in fucose. Fucose is the major monosaccharide that makes up fucoidan. Hence, this dually confirms the fucoidan-rich nature of *C. minima* polysaccharides.

Table 5. Monosaccharide composition of the hot water soluble crude polysaccharides of algae

Sample	Mono sugar (%)					
	Fucose	Rhamnose	Galactose	Glucose	Mannose	Xylose
C. antennina	0.57	22.40	34.24	23.47	11.93	7.40
H. discoidea	0.79	3.10	11.86	52.27	11.91	20.07
H. gracilis	0.86	3.27	12.75	53.81	10.18	19.12
C. racemosa	1.31	5.52	27.61	32.71	17.49	15.36
G. corticata	1.85	8.40	47.13	23.25	11.33	8.03
G. foliifera	1.76	8.05	37.56	34.74	11.83	6.05
A. pygmaea	1.80	0.64	52.84	30.45	10.02	4.25
G. corticata	1.01	10.33	35.63	31.58	14.49	6.96
J. adhaerens	1.66	4.72	29.66	48.41	11.98	3.57
G. edulis	1.93	5.65	59.59	16.71	14.33	1.78
C. minima	33.25	3.70	7.08	29.59	19.24	7.15

4. CONCLUSIONS

Algae are one of fascinating organisms in a marine ecosystem. Recently an especial attention has been remunerated to explore the bioactive functionalities of these organisms. Algae have widened the vocabulary of marine natural products hand have provided new insight into the development of future drug leads. Present bioactivity-screening studies targeting the untapped biomass of Sri Lankan algae report the identification of algae with potential bioactive natural products. Based on these observations *C. minima* indicated anti-oxidant effects evidenced in-vitro studies. Hence, *C. minima* abundant in coastal areas of the country covering Hikkaduwa, Galle, Kalpitiya, and Trinkomale could be used as a potential bioresource to obtain bioactives for the possible development of functional ingredients in food, cosmetics, and pharmaceuticals.

SECTION 2; ENZYME-ASSISTED EXTRACTION, SCREENING OF BIOACTIVITIES, PURIFICATION AND CHARACTERISATION OF BIOACTIVE POLYSACCHARIDES.

ABSTRACT

The use of green extraction techniques is gaining increased interest in natural product research. Enzyme-assisted extraction is such an environmentally friendly and safe extraction approach that enables to obtain higher yields of the extract compared to other organic solvent based extraction techniques. Different types of commercial food grade enzymes mainly composing of carbohydrases and proteases could be utilized for the process. The aim of the current investigation was to employ the enzyme-assisted extraction to obtain bioactives from algae harvested from coastal areas of Sri Lanka and to evaluate their biofunctional properties. Ten different types of food grade carbohydrases and proteases were used to extract ten different algae species. Moreover, further studies were carried out to purify bioactive principals, sulfated polysaccharides from the selected extracts that indicate enhanced biological effects. Based on the observations the carbohydrases, "Celluclast" was found to be effective at obtaining higher yields of extracts compared to other algae species with comparatively better biological functionality. Among the algae species, Celluclast extract of *Sargassum polycystum* indicated the highest DPPH and hydrogen peroxide radical scavenging activity followed by *Chnoospora minima* and *Sargassum natans*. Ferric reducing antioxidant power was higher in *Gracilaria corticata var. ramalinoides*. Anti-inflammatory effects were evaluated via monetarizing the ability to inhibit NO production in LPS induced RAW macrophages. Collectively the enzymatic extracts of the 4 brown algae species, *S. polycystum*, *Sargassum natans*, *P. commersonii*, and *C. minima* demonstrated considerably good anti-inflammatory activity whereas the Celluclast extract of *C. minima* indicated the best effects. For further studies,

Celluclast extracts of *S. polycystum* and *C. minima* were selected successively for evaluating antioxidant and anti-inflammatory activities. *In-vivo* studies using zebrafish *in-vivo* model demonstrated the antioxidant properties of the Celluclast extracts of *S. polycystum* by reducing the H_2O_2 induced ROS levels while having a protective effect. The Celluclast extracts of *C. minima* demonstrated anti-inflammatory potential by lowering the NO and ROS levels in LPS-induced zebrafish embryos while exhibiting a protective effect against the LPS-induced cytotoxicity.

The selected Celluclast extracts of *C. minima* was used in purifying bioactive principals. The identified polysaccharide precipitate of Celluclast extracts from *C. minima* was accordingly purified using a DEAE anion exchange chromatography yielding 4 separate fractions. The purified fractions were analyzed for their chemical composition, structural characteristics and biological functionality. The fraction F4 indicated better anti-inflammatory effects by reducing the NO production ($IC_{50} = 27.82 \pm 0.88\,\mu g/ml$), iNOS expression and expression levels of COX-2, PGE_2 and pro-inflammatory cytokines (TNF-α, IL-1β, IL-6) in LPS-stimulated RAW 264.7 macrophages. Simultaneously F4 could inhibit NO and ROS levels, expression of iNOS and COX-2 in LPS-induced zebrafish embryos while exhibiting a protective effect against the LPS-induced cytotoxicity. The chemical analysis indicated a 1.85 of mean degree of sulfate substitution per anhydro sugar residue in F2. HPAE-PAD analysis of the monosaccharide content indicated increasing amounts of fucose in each successive column fraction accounting a 79.32% in F4. FTIR analysis of F4 indicated vibrational characteristics similar to commercial Fucoidan. The molecular weight of polysaccharides in F4 was distributed with a mean of 60 kDa. Current evaluations confirm that F4 is a fucoidan with potential anti-inflammatory effects. These observations further highlight the possibilities of using polysaccharides of C. minima Celluclast extract as biofunctional ingredients in functional foods, cosmeceuticals, pharmaceuticals and other related consumer products.

1. INTRODUCTION

Evaluation of natural products from marine algae is gaining increased attention as a research tool since past few years, in cosmetic, food and pharmaceutical industry. A variety of biologically active secondary metabolites including polyphenols, sulfated polysaccharides, terpenoids, alkaloids, polyunsaturated fatty acids, peptides, mycosporine-like amino acids and halogenated compounds have been discovered from marine algae [44]. These molecules provide additional health benefits and are active against many types of disease conditions. Unlike many other natural products isolated from terrestrial organisms, these biomolecules possess unique structural and related functional properties that extend the research perspectives for characterization ant to synthesize structural analogs [45]. One of the typical method employed in extracting natural products is to use organic solvents. However, new environmental-friendly extraction techniques are required for natural product research and their industrial applications.

1.1. Enzyme-assistant extraction

Enzyme-assistant extraction (EAE) is one of the innovative technology that enables to obtain a higher extraction efficiency. The enzymes aid in breaking cellular matrix and cell walls enabling the successful extraction of some of the compounds that stay attached to cell walls and inside cytosol [46]. Hydrolytic enzymes that specifically degrade polysaccharides and proteins can be the key to producing novel macromolecular substructures that might have potentially beneficial functionalities. Especially marine algae contain sulfated polysaccharides which are not reported to be present in terrestrial plants that have a range of biological activities. Recently a special interest is paid towards investigating the enzymatic hydrolysis of sulfated algal polysaccharides [47]. Additionally, EAE of algae had been implemented in extracting

43

natural products with antioxidant, anti-inflammatory, anticoagulant and antipoliferative effects [48 Yang, Samarakoon KW, Kwon, Athukorala Y, Jung].

1.2. Antioxidants from marine algae

Apparently, antioxidant effect is a central field of investigation in natural product, and food research as these compounds possess beneficial properties on physiological wellbeing and to counteract oxidative stress and pathogenesis of disease conditions such as cancer, rheumatoid arthritis, atherosclerosis, cardiovascular and neurodegenerative diseases [49]. Alternatively, these compounds can increase the shelf life of food by reducing lipid peroxidation. Among natural antioxidants, phenolic compounds receive an exceptional place as the most abundant antioxidants in marine algae. Moreover, sulfated polysaccharides, peptides/protein hydrolysates, and other minor constituents contribute to the antioxidant activity of these algae extracts [50].

1.3. Anti-inflammatory agents from marine algae

Anti-inflammatory activity is another interesting area of research as inflammatory diseases are gradually becoming a leading cause of health issue in many parts of the world, having a considerable influence on the healthcare costs. Inflammation is a part of the complex stereotypical responses of the body to harmful stimuli. Inflammatory responses are mediated through a complex system of cell signaling pathways that involves cytokines and lipid mediators [51]. Although inflammatory responses are crucial for an organism to counteract infection, chronic inflammation could result in detrimental issues upon the physiological wellbeing by producing an array of degenerative disease conditions that includes inflammatory arthritis, coronary artery diseases, multiple sclerosis, cancer, obesity, atherosclerosis,

migraines, interstitial cystitis, dermatitis, insulin resistance and irritable bowel syndrome [52 Xu H, Barnes]. A descriptive record of anti-inflammatory components of marine algae is given in Fernando et.al. [53]. Since the discovery of substances with anti-inflammatory activity could benefit the mankind in maintaining physiological wellbeing.

1.4. Fucoidans; a sulfated polysaccharide from brown algae possessing desirable biofunctional properties.

Fucoidans are a type of L-fucose rich sulfated polysaccharide unique to brown algae [54]. During past few decades, fucoidans purified from different brown algal species have extensively been studied due to their broad spectrum of desirable biological functionalities that includes anticoagulant, antithrombotic, antitumor, anti-inflammatory, immunomodulatory, anticomplementary, anti-obesity and antioxidant properties. Moreover, fucoidans are effective against congestive hepatopathy, obstructive uropathy and kidney failure as well as have gastric protective effects [55, 56]. The structural complexity of this biopolymer ranges from the basic macromolecular structure that contains fucose monosaccharide units with attached sulfate groups into macromolecules containing a range of different monosaccharide units such as mannose, galactose, glucose, and xylose. Molecular structures of fucoidan are extremely random and depend on the specificity of species and some other factors such as harvesting time and habitat conditions. Since the sequencing of monosaccharides and determination of structural features remains highly challenging [57]. These structural features are most likely to affect the biological activity of these sulfated polysaccharides. However, until now, the relationship between molecular characteristics and bioactivity of sulfated polysaccharides are poorly understood [58]. The anionic sulfate groups of fucoidans have been reported to enhance the nonspecific binding to proteins [57]. Also, the sulfate groups in fucoidans are likely to affect intracellular antioxidant properties and an array of other biofunctional properties [59].

2. MATERIALS AND METHODS

2.1. Analysis of mineral constituents by inductively coupled plasma optical emission spectrometry (ICP-OES).

The analysis was carried out according to the method described by Pasławski and Migaszewski with minor modifications [60]. All glass were used during the analysis were pre-washed using 10% HNO_3. A measured weight of the finely powdered sample was dried in the drying oven at 100°C for 24h. A measured 2.00 g of dried sample was ashed in a furnace oven at 450°C for 6h. A 50.0 mg of ash was dissolved in 2.00 ml of aqua regia under 90°C in sealed glass vials. After, a serial dilution (x10 x50) was performed using 3% analytical grade HNO_3. Samples were filtered using pre-washed syringe filters. The analysis was done using a PerkinElmer OPTIMA 7300DV Inductively Coupled Plasma Spectrometer system (Massachusetts, USA). The equipment was calibrated using a multi-element calibration standard (PerkinElmer N9300233) that contains 10 µg/mL (10 ppm) of Ag, Al, As, Ba, Be, Bi, Ca, Cd, Co, Cr, Cs, Cu, Fe, Ga, In, K, Li, Mg, Mn, Na, Ni, Pb, Rb, Se, Sr, Tl, U, V, and Zn. The elements were detected at least by using two non-overlapping wavelengths.

2.2. Enzyme-assisted extraction (EAE) of marine algae

A known quantity of freeze-dried algae powder was depigmented using 95% EtOH and dried to remove remaining EtOH. The remain was suspended in distilled water, and the pH was adjusted to the optimum conditions of the specified enzymes as indicated in Table 6. After introducing the enzyme the mixture was incubated under continuous agitation for 24h at the optimum temperature specified to each enzyme. Enzymes were heat inactivated by incubating in a boiling water bath at 90-95°C for 10 min. The pH was readjusted to 7.0, and the mixture

was filtered under vacuum. Simultaneously water extract was obtained at 30°C by the same method. The extracts were lyophilized and kept stored at -20°C until analysis.

Table 6. Optimum conditions employed during enzyme assisted extraction

Enzyme	pH	Temperature (°C)
Pepsin	2.0	37
Neutrase	8.0	50
Alcalase	6.0	50
Trypsin	8.0	37
Protomax	6.0	40
Flavourzyme	7.0	50
Kojizyme	6.0	40
Celluclast	4.5	50
Viscozyme	4.5	50
AMG	4.5	60
Termamyl	6.0	60
Ultraflo	7.0	60

2.3. Precipitation of polysaccharides of selected *C. minima* and *S. polycystum* extracts obtained via EAE of depigmented raw material.

For further studies, the selected *C. minima* (350.0 g) and *S. polycystum* (170.0) was depigmented using 70% ethanol. After evaporating off the ethanol, the remaining powder was freeze-dried. The powders were separately suspended in water and pH of the medium was adjusted to 4.5 using 1M HCl to carry out the extraction process using the selected Celluclast enzyme as it gives a higher yield. After, Celluclast was introduced into the medium at a 0.5% of substrate concentration and the mixture was incubated for 24h at 50° C under continuous agitation. The pH of the medium was randomly monitored and maintained at 4.5 during the extraction period. After, the enzyme was inactivated by keeping the mixture in boiling water (95°C) for 10 min. After the hydrolysate was filtered by vacuum and pH was readjusted to 8.0 using 1M NaOH. Alcalase was introduced into the mixture to facilitate the hydrolysis of proteins. The mixture was incubated at 50°C for 24h under continuous agitation. Alcalase was heat inactivated by keeping at 95°C for 10 min. The pH was adjusted to 7.0 and the mixture was filtered under vacuum. Then the mixture was concentrated to 1/3 of its original volume via lyophilization. Four volumes of ethanol (95%) was incorporated with the concentrated extract to facilitate the precipitation of polysaccharides. For precipitation to proceed the mixture was kept at 4°C for 8h. The polysaccharides were separated via centrifugation. The separated polysaccharides were re-suspended in 95% ethanol and centrifuged to wash away the contaminants. The obtained polysaccharides were fully dissolved in DW and lyophilized while in zipper bags to obtain smoothly (soft) distributed polysaccharides.

2.4. Separation of polysaccharides via anion-exchange chromatography

The polysaccharides were separated using ÄKTA start chromatographic system (GE Healthcare Bio-Sciences Co., UK) equipped with a DEAE-Sepharose fast flow column (HiPrep DEAE FF 16/10, GE Healthcare Bio-Sciences Co., UK). The system was pre-equilibrated with 50.0 mM sodium acetate buffer (pH 5.3) and the column separation was carried out with gradient elution starting with 50.0 mM sodium acetate buffer to 2.0 M NaCl in the same buffer. Eluate of the column separation was collected into 72 tubes. Tubes were analyzed for their polysaccharide content by the phenol-H_2SO_4 assay. The eluates in the tubes were pooled into 4 fractions and concentrated via lyophilization. The fractions were purified by removing the ionic contaminants of the column separation by dialysis. Dialysis was carried out using dialysis membranes with a 3.5 kD molecular weight cut-off value (Spectra/Por USA).

2.5. Characterization of the polysaccharides by FTIR and monosaccharide analysis

Polysaccharide characterization was performed both by using FTIR spectroscopy and by monosaccharide composition analysis according to the same method described previously.

2.6. Analysis of antioxidant activities of the samples using colorimetric methods

DPPH radical scavenging assay was performed by mixing 100 µl of different concentrations of the sample with equal volume of 4×10^{-4} M DPPH. Following an incubation period of 30 min, the absorbance was measured at 517 nm. Hydrogen peroxide radical scavenging activity was measured by incorporating 0.1 M phosphate buffer, sample, hydrogen peroxide, 1.25mM ABTS and peroxidase following a 10 min incubation. The absorbance was measured at 405 nm. Ferric reducing/antioxidant power (FRAP) assay was performed to estimate the levels of lipid peroxidation. A 100 µl of sample 2 mg/ml was mixed with 100 µl of DW and mixed with

0.5 mM FeCl$_2$ and 0.5 mM ferrozine. Following a continuous mixing period of 20 min, the absorbance was measured at 562 nm. Calculation of the radical scavenging activity was done with compression to control that uses DW instead of samples. The interference of readings due to sample color was corrected by using necessary sample blanks using DW instead of reactants.

Anti-oxidant activity (%) = [(A$_0$-(A$_1$-A$_2$)]/A$_0 \times 100$

N.B.; A$_0$: absorbance of the control, A$_1$: absorbance of the sample and A$_2$: absorbance of the respective blank.

2.7. Maintenance of cell lines

RAW 264.7 macrophages were maintained in DMEM media supplemented with 10% FBS and 1% antibiotic (penicillin and streptomycin). "Vero" (kidney epithelial cells of an African green monkey) and HL-60 (human leukemia) cancer cells were maintained in RPMI media supplemented with 10% FBS and 1% antibiotic (penicillin and streptomycin). Cells were periodically subcultured and maintained at 37°C with 5% CO$_2$ under a humidified atmosphere. Cells under exponential growth (log phase) were seeded for experiments. Experiments were carried out using appropriate cell line seeded in culture plates. Cytotoxicity of the samples was evaluated as a measurement of cell viability by MTT assay [32]. Readings were obtained using a Synergy HT multi-detection microplate reader (BioTek Inc., Winooski, VT, USA).

2.7.1. Evaluation of anti-inflammatory activity in LPS-stimulated RAW 264.7 macrophages.

The initial evaluation of the anti-inflammatory activity was done by measuring the levels of NO production in LPS-stimulated RAW 264.7 macrophages. For the experiments, RAW cells were seeded in 24 well culture plates for a period of 24h. After, the samples were treated to

each plate reaching a predesignated final concentration. Following another 24h period, the NO levels of the culture media were measured by the Griess assay [32].

2.7.2. Western blot analysis of the expression levels of inflammatory mediators.

RAW 264.7 macrophages were seeded in 6 well plates with $2x10^5$ cells/ml. After a 24h incubation period, different concentrations of the samples were treated into each well. LPS treatment was done after 1h. Following 24h, the cells were harvested, washed with LPS and lysed using lysis buffer containing 50 mm L^{-1}, Tris-HCl (pH. 7.4), 1% Triton X-100, 150 mm L^{-1} NaCl, 0.1% SDS and 1 mm L^{-1} EDTA by periodically vortexing while keeping in ice. The lysate was centrifuged at 16000 rpm for 20 min under 4°C. The protein content of the supernatant was measured using BCA™ protein assay kit. Cell lysates containing 50 μg of protein was subjected to electrophoresis on 12% polyacrylamide gels. The resolved protein bands were blotted onto nitrocellulose membranes, and selected strips of the membranes were blocked in blocking buffer and incubated with the corresponding primary antibody for 8h under at 4°C. After washing the membrane strips with tween-tris buffered saline containing TTBS; 25 mm L^{-1} Tris-HCl, 137 mm L^{-1} NaCl, 0.1% Tween 20, pH 7.4), strips were immersed in the secondary antibody and genteelly shaken for 3h at room temperature. After, the strips were washed again with TBST. Finally, ECL (enhanced chemiluminescence) western blotting detection activator was added onto the strips and fluorescence images were generated by a FUSION SOLO Vilber Lourmat system (Paris, France).

2.7.3. Evaluation of the expression levels of PGE$_2$ and pro-inflammatory cytokines

RAW 264.7 macrophages were pre-seeded in 24 well plates, treated with different concentrations of polysaccharides and co-treated with LPS (1 μg/ml). Following a 24 h period,

the culture media was collected from each separate well. The analysis was carried out for the expression levels of PGE$_2$, IL1-β, IL-6 and TNF-α using enzyme immunoassay kits, following the given instructions.

2.8. Maintenance of zebrafish and obtaining embryos

Experimental zebrafish were purchased from a commercial fish dealer (Seoul Aquarium, Seoul, Korea). The fish were acclimated to the laboratory environment which was controlled under carefully monitored conditions. Fish were kept at 28.5 ± 1°C in purified water supplemented with essential minerals under a 14/10 h light/dark cycle. Fish were fed twice a day with "Tetra GmgH D-49304 Melle". After 2 weeks zebrafish were mated and 8 of eggs and sperms was stimulated by the onset of light. Embryos were obtained within 30 min after the spawning and transferred to a petri dish containing 0.1% (w/v) methylene blue solution for 10 min. After they were transferred into embryo media. Embrionic stages of the developing zebrafish larve is depected in Fig. 8
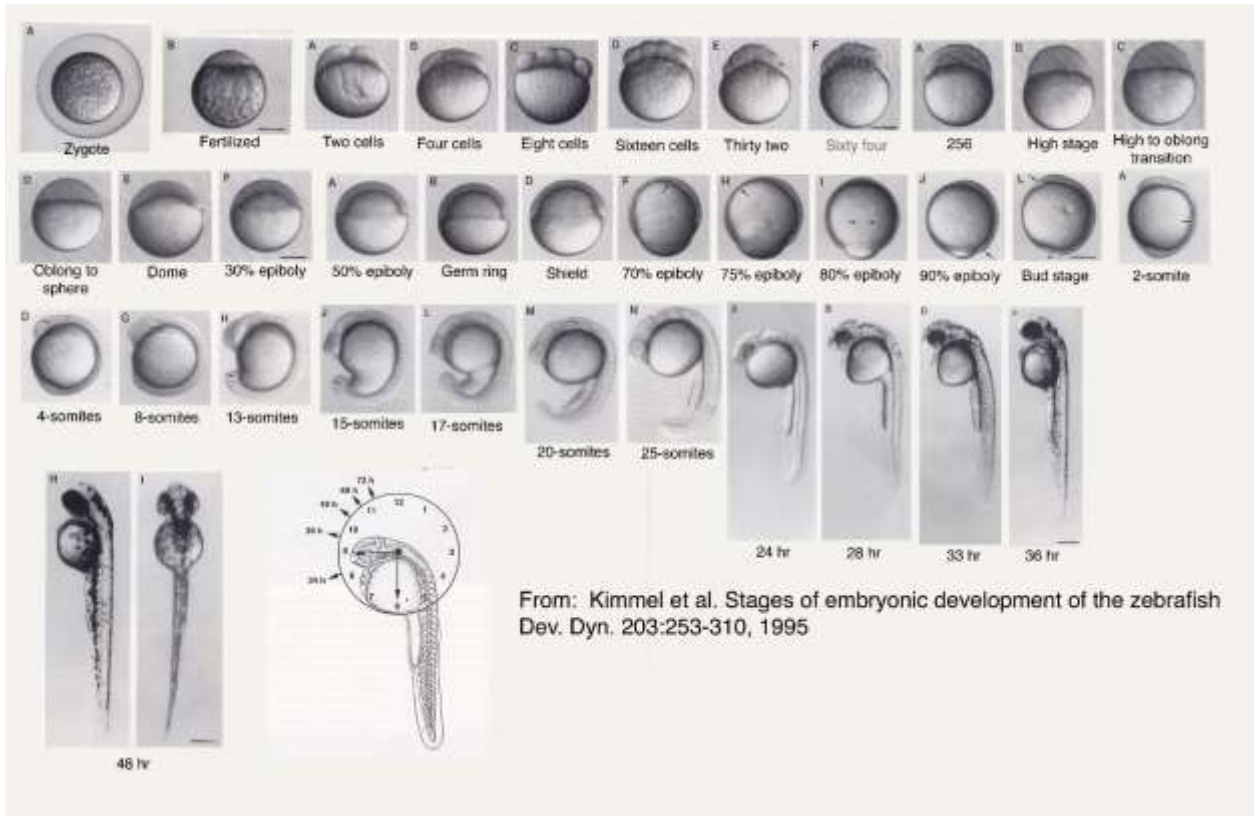
Fig. 8 Stages of development of zebrafish embryos

2.8.1. In vivo evaluation of the anti-inflammatory activity of algae polysaccharides by zebrafish embryos.

The selected healthy zebrafish embryos were mounted in embryo media and randomly and periodically monitored to identify the embryonic stage of development. For the experiments, fish embryos 15 per group were transferred to 12 well plates. Sample / LPS treatment was carried out between the 70% epiboly and 80% epiboly stages, which is observed 7-9 hours after the fertilization. The exposure to sample/stimulators were done only for 24 hours. The embryo media was replaced with new embryo media after each 24 hours. At the 3rd day of postfertilization (dpf), the emerging fish larvae were used to observe the different experimental parameters. Mortality of the embryos and heartbeat rate (by microscope) were periodically monitored during the experimental period.

Parameters such as NO level, ROS level, and cell death was detected by using fluorescence dyes. Accordingly, intracellular ROS levels were detected by using 2,7-dichlorodihydrofluorescein diacetate (DCFH-DA), NO levels by diaminofluorophore 4-amino-5-methylamino-2′7′difluorofluorescein diacetate (DAF-FM DA) and cell death by acridine orange. After incubating the larvae in the medium containing the dye for designated period the fluorescence images were obtained via a fluorescence microscope equipped with a Moticam color digital camera (Motix, Xiamen, China). The intensity of green color in each image was quantified by Image J program.

2.2. Statistical analysis

Results are represented as the mean ± standard deviation based on at least three independent experiments. Significant differences between the parameters were calculated using IBM SPSS

Statistics 20 software using one-way ANOVA by Duncan's multiple range test (DMRT). P-values less than 0.05 (P < 0.05) and 0.001 (P < 0.001) were considered as significant.

3. RESULTS AND DISCUSSION

3.1. Mineral content of algae material

Mineral content of the selected algae material was analyzed based on ICP-OES measurements (Table 7). In general, higher levels of potassium and calcium were evident from the algae species. Especially the algae that had a higher ash content indicated higher levels of calcium. This correlates with their calcified appearance of the thallus. The brown algae indicated the presence of the heavy metal arsenic, which could be resulting from the alginic acid that indicates metal chelating properties.

Table 7. Mineral content of the algae material (given in ppm)

Sample	Metal ion content													
	K	Ca	Mg	Fe	Cu	Mn	Na	Zn	Ni	Al	V	Sr	Ba	As
S. polycystum	4065.0	3295.8	2715.6	4.7	14.5	1.9	825.3	0.0	8.0	53.2	6.6	359.0	14.2	60.1
S. natans	5386.2	3918.2	2008.8	133.1	0.0	3.0	2548.7	0.0	12.9	237.3	0.0	343.6	9.8	81.8
P. commersonii	3182.8	12410.3	4131.4	1637.6	13.0	38.4	618.0	0.0	20.3	2657.5	49.0	326.1	9.1	191.0
C. minima	3745.8	3425.3	1436.2	127.1	7.4	4.5	670.4	0.0	11.5	98.2	0.0	504.1	8.9	41.7
C. herpestica	2905.4	16732.3	1567.0	1436.7	10.0	24.4	3776.8	0.0	18.3	1770.7	0.0	230.5	10.4	171.2
C. antennina	12743.7	2727.9	938.1	559.2	0.0	13.0	1077.7	0.0	16.2	164.7	0.4	33.8	11.1	145.2
U. fasciata	588.4	5513.5	4492.1	422.2	0.0	5.4	1241.4	0.0	8.0	474.4	12.8	83.4	12.6	10.1
A. pygmaea	4367.2	1002.8	642.0	94.5	0.2	5.3	714.1	0.0	4.0	35.3	7.9	12.7	-0.2	35.4
G. corticata	2951.9	4099.2	1091.0	0.0	19.5	5.7	91.5	4.7	2.3	27.8	3.3	28.1	35.0	23.6
G. lithophila	2963.0	2668.5	2353.5	0.0	4.8	6.0	2520.4	0.0	3.1	27.7	2.6	33.4	6.8	0.0

Results represents means of at least triplicate determinations.

3.2. Extraction yields algae extracts obtained via enzyme-assisted extraction.

Enzymatic extraction is considered as a green extraction technique that improves the efficiency of extraction process which facilitates the release of bioactive principals. During the present experiments, five different carbohydrases and five different proteases were used to extract the algae material (Table 8). Among the used enzymes, Celluclast gave the highest yields compared to other enzymes for all the algae material. Among the investigated algae *Chaetomorpha antennina*, *Gracilaria corticata* and *Grateloupia lithophila* gave the highest yields compared to other algae. The yield of water and ethanol extracts were lower than the enzymatic extracts. However, the results could not be directly co-related as different enzymes were used with different pH and at different temperatures. The extraction yield was comparatively low in *Chnoospora minima* and *Sargassum polycystum*.

Table 8. Yields of enzyme-assisted extracts of the algae

	Algae	Enzyme-assisted extraction										
		Protamex	Kojizyme	Flavourzyme.	Alcalase	Neutrase	Viscozyme	Celluclast	AMG	Termamyl	Ultraflo	D.W.
	Brown algae											
1	*S. polycystum*	10.00 ± 0.84	10.00 ± 0.92	14.00 ± 0.51	12.50 ± 1.25	9.00 ± 1.2	12.5 ± 1.28	15 ± 0.95	14.5 ± 0.52	13 ± 0.94	10.5 ± 0.23	5.5 ± 0.21
2	*S. natans*	19.00 ± 0.56	20.00 ± 0.85	20.00 ± 0.05	21.50 ± 0.36	16.00 ± 0.71	21 ± 0.95	23.5 ± 0.92	22.5 ± 0.95	22 ± 1.17	21.5 ± 0.48	13.5 ± 0.84
3	*P. commersonii*	19.50 ± 0.28	20.50 ± 1.2	21.50 ± 0.23	18.50 ± 0.95	23.00 ± 0.49	21.5 ± 0.82	26 ± 1.25	23.5 ± 0.86	22.5 ± 0.81	17.5 ± 0.15	14.5 ± 0.22
4	*C. minima*	6.50 ± 0.95	9.50 ± 0.56	10.50 ± 0.53	9.00 ± 0.49	6.50 ± 0.5	9 ± 0.97	12 ± 0.86	8.5 ± 0.77	8 ± 0.77	6.5 ± 0.69	4 ± 0.34
	Green algae											
5	*C. herpestica*	11.00 ± 0.26	13.00 ± 0.95	14.00 ± 0.76	13.00 ± 0.35	12.00 ± 1.14	14.5 ± 0.57	17.5 ± 0.95	14.5 ± 0.76	14 ± 0.62	15 ± 0.17	7.5 ± 0.5
6	*C. antennina*	33.50 ± 0.78	35.00 ± 0.82	36.00 ± 0.6	33.50 ± 0.31	34.00 ± 0.5	33.5 ± 1.96	39.5 ± 0.81	35.5 ± 1.28	34.5 ± 0.84	37.5 ± 0.58	26.5 ± 0.24
7	*U. fasciata*	23.50 ± 0.29	23.00 ± 0.92	27.00 ± 0.15	26.00 ± 0.69	25.50 ± 0.63	25 ± 1.83	27 ± 0.98	25.5 ± 0.79	26 ± 1.24	24 ± 0.51	13 ± 0.38
	Red algae											
8	*A. pygmaea*	15.50 ± 0.17	16.00 ± 0.64	15.00 ± 0.87	13.50 ± 0.57	12.50 ± 0.46	17 ± 0.49	17.5 ± 0.67	16.5 ± 0.88	16.5 ± 0.97	12 ± 0.91	8.5 ± 0.43
9	*G. corticata*	29.50 ± 0.72	29.00 ± 0.72	33.00 ± 0.87	33.50 ± 1.18	33.00 ± 0.87	33.5 ± 1.74	36 ± 0.83	34.5 ± 0.71	34 ± 0.29	29.5 ± 0.7	20.5 ± 0.33
10	*G. lithophila*	35.50 ± 0.95	36.50 ± 0.91	36.50 ± 0.4	28.00 ± 1.02	25.50 ± 0.36	36 ± 1.11	40 ± 0.96	36 ± 1.14	37 ± 0.57	34 ± 0.22	23 ± 0.17

Results represents means ± standard deviation of at least triplicate determinations.

3.3. Antioxidant activities of the algae crude polysaccharides from enzyme assisted extracts of algae.

Antioxidant activities were determined by colorimetric methods that allow screening a large number of samples at once. Accordingly, DPPH, hydrogen peroxide scavenging and ferric reducing antioxidant power were determined. Fig. 9-11 represent the antioxidant activities of the polysaccharides obtained from enzyme assisted extraction. Celluclast extract of *S. polycystum* indicated the highest DPPH and hydrogen peroxide radical scavenging activity at the measured concentration of 2 mg/ml (57.23% and 39.10%). The Water extract of *G. corticata var. ramalinoides* indicated the highest ferric reducing antioxidant power accounting a value of 92.92%. This result was unexpected but might be resulting due to the chelation of Fe^{2+} by polysaccharides in *G. corticata var. ramalinoides.*
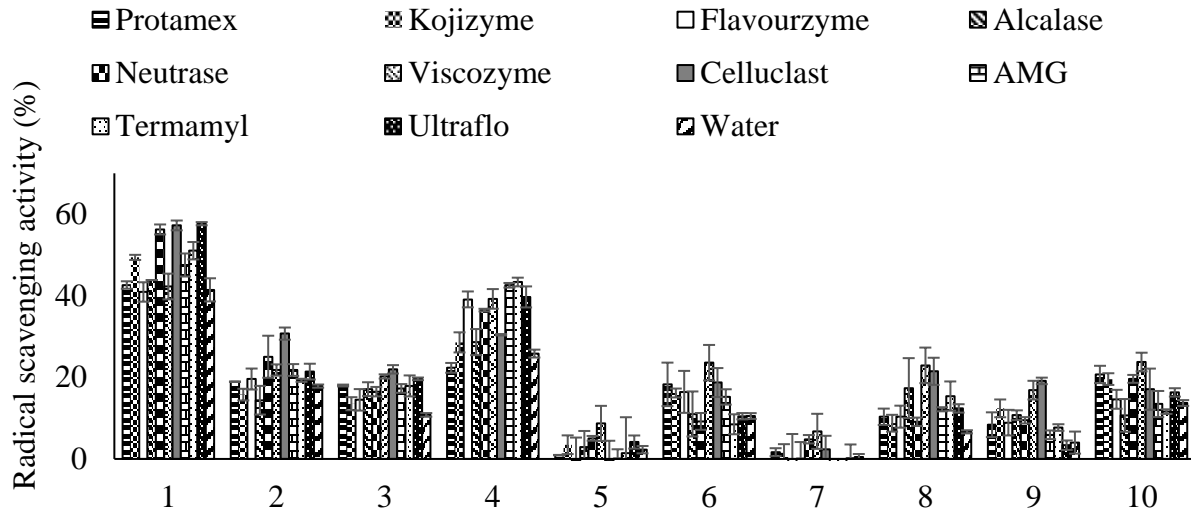
Fig. 9 DPPH radical scavenging activity of the polysaccharide precipitates obtained via enzymatic extraction of algae material. Experiments were carried out in triplicate, and the results are represented as means ± SD.
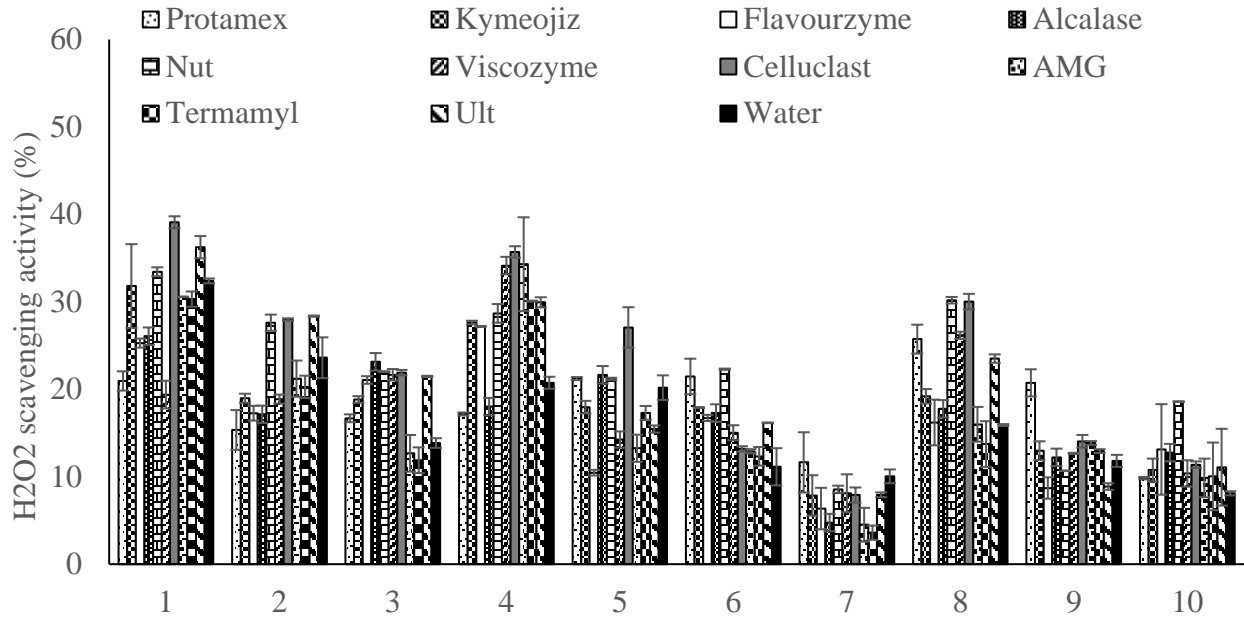
Fig. 10 Hydrogen peroxide radical scavenging activity of the polysaccharide precipitates obtained via enzymatic extraction of algae material. Experiments were carried out in triplicate, and the results are represented as means ± SD.
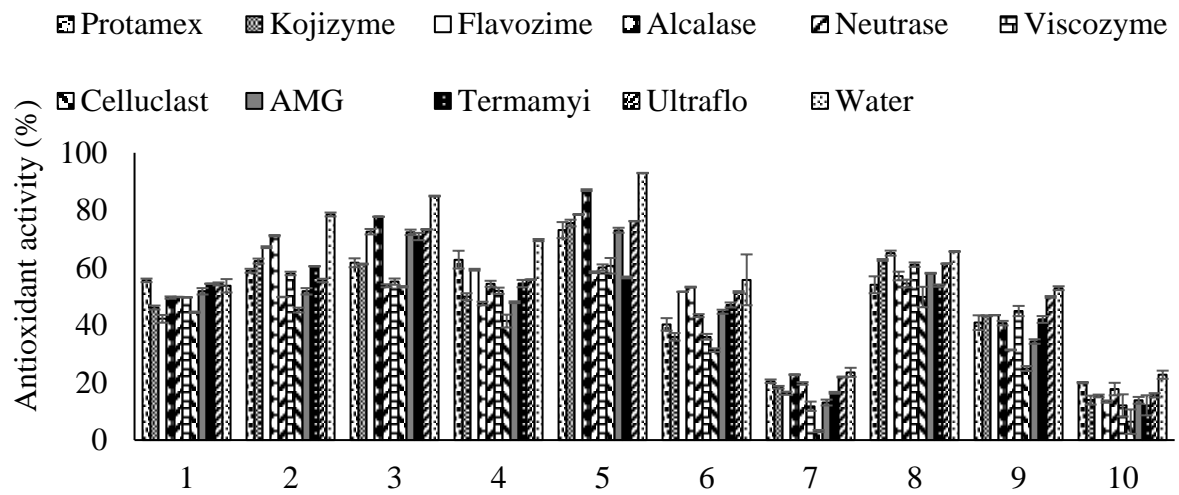
Fig. 11 Ferric reducing antioxidant power of the polysaccharide precipitates obtained via enzymatic extraction of algae material. Experiments were carried out in triplicate, and the results are represented as means ± SD.

3.4. Sample toxicity of enzyme-assisted extracts of algae upon normal cells

Fig. 12 indicate the cytotoxicity levels of the enzymatic extracts of the algae. Among the algal extracts, *G. corticata var. ramalinoides* extracts obtained from different enzymes indicated a considerable toxicity level compared to other algal extracts. Except for that all other algae extracts were found be safe for cell culture studies within the investigated concentration range of 25 – 100 µg/ml.

3.5. Anti-inflammatory effects of the algal extracts obtained by enzyme assisted extraction

Fig. 13 indicate the anti-inflammatory activities of the enzyme-assisted extracts as a measure of NO production in LPS-stimulated RAW macrophages along with the cell viability. Collectively the enzymatic extracts of the four brown algae species, *Sargassum polycystum*, *Sargassum natans*, *Padina commersonii*, and *Chnoospora minima* demonstrated considerably good anti-inflammatory activity compared to the extracts of the other algae with a cell viability of >80% within the concentration range of 25 – 100 µg/ml. Among the investigated algal extracts, the Celluclast extract of *Chnoospora minima* indicated the best anti-inflammatory effect. Hence, the four of these Celluclast extracts of the brown algae could be selected for further evaluation of their bioactive properties.
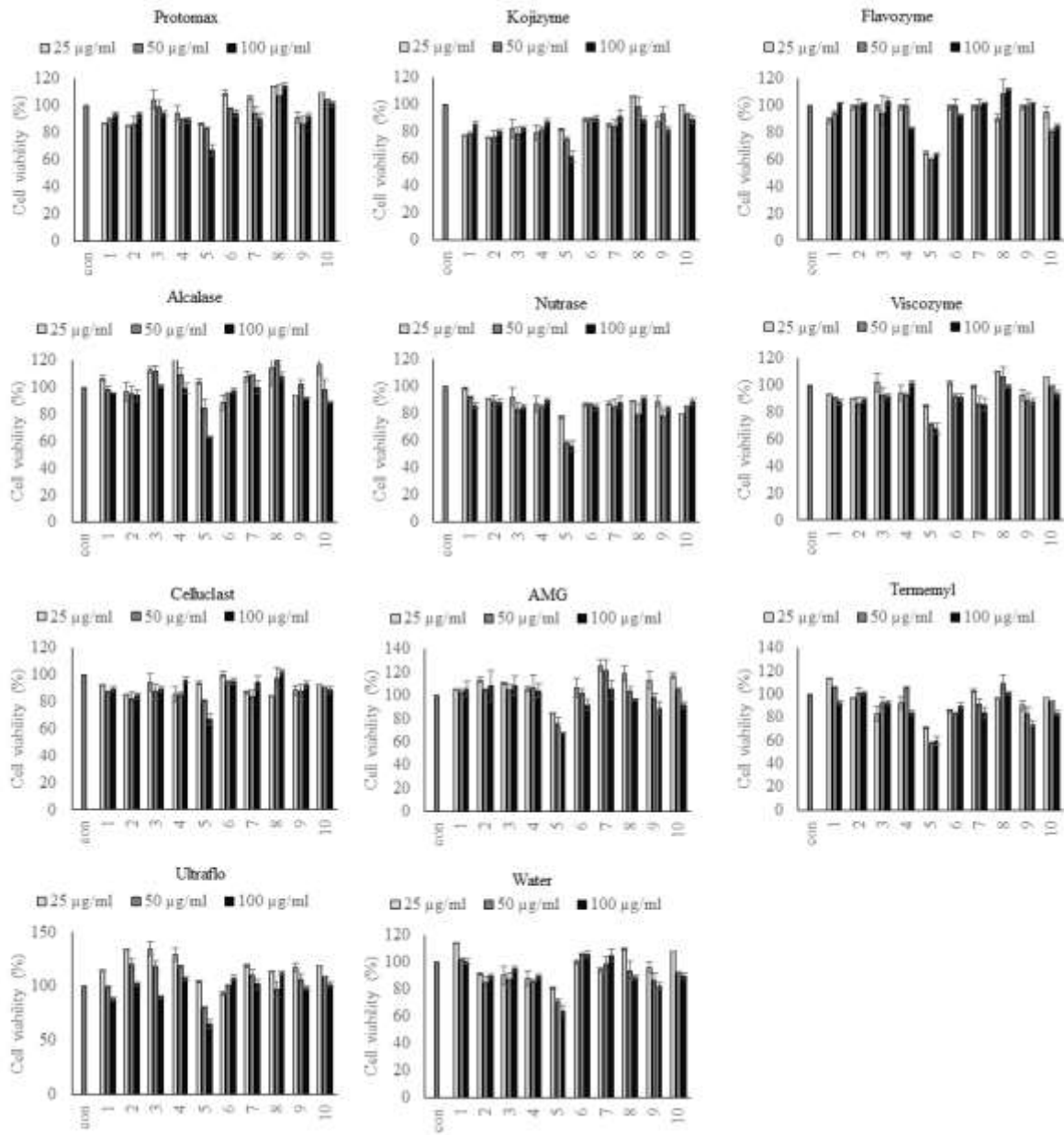
Fig. 12 Sample toxicity of the algal extracts. Results represent the percentage of "Chang" cell viability 24 hours after the sample treatment. Values were obtained from three independent experiments. The results are represented as means ± SD.
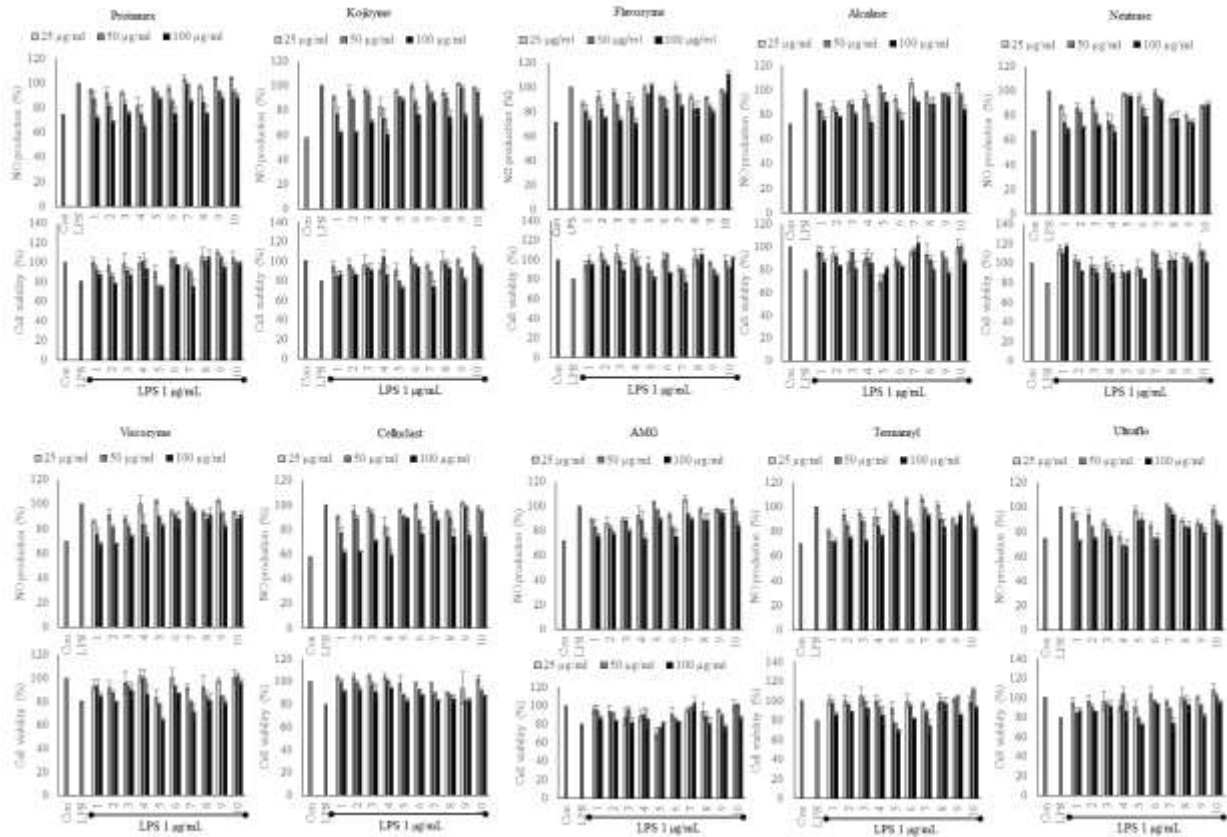
Fig. 13 Anti-inflammatory activity of algal extracts obtained by enzyme assisted extraction as a measure of inhibition of NO production and its protective effects against LPS induced cytotoxicity in RAW 264.7 macrophages. RAW cells were pretreated with different sample concentrations and co-treated with LPS (1 µg/ml). After 24h, culture media was retrieved for the analysis of NO levels using Griess assay and MTT assay was adopted for the determination of cell viability. Experiments were carried out in triplicate, and the results are represented as means ± SD.

66

3.6. Effect of Celluclast extract of *C. minima* upon LPS-induced iNOS, COX-2, PGE$_2$ and TNF-α protein expression in LPS-induced RAW cells.

Evaluating the expression levels of pro-inflammatory cytokines and inflammatory mediators is a convenient approach to assessing the anti-inflammatory activity of phytochemicals. As shown in Fig. 14, the LPS treatment resulted in a significant increase of the cytokine production compared to the control. However, the treatment of CCm effectively suppressed the expression levels of iNOS, COX-2, PGE$_2$ and TNF-α in a dose-dependent manner. Further, the observed reduction of NO production in RAW 264.7 macrophages could be attributed to the downregulation of iNOS expression.
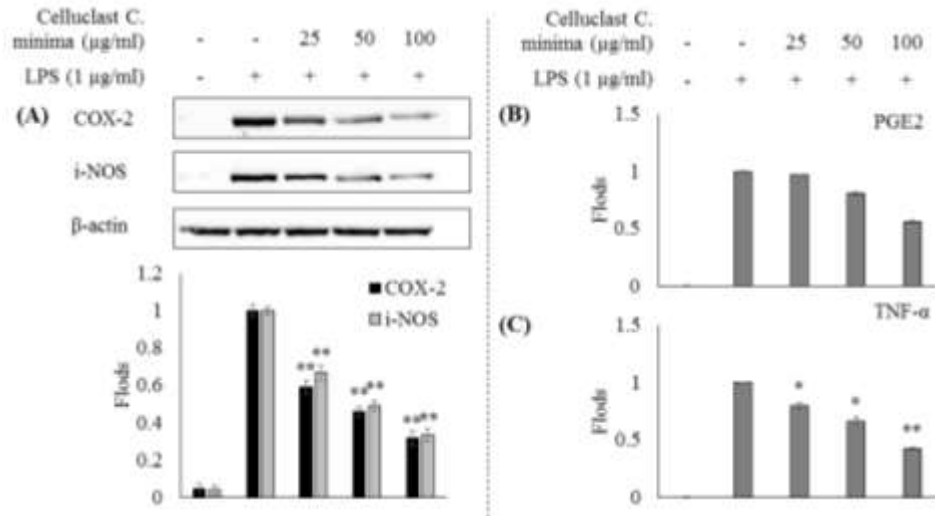
Fig 14 Effects of the Celluclast extract of C. minima on LPS-induced iNOS and COX-2 protein expression and pro-inflammatory cytokine production in RAW 264.7 cells. Expression analysis of (A) iNOS and COX-2 levels using western blot, (B) PGE_2 and (C) TNF-α levels using Elisa kits. Results were obtained with 3 independent experiments and represented as their means. Error bars accounts for the standard deviations. $* p < 0.05$, $** p < 0.001$ were considered as significant compared to the control.

3.7. Protective effect of Celluclast extract of *S. polycystum* against H_2O_2-induced oxidative stress and cell death in zebrafish

The survival rate for the zebrafish treated with 10 mM H_2O_2 after 5dpf was 58.6%, whereas the treatment of Celluclast extract of *S. polycystum* (200 µg/ml) increased it up to 93.0% (results not shown). The heart beating rate at 2dpf was increased up to 112.2% in zebrafish treated with 10 mM H_2O_2 with an average of 160 beats/min. The treatment of Celluclast extract of *S. polycystum* (200 µg/ml) reduced the rate to the normal levels (100%) with an average of 143 beats/min (results not shown). Further, the cell death of zebrafish caused by the oxidative stress was observed by acridine orange staining (Fig. 15). The decreasing fluorescence intensities indicate that treatment of Celluclast extract of *S. polycystum* (200 µg/ml) effectively reduced the cell death caused by H_2O_2-induced oxidative stress to normal levels. Intracellular ROS levels were simultaneously analyzed using DCHF-DA staining method (Fig. 15). Once again, Celluclast extract of *S. polycystum* (200 µg/ml) effectively reduced the intracellular ROS levels back to similar levels observed in the control.
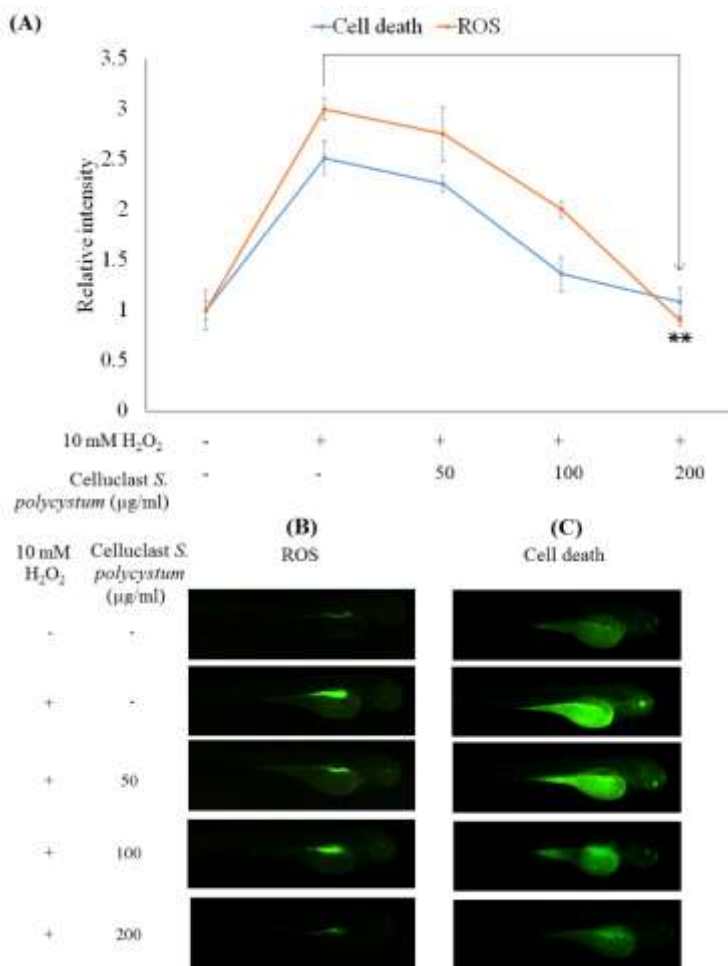
Fig. 15 In vivo evaluation of the protective effect of CSp against hydrogen peroxide-induced oxidative stress and cell death in zebrafish. (A) Relative fluorescence intensities of ROS levels and cell death. (B) Microscopic fluorescence images of ROS levels in Zebrafish larvae (stained with DCF-DA). (C) Microscopic fluorescence images of cell death in Zebrafish larvae (stained with acridine orange). At 3 hpf, embryos mounted in embryo media containing 1.00 ml of 0.2 mM PTU. After 1h embryos were treated with 50, 100 and 200 μg/ml of CSp. Again after 1h, 10 μg/ml H2O2 was introduced to the embryos. At 3dpf zebrafish larvae were examined using fluorescence staining methods. Results were obtained with 3 independent experiments and * $p < 0.05$, ** $p < 0.001$ were considered as significant compared to the control.

3.8. Anti-inflammatory activity of a Celluclast extract of *C. minima* against LPS-induced NO production, oxidative stress and cell death in zebrafish.

The heart beating rate showed a marked increase upon LPS treatment in Zebrafish up to 113.4% (161 beats/min). Celluclast extract of *C. minima* (100 µg/ml) treatment effectively reduced it back to the normal level (142 beats/min) (results not shown). The survival rate of the LPS treated zebrafish at 5dpf was 51.7%, but the treatment of Celluclast extract of *C. minima* at100 µg/ml successfully increased the survival rate up to 93.1%. These trends indicated a dose-dependent response (results not shown). As Fig. 16 indicate LPS treatment increased the cell death, ROS production and NO production in Zebrafish at 3dpf, whereas Celluclast extract of *C. minima* treatment at 100 µg/ml effectively evoked the levels back to the levels similar to control. The high fluorescence intensity of the LPS treated positive control group of zebrafish indicates increased NO production. Treatment of Celluclast extract of *C. minima* effectively reduced the NO levels indicating anti-inflammatory effects.
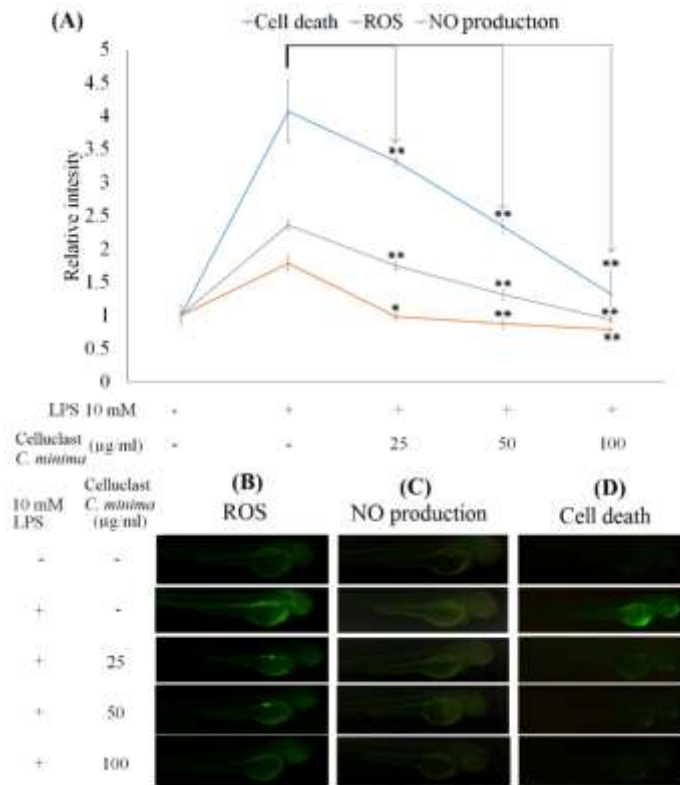
Fig. 16 In vivo evaluation of the protective effect of CCm against LPS-induced NO production, oxidative stress and cell death in zebrafish. (A) Relative fluorescence intensities of ROS levels NO production and cell death. (B) Microscopic fluorescence images of ROS levels in Zebrafish larvae (stained with DCF-DA). (C) Microscopic fluorescence images of NO levels in Zebrafish larvae (stained with DAF-DM-DA) (D) Microscopic fluorescence images of cell death in Zebrafish larvae (stained with acridine orange). At 3 hpf, embryos mounted in embryo media containing 1.00 ml of 0.2 mM PTU. After 1h embryos were treated with 25, 50 and 100 µg/ml of CCm. Again after 1h, 10 µg/ml LPS was introduced to the embryos. At 3dpf zebrafish larvae were examined using fluorescence staining methods. Results were obtained with 3 independent experiments and * p < 0.05, ** p < 0.001 were considered as significant compared to the control.

3.9. Yield and chemical composition of polysaccharides obtained from selected *S. polycystum* (SPP) and *C. minima* (CMP) samples.

The color of the obtained polysaccharides was brownish/off white. The polysaccharide content in both precipitates was higher than the other constituents indicating the efficiency of the followed methodology in obtaining polysaccharides (Table 9). Compared to CMP, SPP gave the highest yield, sulfate content and polyphenol content. In fact, the SPF indicated a ratio of relatively higher sulfate content relative to its polysaccharide content. The degree of sulfate substitution per anhydro sugar residue was respectively obtained as 0.62 and 0.82 for CMP and SPP. The relatively lower protein content in both samples indicates that protein hydrolysis via Alcalase is a useful strategy to get ethanol precipitates of polysaccharides with less protein contamination. Here the hydrolysis products of protein become much soluble in water whereas the addition of ethanol that reduces the dielectric constant of the medium fails to precipitate those hydrolyzed products. Hence allowing to obtain polysaccharides in a higher yield.

제주대학교 중앙도서관
JEJU NATIONAL UNIVERSITY LIBRARY

Table 9. Proximate composition of chemical components in the obtained polysaccharides

Sample	Yield	Carbohydrates		Protein	Polyphenol	Ash	Moisture
		Polysaccharide	Sulfate				
CMP	**8.39**	71.46	23.52	1.25	3.01	1.20	1.18
SPP	**12.16**	62.95	27.52	0.15	3.43	0.50	1.06

Results are based on triplicate determinations.

3.10. Anion exchange chromatography separation of CMP gave 4 different fractions

Fig. 17 show the DEAE-Sepharose column separation and distribution of polysaccharide content in each tube. According to the Fig. 17 separate fractions were identified from the column eluates. The respective tubes were pooled accordingly, concentrated and dialyzed to remove salt contaminants. Based on the chemical composition of each fraction, F1 indicated the highest yield and polysaccharide content. However, the sulfate content of F1 was lower than the rest. The polysaccharide content of the fractions showed a declining pattern whereas the sulfate content indicated a gradual increase with the fractions obtained sequentially. This increasing pattern of sulfate substitution relates with the increasing anionic characteristics of the polysaccharides. It goes with the fact that increasing concentrations of NaCl facilitate the elution of anionic molecules. Accordingly, the highest sulfate content was recorded from F4. The lower levels of proteins and polyphenols observed in each fraction could be considered negligible.
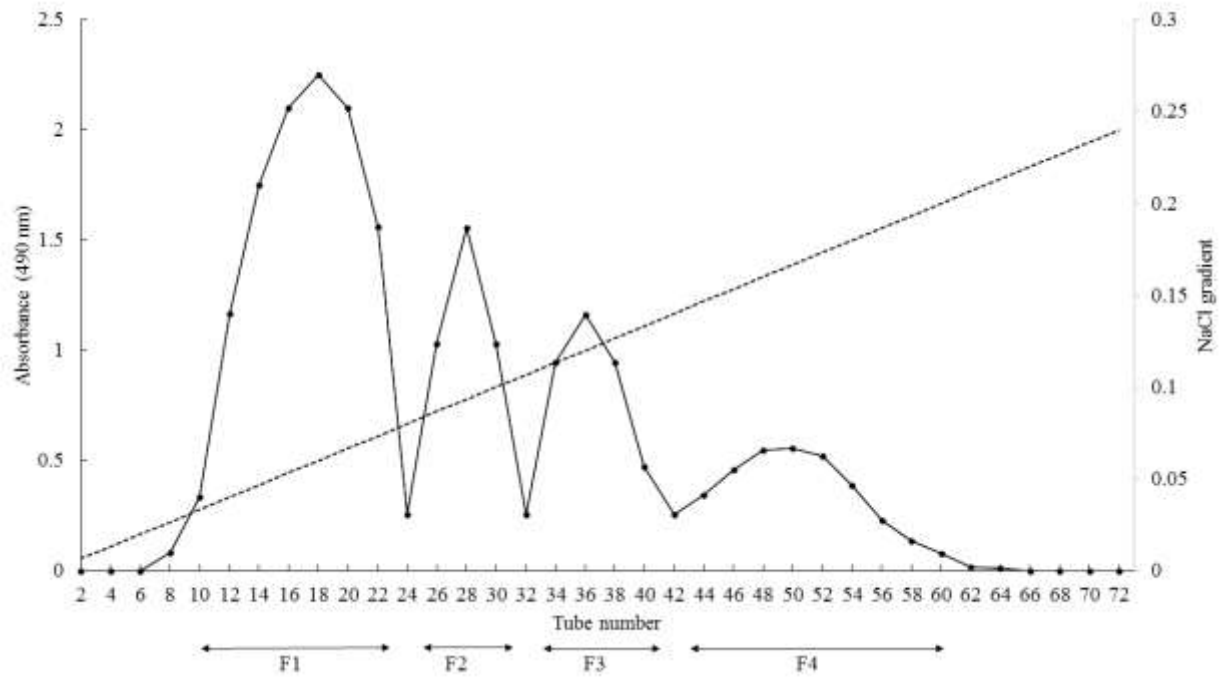
Fig. 17 Purification of CMP using DEAE-cellulose anion exchange chromatography. CMP was loaded to a DEAE-cellulose column (100 mm×16 mm) pre-equilibrated in 50.0 mM acetate buffer (pH 5.3). The column was eluted with an increasing gradient of NaCl (0.0-2.0 M) in the same buffer. Four fractions (F1, F2, F3, and F4) were identified based on the polysaccharide content measured by the phenol-sulfuric assay.

3.11. FTIR characterization of the polysaccharides indicated the presence of fucoidan in sub-fractions.

The region that represents the fingerprint of polysaccharides (500-2000 cm⁻¹) was used for the prediction of IR bond vibrational modes. The peak at 1035 cm⁻¹ represents the FTIR band characteristic to polysaccharides that signify the C─O─C stretching vibrations of glycosidic bridges. Brown algae contain some polysaccharides mainly including alginic acid and [61, 62]. The target of the current study was to purify and analyze the anti-inflammatory potential of a homogenous fraction of fucoidan. As indicated in Fig. 18 All subfractions indicated vibrational patterns that show characteristic features of fucoidan. The broad and intense peak between 1220-1270 cm⁻¹ signifies the stretching vibration of S═O bonds in sulfate groups connected to monosaccharide units. The peak at 845 cm⁻¹ corresponding to the bending vibration of C─O─S further confirms this speculation [63 & Pelegrín, 2015]. The band at 1135 cm⁻¹ observed in commercial fucoidan standard and much weakly in F4 could be assigned to the glycosidic (C─O─C) bond [64]. The peaks at 1616 cm⁻¹ were arising from the bending vibrations of H─O─H bond in water. This suggests the presence of moisture in the samples [65]. Differences in spectral profile of the fractions F1, F2 and F3 were noticed with the appearance of a sharp peak centering 1430 cm⁻¹, which was absent in commercial fucoidan and F4. The relatively intense peaks at 845 cm⁻¹ and between 1220-1270 cm⁻¹ observed in F4 and commercial fucoidan signifies a higher degree of sulfate substitution compared to the other fractions. In fact, the intensity of the peaks between 1220-1270 cm⁻¹ was increasing in order F1 < F2 < F3 < F4, which suggest increasing sulfate content in the fractions.
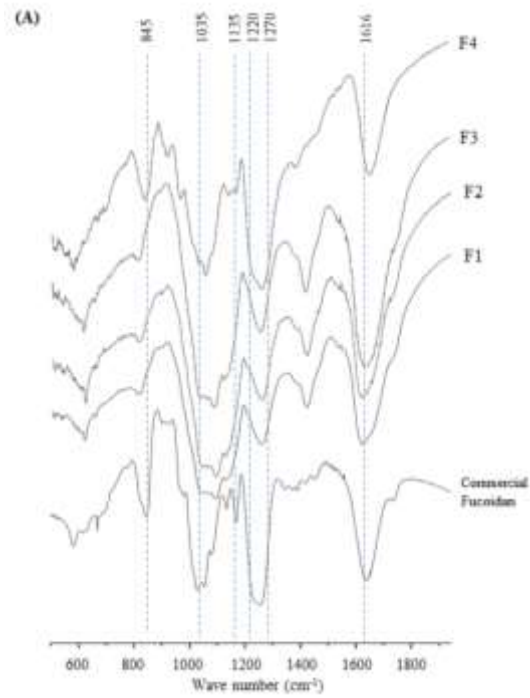
Fig. 18 Characterization of the structural features of CMP subfractions using FTIR spectroscopy. FTIR spectra of CMP subfractions compared to standard fucoidan was utilized for the spectral analysis.

3.12. NMR analysis of F4 indicated the structural characteristics of a fucoidan

Proton NMR analysis of the purified F2,4 (Fig. 19) indicated peaks typical of fucoidan as reported by Chevolot et al. and Mulloy et al. [35, 36]. The unresolved widened peaks between 5.3-5.6 ppm represent the anomeric protons of α-L-fucopyranosyl units. The two sharp unresolved peaks at 1.15 and 1.40 can represent methyl groups of fucose units. The overlapping and broadening of observed ^{1}H NMR peaks limited the ability to give a complete description of its structural characteristics. Sulfated polysaccharides generally have a complex and heterogeneous structures lacking regularity. The presence of sulfate groups often interrupts with the NMR determination of connectivity and branching. Hence, chemical alterations including desulfation and deacetylation are generally performed before NMR analysis [17]. Also, we were unable to obtain a clear ^{13}C NMR spectrum for the F2,4 (meager signal-to-noise ratio) mainly due to the heterogeneity and structural complexity of the molecules.
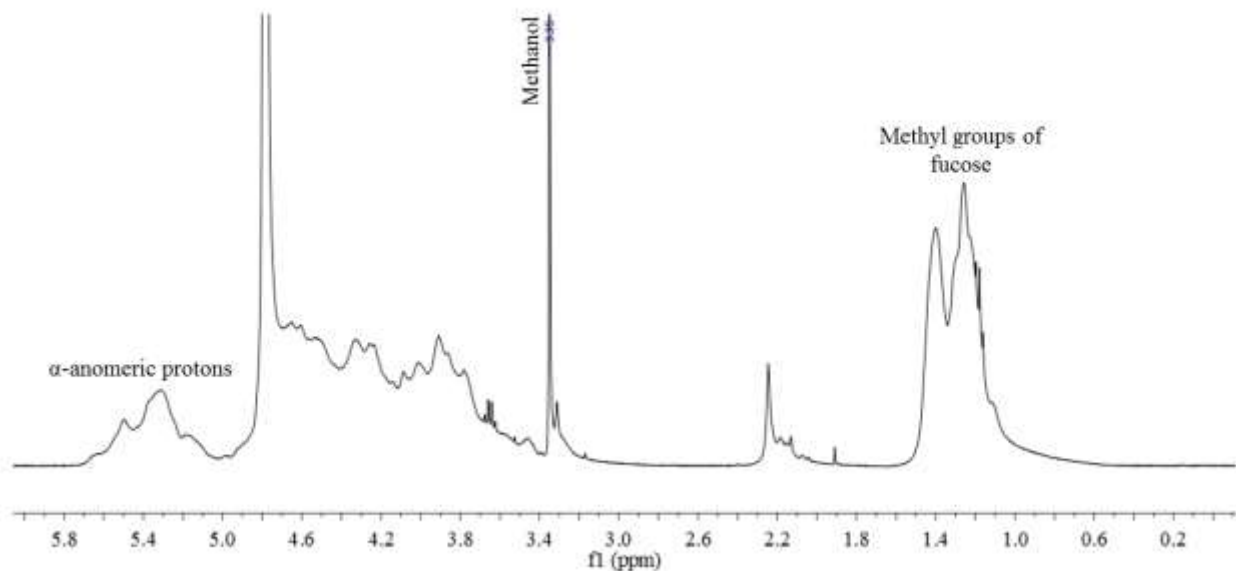
Fig. 19 ^{1}H NMR spectra of the F2,4 fraction. NMR spectrum of the F2,4 was obtained using a JEOL JNM-ECX400, 400 MHz spectrometer (Japan) at 33 k. The sample was repeatedly dissolved in deuterium oxide and lyophilized for five times for deuterium exchange. Finally, F2,4 was dissolved in deuterium oxide (4.65 ppm) and mixed with 2 µl of deuterated methanol (3.35, 4.78 ppm) as the internal standard [17].

3.13. Monosaccharide content analysis indicated the abundance of fucose in F4

Biological functionality of sulfated polysaccharides could depend upon several key molecular features such as the monosaccharide composition, sequence, branching pattern and a number of reducing end groups, the degree of sulfation and the substitution pattern of sulfate groups. Since the monosaccharide composition of each F2 subfraction was analyzed using HPAE-PAD chromatography to understand the relationship between monosaccharide composition and the anti-inflammatory potential of the polysaccharides. Polysaccharide fractions were hydrolyzed using 4 M of trifluoroacetic acid before the analysis. However, the weight of total monosaccharide content of each sample indicated a certain deviation from the sample weight injected into the column. Hence, the undetected portion indicated as "others" may represent unhydrolysed polysaccharides, sulfates and possibly other minor contaminants. All subfractions of F2 contained fucose and galactose. It is interesting to note that fraction F4, which indicated a profound anti-inflammatory activity was highly rich in fucose (79.32%). The corresponding HPAE-PAD spectrum of standard monosaccharide mixture and F4 are shown in Fig. 20; (B and C). Interestingly, the amounts of fucose were increasing in order F1<F2<F3<F4 whereas the galactose levels were declining. Three out of the four column eluates had >70% of fucose content. Fig. 20; (C) indicate the intense HPAE-PAD peak corresponding to fucose of the F4 fraction. Increased sulfate content marks increase anionic characteristics of the polysaccharides. The anion exchange DEAE-cellulose column purification facilitates the elution of anionic substances with the increasing NaCl concentration. The growing pattern of sulfate content both evidenced by the chemical assay (Table 9) and FTIR analysis (Fig. 18) and the fucose content of the CMP relates with the increasing anionic characters of the polysaccharides. These results clarify the effective separation efficiency of sulfated polysaccharides by DEAE anion exchange chromatography. Based on the chemical assays the

mean degree of sulfate substitution per anhydro sugar residue in F4, rich in fucose was estimated as 1.85. Fucose is the major polysaccharide in fucoidan unique to brown algae. It is a deoxyhexose sugar, which could be substituted with sulfate groups. Chevolot *et al.* report the presence of 2,3-disulphated fucose, 2-sulphated fucose and less abundant 2,3-disulphated fucose and 2-monosulphated fucose residues in the brown algae *A. nodosum* [66]. Fucoidans from *Fucus vesiculosus* and *Ascophyllum nodosum* have increasingly been investigated and described as mainly consisting of l-fucopyranose residues with α-(1→2) or α-(1→3) glycosidic linkages [62, 67 Williams, & Clark, 1993].
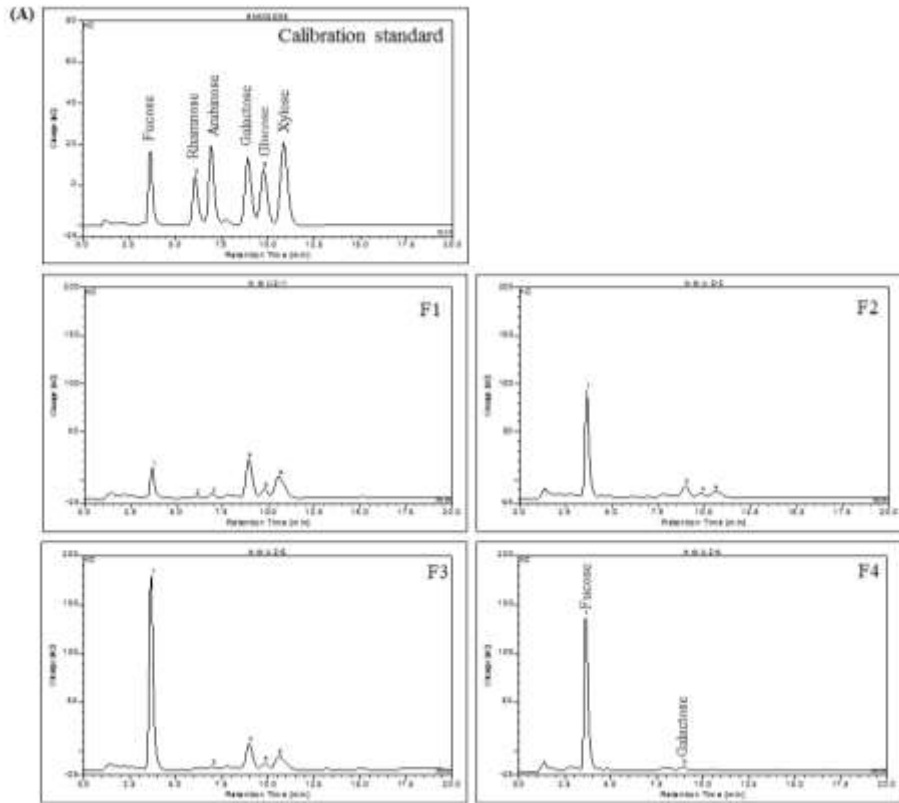
Fig. 20 Characterization of the structural features of CMP subfractions using monosaccharide analysis. Monosaccharide content of each CMP subfraction was analyzed using an HPAE-PAD spectrum comparing with a standard monosaccharide mixture.

3.13. The fraction F4, efficiently inhibited the LPS induced NO production in RAW 264.7 macrophages.

Lipopolysaccharides could stimulate the inflammatory responses in RAW 264.7 macrophages marked by an increased production of NO. As indicated in Fig. 21, LPS treatment resulted in an increased NO production in RAW 264.7 macrophages indicating increased NO production. Co-treatment with the column fraction F4 could effectively inhibit the NO production in a dose-dependent manner with an IC_{50} of 27.82 ± 0.88 µg/ml. Moreover, the column fractions indicated an ordered pattern of NO inhibitory activities (F4 > F3 > F2 > F1). The cytotoxicity of LPS (1µg/ml) treatment caused the reduction of the cell viability nearing 70%. Interestingly, co-treatment of column fractions revoked the cytotoxic effect of LPS on RAW 264.7 macrophages showing increased cell viability. These observations further highlight the cytoprotective effects of all the column fractions against LPS induced cytotoxicity.
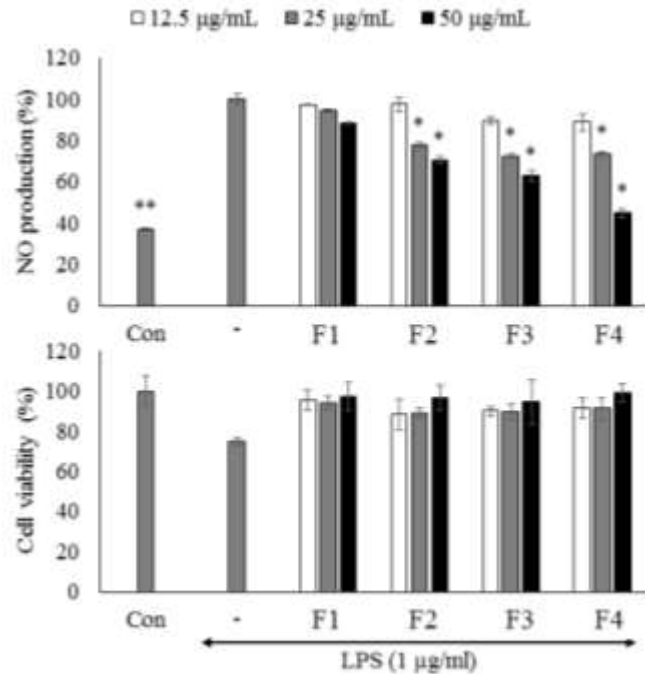
Fig. 21 Anti-inflammatory activity of CMP subfractions as a measure of inhibition of NO production and its protective effects against LPS induced cytotoxicity in RAW 264.7 macrophages. RAW cells were pretreated with different sample concentrations and co-treated with LPS (1 µg/ml). After 24h, culture media was retrieved for the analysis of NO levels using Griess assay and MTT assay was adopted for the determination of cell viability. Experiments were carried out in triplicate, and the results are represented as means ± SD. Values are significantly different from the positive control (LPS treated group) at *P < 0.05 and **P < 0.001.

3.14. The fraction F4 could downregulate the expression of iNOS, COX-2, PGE$_2$ and pro-inflammatory cytokines in RAW 264.7 macrophages.

Chronic inflammation is a detrimental pathological condition characterized by the upregulation of pro-inflammatory mediators that cause tissue destruction. Some immune cells including neutrophils, macrophages, and eosinophils are involved in the pathogenesis of inflammation through the production of inflammatory cytokines [53]. These inflammatory responses are mediated through a complex system of signaling pathways that regulate cellular responses [68, 69]. iNOS, COX-2, PGE$_2$ and proinflammatory cytokines such as TNF-α, IL1-β, and IL-6 are some of the key inflammatory mediators, which could be used to evaluate cellular responses and thereby anti-inflammatory activity of phytochemicals[68]. As evident from western blot analysis, (Fig. 22) treatment of F4 downregulated the LPS induced expression of iNOS and COX-2 in a dose-dependent manner. The down-regulation of iNOS expression successively results in the inhibition of NO production in RAW 264.7 macrophages. Prostaglandins, which are involved in causing a host of detrimental inflammatory responses eventually leads to tissue destruction [69]. F4 could significantly reduce the PGE$_2$ production in LPS stimulated cells indicating a promising anti-inflammatory activity.
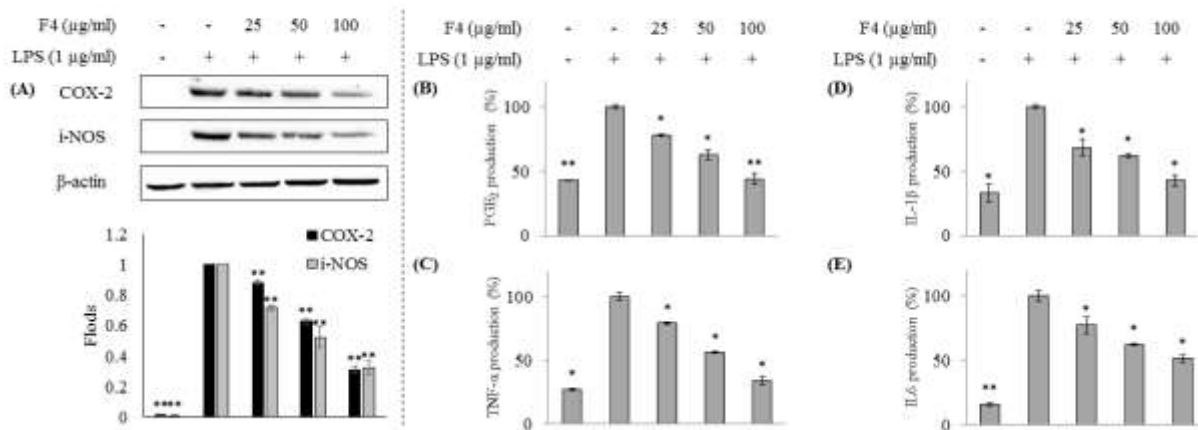
Fig. 22 The effects of F4 upon the mediation of inflammatory regulators. (A) Western blot analysis of the expression levels of iNOS and COX-2. Analysis of the downregulation of (B) PGE$_2$ and pro-inflammatory mediators including (C) TNF-α, (D) IL1-β and (E) IL-6 in LPS stimulated RAW 264.7 macrophages. RAW cells were pretreated with different concentrations of F4 and co-treated with LPS (1 µg/ml). After 24h, culture media was retrieved for the analysis of PGE$_2$, TNF-α, IL1-β, and IL-6. Simultaneously the cells were harvested for the analysis of iNOS and COX-2 expression using western blot analysis. Experiments were carried out in triplicate, and the results are represented as means ± SD. Values are significantly different from the positive control (LPS treated group) at *P < 0.05 and **P < 0.001.

87

3.15. *In vivo* anti-inflammatory effects of F4 indicated the ability to inhibit NO production, ROS production, and cell death in LPS stimulated zebrafish embryos.

Anti-inflammatory effects of F4 were evaluated under *in vivo* conditions using zebrafish embryo model. Zebrafish animal model is recently gaining popularity over other animal models in mimicking human disease conditions. As indicated in Fig. 23, LPS (10 µg/ml) stimulation of zebrafish embryos caused a significant upregulation of NO and ROS production with an increased cell death. The comparatively higher fluorescence intensity in LPS treated zebrafish embryos dually explains this phenomenon. However, the co-treatment of F4 could effectively reduce the NO, ROS and cell death levels in LPS stimulated zebrafish embryos in a dose-dependent manner. These observations further confirm the potential anti-inflammatory effects and cytoprotective effects of F4 on LPS stimulated zebrafish embryos.
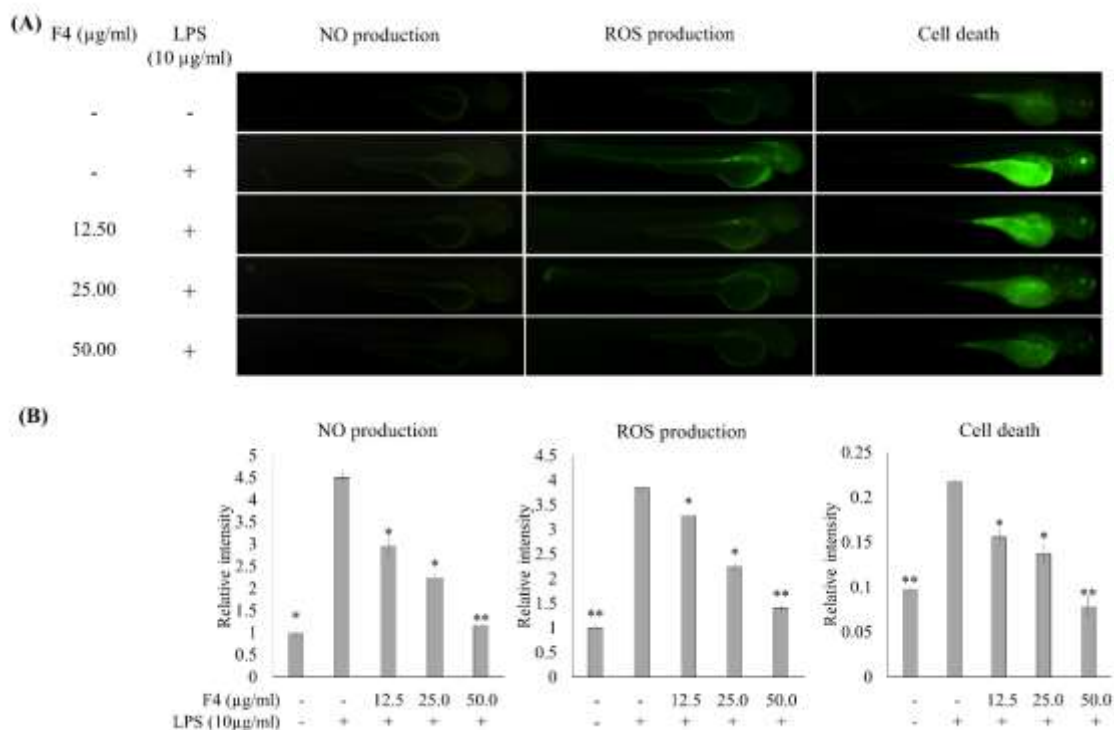
Fig. 23 In vivo evaluation of anti-inflammatory effects of F4 in LPS stimulated zebrafish embryos. F4 was treated to zebrafish embryos at different concentrations, stimulated with LPS (10 µg/ml) and fluorescence images were taken after 3 dpf using respective fluorescence probe dyes. (A) Fluorescence images of the zebrafish embryos representing NO production, ROS level and proportion of dead cells. (B) Quantitative interpretation of the average intensity of green fluorescence emitted by the corresponding zebrafish larvae group. Experiments were done in triplicate, and the results are expressed as mean ± SD. Values are significantly different from the positive control (LPS treated group) at *P < 0.05 and **P < 0.001.

89

4. CONCLUSIONS

Enzyme-assistant extraction is considered as a safe and inexpensive method to obtain bioactives from plant material compared to the conventional methods. The enzymatic extracts of the ten different Sri Lankan marine algae yielded in a higher polyphenolic content with profound antioxidant and anti-inflammatory activities respectively in the Celluclast extract of *S. polycystum* and *C. minima* both in *in-vitro* and *in vivo* Zebrafish model systems. In addition to the two studied algae, Celluclast extracts of *S. natans* and *P. commersonii* abundant in Hikkaduwa area could possess the potential to be utilized in the development of functional material. Collectively the enzymatic extraction using Celluclast could be an efficient method of obtaining bioactives from algae. Further, EAE could be employed in the industrial manufacture of algae-based functional ingredients.

Moreover, the current findings reveal an inexpensive, efficient green extraction method to obtain fucoidan with a higher purity from the under-explored brown algae *C. minima* harvested from Sri Lanka. Moreover, we elaborated the potential anti-inflammatory activity of a purified fraction of fucoidan (F4) using anion exchange chromatography. The fraction F4 could effectively inhibit the nitrous oxide (NO) production in RAW 264.7 macrophages (IC_{50} of 27.82 ± 0.88 µg/ml). Moreover, F4 could downregulate the expression of PGE_2, one of the major mediator of inflammation and could inhibit the expression of pro-inflammatory cytokines including TNF-α, IL1-β, and IL-6 in LPS stimulated RAW 264.7 macrophages in a dose-dependent manner. In vivo zebrafish embryo experiments indicated that F4 possess the ability to downregulate the production of NO and ROS levels in LPS stimulated zebrafish embryos while increasing the protective effect against cell damage caused by LPS. Molecular properties of F4, which was evaluated by FTIR and monosaccharide composition analysis, agree with the structural properties of fucoidan. These

findings confirm the anti-inflammatory potential of fucoidan purified from the *C. minima* by means of enzyme-assisted extraction using Celluclast. These sulfated polysaccharides with a host of other possible potential functionalities, which is to be evaluated in near future could be efficiently utilized in the manufacturing of functional ingredients for the food, pharmaceutical, and cosmetic industry.

SECTION 3; SCREENING BIOACTIVITIES OF 70% ETHANOL EXTRACTS OF SRILANKAN ALGAE AND PURIFICATION OF BIOACTIVE PRINCIPALS.

ABSTRACT

Identification and evaluation of biofunctional properties of marine natural products receive a tremendous importance in modern natural product research. The aim of current study was to explore the biofunctional properties of 70% ethanol extracts of algae including *Ahnfeltiopsis pygmaea*, *Gracilaria corticata var. ramalinoides*, *Chnoospora minima* and *Caulerpa racemose* harvested from Sri Lanka and to identify the active principals. Extracts of *C. minima* and *C. racemose* indicated desirable antioxidant anti-inflammatory and anti-cancer activities. The selected extracts were further purified using solvent/solvent separation, open column chromatography and PTLC based on bioassay-guided methods. Active principals were characterized by CG-MS/MS analysis and NMR techniques. The isolated C2 compound indicated the ability to decrease the levels of NO production in LPS-stimulated RAW 264.7 macrophages. Moreover, C2 downregulated the expression levels of iNOS, COX-2, and PGE_2 as well as pro-inflammatory cytokines. Hence, the ethanol extracts of *C. minima* and *C. racemose* or the purified compounds possess the potential to be incorporated into a functional material in cosmeceuticals, pharmaceuticals, and functional food. Moreover, these observations highlight the importance of exploring untapped algae bioresources in Sri Lanka.

1. INTRODUCTION

From ancient times, natural products of plant and animal origin have been used to treat many disease conditions. Hence, the exploration of bioactive natural products is one of the major strategy involved in discovering potential pharmaceutical agents or drug leads. Based on today's knowledge base regarding medicinal chemistry, many investigations have been done on natural products from terrestrial environment, and have proven their effectiveness and biocompatibility. However marine environment remains as an under-exploited natural habitat with a vast diversity of organisms with potentially bioactive metabolites [8]. During the recent few decades, there has been an increasing demand for research focused on isolating bioactive secondary metabolites of marine organisms. Many of the studied bioactive compounds in the marine environment have been isolated from invertebrates such as sponges, tunicates, mollusks or hydrozoans. Recent investigations have highlighted the importance of bioactive natural products of plant origin as potential agents for many disease conditions. These metabolites include polyphenols, terpenoids, proteins, peptides, alkaloids, polyunsaturated fatty acids, polysaccharides and many types of other metabolites. Still many of this marine-derived potentially active drug candidates are under pre-clinical trials while some are already in the market [70].

1.1. Bioactive phenolic metabolites of marine algae

Phenols or Polyphenolic compounds are one of the largest and diverse groups of secondary metabolites consisting of nearly 8000 natural compounds with important biological functionalities centered on their highly potential antioxidant properties [71] [72]. The structural features common to these molecules is the presence of phenol groups. Based on the number of phenyl substituents, their connectivity and connectivity of other functional groups, phenolic compounds can be found

as simple phenols and polyphenols [73]. These renowned phytochemicals are further classified into different groups based on their structure from simple phenols to much complex molecules including phenolic acids, tannins, coumarins, lignins, lignans, flavonoids, stilbenes, and into several other classes [74]. The biosynthesis of polyphenols proceeds through two basic pathways including shikimic acid and acetate-malonate pathway [75]. Simple phenolic compounds and phenolic acids are the metabolites of the shikimic acid pathway. However, the biosynthesis of complex polyphenol derivatives including flavonoids proceeds via shikimic acid and acetate-malonate pathways [76, 77].

Marine algae, especially the brown algae have been identified as a reservoir of bioactive polyphenolic compounds. These compounds have demonstrated interesting bioactive properties including antioxidant, free radical scavenging, anti-inflammatory, anti-cancer, antimicrobial, antidiabetic and several other bio functionalities indicating their potential to be used as functional ingredients and pharmaceuticals [14]. Phenolic acids found in algae includes salicylic acid, gallic acid, caffeic acid, protocatechuic acid, gentisic acid, p-hydroxybenzoic acid, chlorogenic acid, vanillic acid, syringic acid, ferulic acid, salicylic acid, 2,3-dihydroxybenzoic acid, p-coumaric acid, and cinnamic acid. Flavonoids are another interesting group of polyphenolic compounds with an immense structural diversity abundant in terrestrial plants. Recently their existence has been reported from marine algae. Some of the flavonoids reported from algae include acanthophorin A, acanthophorin B, tiliroside, catechin, epigallocatechin, epicatechin, epigallocatechin gallate, quercetin, daidzin, genistin, ononin, sissotrin, formononetin, and biochanin. Phlorotannins represent a complex group of polyphenolic compounds mainly confined to brown algae. Some of the phlorotannins include phlorofucofuroeckol A, dieckol, dioxinodehydroeckol, eckstolonol, triphlorethol-A, fucosterol, phloroglucinol, eckol, fucodiphloroethol G, 7-phloro eckol, and 6,6'-

bieckol, 2-phloroeckol. Apart from these polyphenolic compounds, different classes of phenolics have been reported from algae [14].

These compounds are renounced for their antioxidant activity hence are at the center of investigations to be implemented as natural antioxidants in food, cosmeceuticals, and other consumer products. A recent publication by Kirke et al. describes the stability of phenolic compounds under different environmental and physical conditions [78].

1.2. Bioactive terpenoid derivatives

Terpenoids represent a broad and diverse group of secondary metabolites derived from C5 isoprene building blocks. They are biosynthesized in all organisms via two major pathways that include mainly the Mevalonic acid pathway and by 2-C-methyl-D-erythritol 4-phosphate/1-deoxy-D-xylulose 5-phosphate pathway. Terpenoids are functional molecules that play a pivotal role in an organism as mediators of signaling pathways. In plants, they are involved in primary functions such as for the growth and development. Terpenoids from plant origin have been used in a variety of applications as flavoring agennntsss, fragrances, pharmaceuticals, insecticides, and industrial compounds.

1.3. Bioactive polyunsaturated fatty acids

Algae represent photosynthetic organisms with a wide distribution of different types of lipids owing to their great habitat diversity. They consist of glycolipids (glycosylglycerides), phospholipids, and non-polar glycerolipids some showing similar structural features to higher plants. Lipids such as betaine and several unusual structures of lipids that are characteristic of a

particular species have been reported from algae. Interestingly Algae have reported containing lipids with significantly longer chain length and unsaturation than the once that have been reported from terrestrial plants [79]. Algal lipids have a large commercial value and a higher demand for alternative sources of biofunctional n -3 polyunsaturated fatty acids (PUFAs), widely employed as functional food ingredients [80, 81].

2. MATERIALS AND METHODS

2.1. Extraction of algae using 70% EtOH

It is a accepted procedure to utilize 70% EtOH to extract polyphenolics and many of the antioxidant phytochemicals. Hence, the selected algae samples were extracted using 70% EtOH. Extraction was done in triplicate to increase the product yield. The solvent was evaporated off employing vacuum. The crude obtained was stored at -20°C until further utilization.

2.2. Solvent/solvent fractionation and purification of the selected 70% ethanol extracts of the algae

The crude of the selected 70% ethanol extracts of the algae was completely dissolved in distilled water and sequentially fractionated between hexane, chloroform and ethyl acetate in order of increasing the polarity. The solvents were evaporated using a rotary evaporator under vacuum at 40°C.

2.3. HPLC and GC-MS/MS analysis

HPLC analysis was used as a guide at each step of separation and purification. The analysis was performed using a Waters, SunFire, C18, 5μ, 4.6 x 250 mm column connected to a Waters HPLC system. The system was equipped with a Waters 2998 Photodiode Array (PDA) detector. The temperature of the column oven was maintained at 35°C. A mobile phase solvent system comprising of acetonitrile and deionized water was used to achieve the separation. GC-MS/MS analysis was done using a Shimadzu GCMS-TQ8040 system (from Japan) equipped with a Rtx-5MS fused-silica capillary column (30.0mx0.25mm i.d. 0.25μm). Iron source temperature 200°C, scan range 50-500 m/z, GC oven program; 260°C, 3 min, 6°C/min to 320°C, 5°C/min to 330°C, 2 min. Helium at a constant flow rate of 0.73 ml/min was used as the carrier gas. Sample injection was done by splitless mode.

2.4. Silica open column chromatographic purification

The selected solvent fractions were further purified using silica open column chromatography. Initially, the separation was performed using a column with a diameter of 10.00 cm but with a short height (10 cm). The column was pre-equilibrated in 20% ethyl acetate in hexane and eluted with six different mobile phase solvent systems containing increasing proportions of ethyl acetate. Among the six eluates CRHF1 which indicated potential effects were further purified using a second open column. An open column (3.00 cm diameter and 70 cm height) was used to achieve a good separation. The column was pre-equilibrated in hexane and eluted with different solvent systems containing increasing proportions of ethyl acetate. Based on the biofunctional properties

the selected CRHF1-F1 fraction was spotted on a PTLC plate and developed in 100% hexane. Compounds indicating a good separation was isolated from the PTLC.

2.5. NMR analysis

The compounds were dissolved in deuterated chloroform and analyzed using a JNM-ECX400 NMR system (JEOL, Japan) with a 40TH5AT/FG Probe. Gradient shim was automatically executed to obtain better NMR resolution. Experiments were done for proton, ^{13}C, DEPT, COSY, and HMBC.

2.6. Evaluation of anti-inflammatory activity in LPS-stimulated RAW 264.7 macrophages.

The initial evaluation of the anti-inflammatory activity was done by measuring the levels of NO production in LPS-stimulated RAW 264.7 macrophages. For the experiments, RAW cells were seeded in 24 well culture plates for 24h. After, the samples were treated to each plate reaching a predesignated final concentration. Following another 24h period, the NO levels of the culture media were measured by the Griess assay [32].

2.7. Evaluation of antiproliferative effects of algae material against carcinoma cells.

Cancer cells were cultured in multi-well plates with 1×10^5 cells/ml and incubated for 24h. Then different concentrations of the samples were treated into each well. MTT assay was carried out after 24h to determine the proportion of viable cells.

2.8. Observation of apoptotic/necrotic body formation.

DNA specific fluorescence dyes were used to identify the apoptotic and necrotic cells. Accordingly, Hoechst 33342 stain the nuclear matter, which can be observed by bright blue fluorescence. Hence, chromatin condensation and nuclear fragmentation could be identified by the morphology. Acridine orange/ethidium bromide simultaneous staining (double staining) method allow to separately distinguish apoptotic and necrotic cells based on the color and nuclear fragmentation. For the experiments, cells were seeded in 24 well culture plates and incubated for 24h. Sample treatment was performed and re-incubated for an additional 24h period. A 5 µl of Hoechst 33342 (10 µg/mL) or 10 µl of acridine orange/ethidium bromide dye mix (each 100 µg mL^{-1}) was treated into each well. Following a 10 min of incubation period cells were washed with PBS and observed using a fluorescence microscope equipped with a CoolSNAP-Pro color digital camera [82, 83].

2.9. Flow cytometric analysis of the cell cycle

The proportion of cells in the sub-G1 that represents the apoptotic hypodiploid cells were analyzed using flow cytometry [84]. Cells were seeded in 6 well culture plates (2×10^5 cells/ml) and incubated for 24h. Sample treatment was performed and re-incubated for an additional 24h period. The cells were harvested either by detaching from the plate using pipetting with PBS or by adding trypsin followed by pipetting with PBS. Cells (alive and apoptotic) were collected by centrifugation and fixed in 70% ethanol at 4 °C for 30 min. Before analysis, the ethanol was removed by centrifugation, and the cells were re-suspended in 2 mM Sodium Ethylenediaminetetraacetate (EDTA) in PBS and washed with the same solution. Ten the cells were re-suspended in a solvent containing PI (100 µg/ml) and RNase (µg/ml) and kept for 30 min

at room temperature. Flow cytometric analysis was performed using FACSCalibur flow cytometer (Becton Dickinson, San Jose, USA).

2.10. Evaluation of the expression levels of proteins by western blot analysis.

RAW 264.7 macrophages were seeded in 6 well plates with $2x10^5$ cells/ml. After a 24h incubation period, different concentrations of the samples were treated into each well. LPS treatment was done after 1h. Following 24h, the cells were harvested, washed with LPS and lysed using lysis buffer containing 50 mm L^{-1}, Tris-HCl (pH. 7.4), 1% Triton X-100, 150 mm L^{-1} NaCl, 0.1% SDS and 1 mm L^{-1} EDTA by periodical vortexing while keeping in ice. The lysate was centrifuged at 16000 rpm for 20 min under 4°C. The protein content of the supernatant was measured using BCA™ protein assay kit. Cell lysates containing 50 µg of protein was subjected to electrophoresis on 12% polyacrylamide gels. The resolved protein bands were blotted onto nitrocellulose membranes, and selected strips of the membranes were blocked in blocking buffer and incubated with the corresponding primary antibody for 8h under at 4°C. After washing the membrane strips with tween-tris buffered saline containing TTBS; 25 mm L^{-1} Tris-HCl, 137 mm L^{-1} NaCl, 0.1% Tween 20, pH 7.4), strips were immersed in the secondary antibody and genteelly shaken for 3h at room temperature. After, the strips were washed again with TBST. Finally, ECL (enhanced chemiluminescence) western blotting detection activator was added onto the strips, and fluorescence images were generated by a FUSION SOLO Vilber Lourmat system (Paris, France).

2.11. *In vivo* evaluation of the NO, ROS levels and cell death in zebrafish embryo model.

Zebrafish larvae three from each well were transferred to wells of 24 well plates and mounted in designated volume of embryo media. Different fluorescent probe dyes were applied and incubated in the dark for designated period to determine the different parameters. 2,7-dichlorodihydrofluorescein diacetate (DCFH-DA) for intracellular ROS levels, acridine orange for the determination of cell death and diaminofluorophore 4-amino-5-methylamino-2′7′difluorofluorescein diacetate (DAF-FM DA) for the determination of levels of NO. After incubation with dye, the larvae were washed by fresh embryo media and mounted in microscopic well depression slides and anesthetized using 0.003% MS-222 (Tricaine methanesulfonate) and visualized under a fluorescent microscope equipped with Moticam color digital camera (Motix, Xiamen, China). The fluorescence intensity of the larval images was quantified using Image J program [85].

2.12. Statistical analysis

Results are represented as the mean ± standard deviation based on at least three independent experiments. Significant differences between the parameters were calculated using IBM SPSS Statistics 20 software using one-way ANOVA by Duncan's multiple range test (DMRT). P-values less than 0.05 ($P < 0.05$) and 0.001 ($P < 0.001$) were considered as significant.

3. RESULTS AND DISCUSSION

3.1. Extraction yields of 70% ethanol extracts and their proximate chemical composition.

Based on the amount available, four of the selected algae samples were subjected to extraction using 70% ethanol. Accordingly, 50 g of *Ahnfeltiopsis pygmaea,* 45 g of *Gracilaria corticata var. ramalinoides* 65 g of *Chnoospora minima* and 90 g of *Caulerpa racemose* were extracted using 70% ethanol. The red algae, *G. corticata,* gave the highest yield of $5.8 \pm 0.22\%$. The highest polyphenolic content was recorded from the 70% ethanol extract of *C. minima* (2.84%). C. racemose extract indicated 8.32% sterol content (Table 10).

Table 10. Extraction yields of 70% ethanol extracts and their proximate chemical composition.

Source of the 70% ethanol extract	Content (%)				
	Yield	Polyphenol	Sterol	Polysaccharide	Protein
C. minima	4.1 ± 0.14	2.84 ± 0.31	6.21 ± 0.63	1.57 ± 0.52	1.22 ± 0.05
C. racemosa	4.5 ± 0.48	0.83 ± 0.25	8.32 ± 0.50	2.50 ± 0.15	1.70 ± 0.18
A. pygmaea	3.9 ± 0.15	0.60 ± 0.25	5.22 ± 0.60	1.55 ± 0.13	1.65 ± 0.52
G. corticata	5.8 ± 0.22	0.75 ± 0.50	5.70 ± 0.48	2.05 ± 0.08	1.52 ± 0.25

Results represent mean ± S.D. of triplicate determinants

3.2. Radical scavenging activities of the algae 70% ethanol extracts.

Table. 11 indicate the radical scavenging activities of the crude 70% ethanolic extracts of the used algae. According to the results, *C. minima* indicated the best DPPH and alkyl radical scavenging activity (0.05 and 0.07 mg/mL) respectively. The best hydroxyl radical scavenging was observed for *C. racemose*. This could be related to the abundant polyphenol content of that extract.

Table 11. Radical scavenging activities of the algae 70% ethanol extracts.

Sample name	Radical scavenging activity (IC$_{50}$ mg/mL)		
	DPPH radical	Alkyl radical	Hydroxyl
G. corticata var. ramalinoides	3.43 ± 0.04	1.19 ± 0.19	6.89 ± 1.82
A. pygmaea	3.27 ± 0.25	0.14 ± 0.17	5.45 ± 0.10
C. minima	0.05 ± 0.01	0.07 ± 0.0	2.79 ± 0.05
C. racemosa	0.915 ± 0.057	0.319 ± 0.014	0.182 ± 0.02

Results represent mean ± S.D. of triplicate determinants

3.3. Anti-inflammatory activity and sample toxicity of extracts obtained by 70% ethanol

The anti-inflammatory effects were evaluated on RAW 264.7 murine macrophages by using 70% ethanolic extracts of the four selected algae. All extracts demonstrated a declining pattern of NO production with increasing sample concentrations (Fig. 24). Especially, *C. racemose* 70% ethanol extract indicated comparably better anti-inflammatory properties than the other algal extracts with an IC_{50} value of 13.5 µg/ml. The corresponding RAW cell viability at the IC_{50} value was 82.72%. The proportion of viable cells went down to 69.00% upon LPS treatment. However, with initial sample concentrations, the increasing pattern of cell viability indicate that samples possess a protective effect against the LPS induced cytotoxicity. The results suggest that *C. racemose* 70% ethanol extract could be used as an inflammation preventive agent bellow 50 µg/ml concentration. Hence, *C. racemose* 70% ethanol extract was selected for further evaluations targeting the isolation of bioactive compounds.
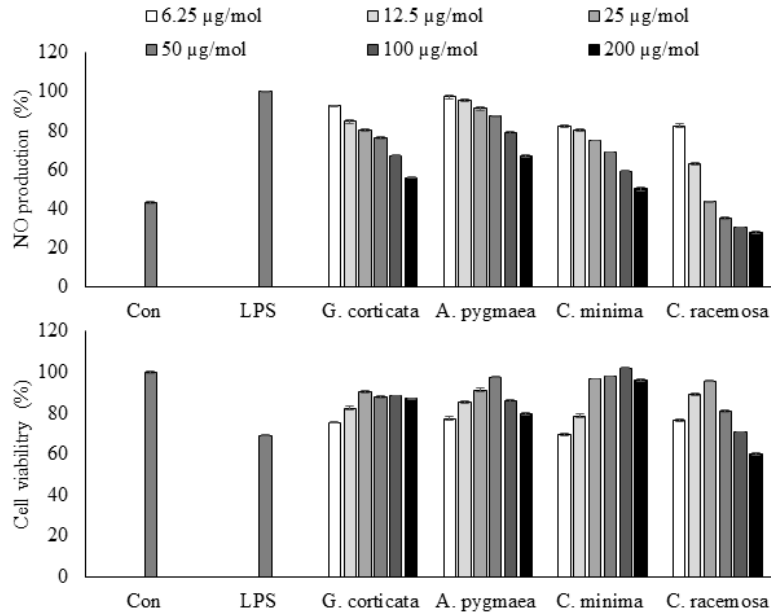
Fig. 24 Anti-inflammatory activity of 70% ethanol extracts of the selected algae. Evaluations were done as a measure of inhibition of NO production and its protective effects against LPS induced cytotoxicity in RAW 264.7 macrophages. RAW cells were pretreated with different sample concentrations and co-treated with LPS (1 µg/ml). After 24h, culture media was retrieved for the analysis of NO levels using Griess assay and MTT assay was adopted for the determination of cell viability. Experiments were carried out in triplicate, and the results are represented as means ± SD. Values are significantly different from the positive control (LPS treated group) at *P < 0.05 and **P < 0.001.

107

3.4. Anti-Cancer Effects

Anti-cancer activity was evaluated using the 70% ethanol extracts of the selected algae on HL-60 leukemia cell line and MCF-7 breast cancer cell line. Fig. 25 indicate that the 70% ethanol extract of *C. racemose* and *C. minima* are demonstrating potential anti-cancer effects compared to other extracts. The proportion of viable cells indicated a declining pattern with increasing sample concentrations. At 200 µg/ml, the cell viability of HL-60 cells reached to 60.32 % and 65.83% upon the consecutive treatment of *C. racemose* and *C. minima* ethanol extracts. The effects were less prominent in MCF-7 cells compared to that of HL-60. However, consecutive treatment of *C. racemose* and *C. minima* ethanol extracts reduced the cell viability of MCF-7 cells to 72.83% and 70.32 respectively thereby demonstrating anticancer effects.
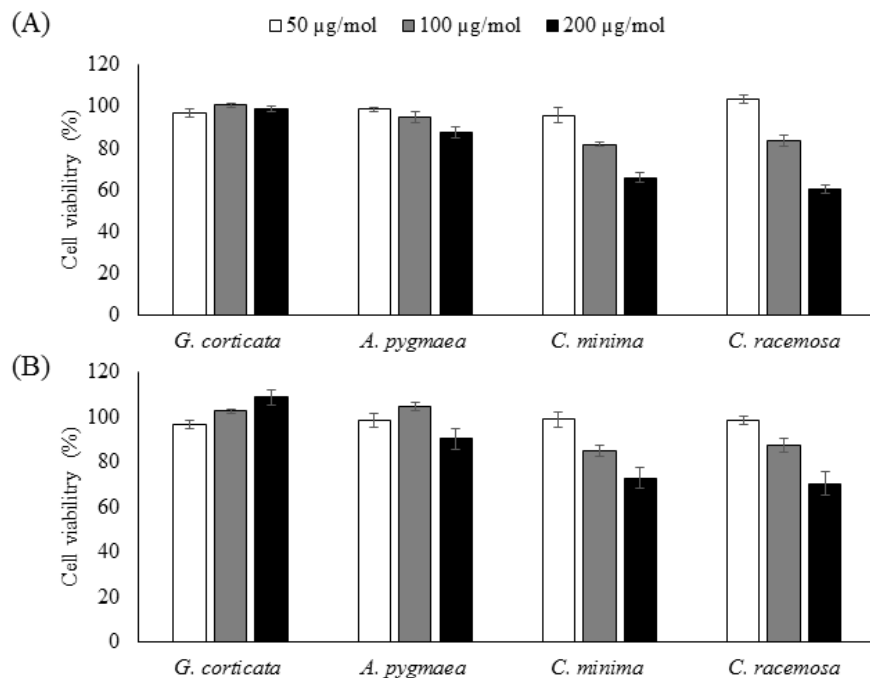
Fig. 25 Anti-cancer effects of the ethanolic extracts of four algae species. Evaluations were done against (A) HL-60 and (B) MCF-7 cell lines. The cells were seeded in 96 well culture plates and treated with different concentrations of samples. The viability of the cells was measured after 24h by MTT assay.

3.5. Yields of solvent fractions of the selected algae extracts and their chemical composition

The 70% ethanol extracts of *C. minima* and *C. racemose* were sequentially separated into solvent fractions, hexane, chloroform and ethyl acetate. Table 12 represent their yields and respective chemical composition. Among the fractions, hexane fraction of each alga indicated a higher yield with a higher content of sterols. The highest content of polyphenol was recorded from the ethyl acetate fraction of each algae extract. However, in both algae, the ethyl acetate fraction had the lowest yield.

Table 12 Yields and chemical composition of the solvent fractions of the selected algae extracts

Sample	Fraction	Yield (%)	Polyphenol content (%)	Sterol content (%)
C. racemose	CRH	53.00	0.11 ± 0.08	20.83
	CRC	19.75	0.25 ± 0.05	8.31
	CRE	4.12	0.96 ± 0.06	2.10
	CRW	16.33	0.62 ± 0.02	0.25
	CMH	48.72	0.82 ± 0.0	17.58
C. minima	CMC	21.52	0.88 ± 0.0	5.20
	CME	8.10	2.414 ± 1.32	1.88
	CMW	22.05	1.039 ± 0.44	0.11

Results represent mean ± S.D. of triplicate determinants

3.6. Free radical scavenging activity of the solvent fractions of selected algae

The free radical scavenging activity of the solvent fractions of selected algae was evaluated based on ESR spectroscopy (Table 13). The ethyl acetate fraction of each algae extracts indicated better free-radical scavenging ability towards all investigated experiments. The next best anti-oxidant activity was recorded from the water fraction of each algae extract.

3.7. Cytotoxicity of the obtained solvent fractions

Cytotoxicity of the solvent fractions was evaluated using the normal kidney cell line "Vero". As shown in Fig. 26 hexane, chloroform, and ethyl acetate solvent fractions of both *C. minima* and *C. racemose* indicated toxicity at higher concentrations (200 µg/ml). Hence, the concentrations of 100 µg/ml were selected for carrying out further experiments. However, the water fraction indicated increasing cell viability with increasing sample concentrations.

Table 13. Free radical scavenging activity of the solvent fractions.

Fraction	Free radical scavenging activity (mg/mL)		
	DPPH radical	Alkyl radical	Hydroxyl radical
CRH	>2	0.33 ± 0.04	0.82 ± 0.02
CRC	1.38 ± 0.43	0.22 ± 0.02	0.25 ± 0.02
CRE	0.76 ± 0.66	0.09 ± 0.01	0.05 ± 0.04
CRW	1.07 ± 0.61	0.12 ± 0.05	0.14 ± 0.04
CMH	>2	0.65 ± 0.32	0.52 ± 0.00
CMC	>2	0.57 ± 0.20	0.22 ± 0.04
CME	0.10 ± 0.02	0.16 ± 0.08	0.11 ± 0.04
CMW	0.21 ± 0.0	0.05 ± 0.01	0.12 ± 0.04

Results represent mean ± S.D. of triplicate determinants
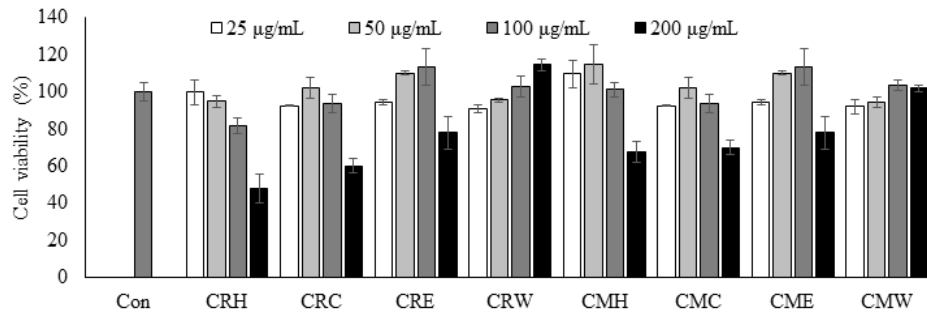
Fig. 26 Cytotoxicity of the solvent fractions. Vero cells were seeded in 96 well culture plates and treated with different concentrations of samples. The viability of the cells was measured after 24h by MTT assay.

3.8. Anti-inflammatory activity of the solvent fractions against LPS-induced NO production and protective effects against LPS-induced cytotoxicity.

Anti-inflammatory activity of the solvent fractions was evaluated using LPS-stimulated RAW macrophages. As indicated in Fig. 27, LPS-stimulation promptly increased the NO production causing a reduction in cell viability. Treatment of hexane and ethyl acetate fractions of both *C. minima* and *C. racemose* reduced the NO production levels while increasing RAW cell viability compared to the LPS-only group. Among the evaluated samples, CRE indicated the best potent anti-inflammatory activity and cytoprotective effects. However, due to the minor yield and lack of enough sample amount CRE could not be further purified to isolate pure compounds. Hence CRH that indicated potential anti-inflammatory effects was selected for further analysis due to the higher yield and available amount.
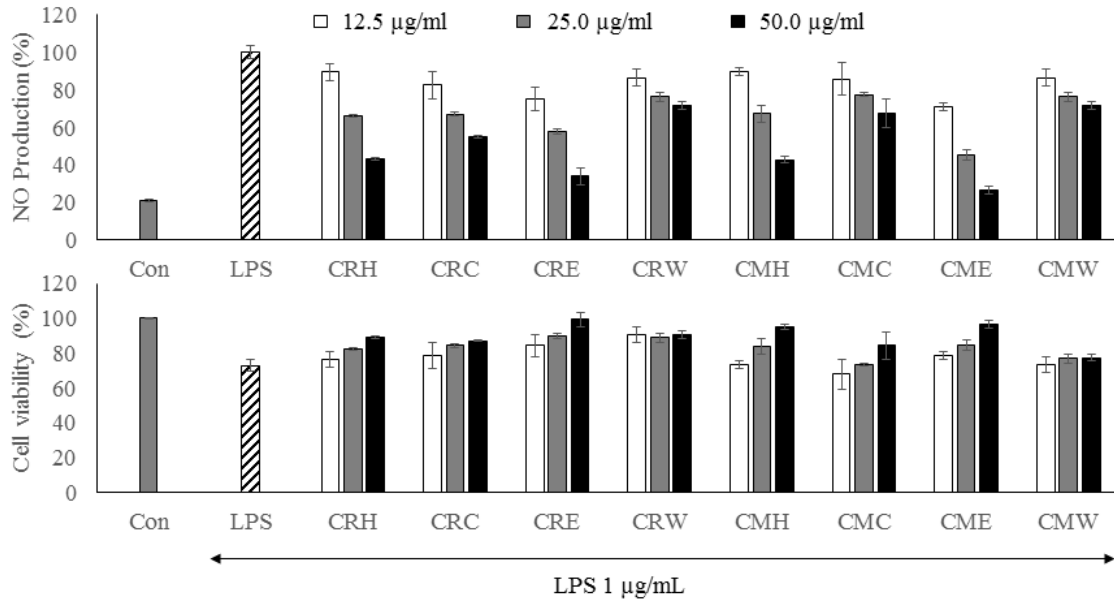
Fig. 27 Anti-inflammatory activity of the solvent fractions. Measurements were carried out to evaluate LPS-induced NO production and protective effects against LPS-induced cytotoxicity. RAW macrophages were seeded in 24 well culture plates and treated with different concentrations of samples and co-treated with LPS. After 24h the viability of the cells was measured by MTT assay, and the NO production was evaluated by the Griess assay.

116

3.9. Anti-cancer activity of the solvent fractions

Anticancer activity of the solvent fractions was assessed using HL-60 (human promyelocytic leukemia) and MCF-7 (human breast adenocarcinoma) cell lines (Fig. 28). Hexane and ethyl acetate fractions of both *C. minima* and *C. racemose* indicated potential anticancer properties upon both investigated cell lines causing an immediate reduction in the cell viability. However, as reported in the previous section, higher sample concentrations caused cytotoxic effects on normal cells. Hence, the concentrations of 100 µg/ml could be selected as safe for evaluation of their anti-cancer activity.
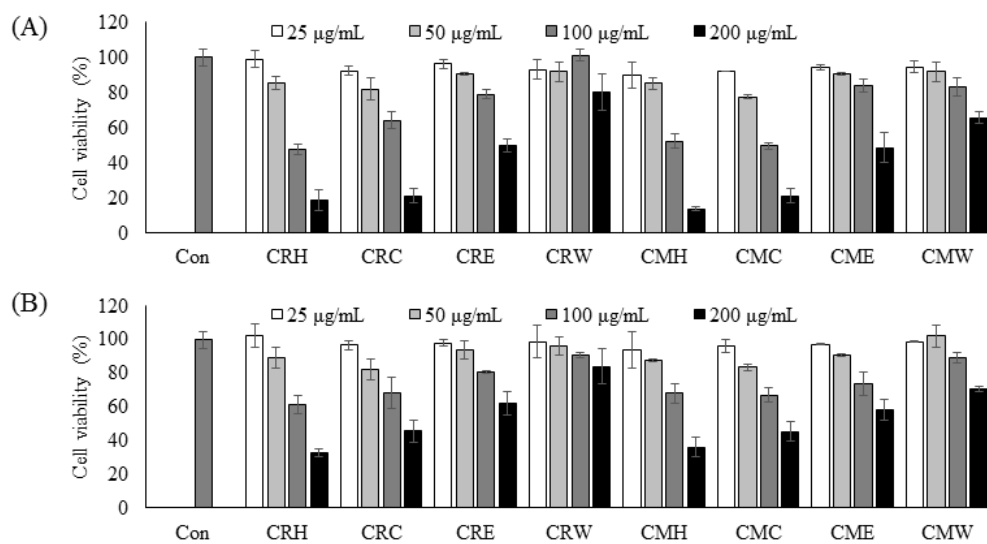
Fig. 28 Anti-cancer activity of the solvent fractions of C. racemose and C. minima 70% ethanol extracts. Against (A) HL-60 and (B) MCF-7 cancer cell lines. Cells were seeded in 96 well culture plates and treated with different concentrations of samples. The viability of the cells was measured after 24h by MTT assay.

3.10. Identification and purification of bioactive constituents

Chloroform and ethyl acetate fractions of the *C. minima* and *C. racemose* extracts were examined

via HPLC using a reverse phase column (Waters, SunFire, C18, 5µ, 4.6 x 250 mm) to resolve the

fractions to identify the distribution of chemical constituents according to polarity and to confirm

the separation efficiency of solvent/solvent fractionations. Fig 29 indicate the HPLC profiles of

the fractions above. However, identification of the compounds corresponding to each peak remains

unconcluded.
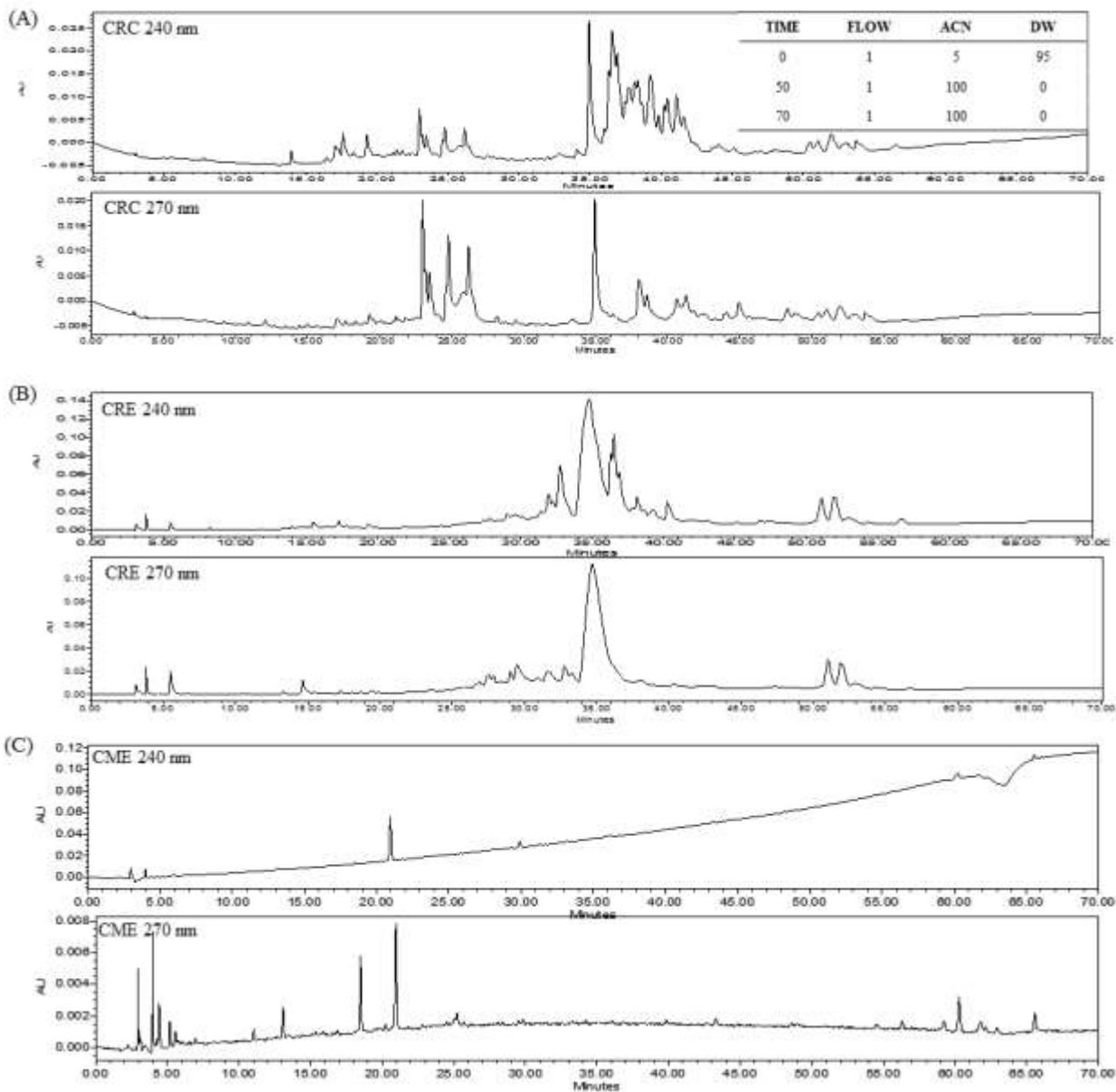
Fig. 29 HPLC analysis of the chloroform and ethyl acetate fractions from *C. minima* and *C. racemose*. Samples were prepared at a 5 mg/ml concentration in methanol and resolved by reverse phase HPLC column. The analysis was done using a PDA detector. (A) CRC, (B) CRE and (C) CME.

The Hexane and chloroform fractions of *C. minima* and *C. racemose* that indicated a higher sterol content were evaluated via GC-MS/MS analysis. Fig. 30 indicate the GC profiles of the tested fractions along with identified compounds. The results indicated the presence of Cholest-5-en-3-ol, 22,23-methylenecholestene-3B-ol and Stigmasta-5,24(28)-dien-3-ol in CMH and 22,23-methylenecholestene-3B-ol and Stigmasta-5,24(28)-dien-3-ol in CMC. However, CRH and CRC did not indicate gave a reliable GC-MS/MS profile. Nevertheless, further studies are in need to isolate and evaluate the functionality of these individual components.
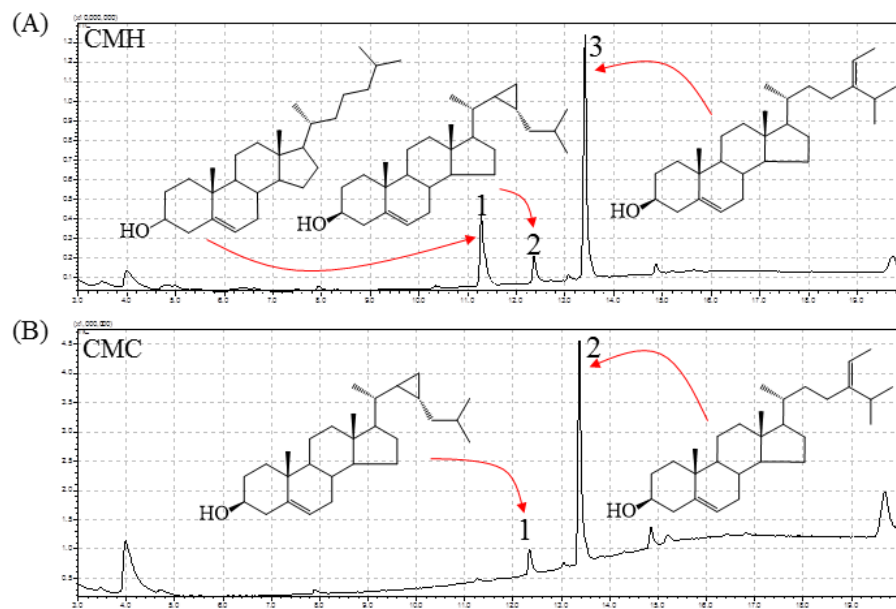
Fig. 30 GC-MS/MS analysis of the solvent fractions. (A) GC profile of CMH indicating ((A) 1) Cholest-5-en-3-ol, ((A) 2) 22,23-methylenecholestene-3B-ol and ((A) 3) Stigmasta-5,24(28)-dien-3-ol and (B) GC profile of CMC indicating ((B) 1) 22,23-methylenecholestene-3B-ol and ((B) 2) Stigmasta-5,24(28)-dien-3-ol.

122

3.11. Further purification of CRH using silica open column chromatography and preparative thin-layer-chromatography.

Based on the anti-inflammatory potential and comparatively higher yield, CRH was selected for further studies to isolate bioactive principals. Accordingly, two consecutive silica open column chromatographic purification steps were performed to resolve and purify the active fractions. Fig. 31 indicate the anti-inflammatory activity of the purified fractions in each step of the purification. Accordingly, the 20% ethyl acetate and 80% hexane eluate (CRHF1) indicated the best anti-inflammatory potential among the other eluates of the first open column. Further separation of the CRHF1 by second open column gave six consecutive fractions (Fig. 31 (B)) whereas the anti-inflammatory activity was prominent in CRHF1-F1. TLC analysis of the fractions indicated that CRHF1-F1 contain easily separable two major compounds. Hence, the compounds (C1 and C2) in CRHF1-F1 was isolated with the aid of PTLC (Fig. 31 (C)).
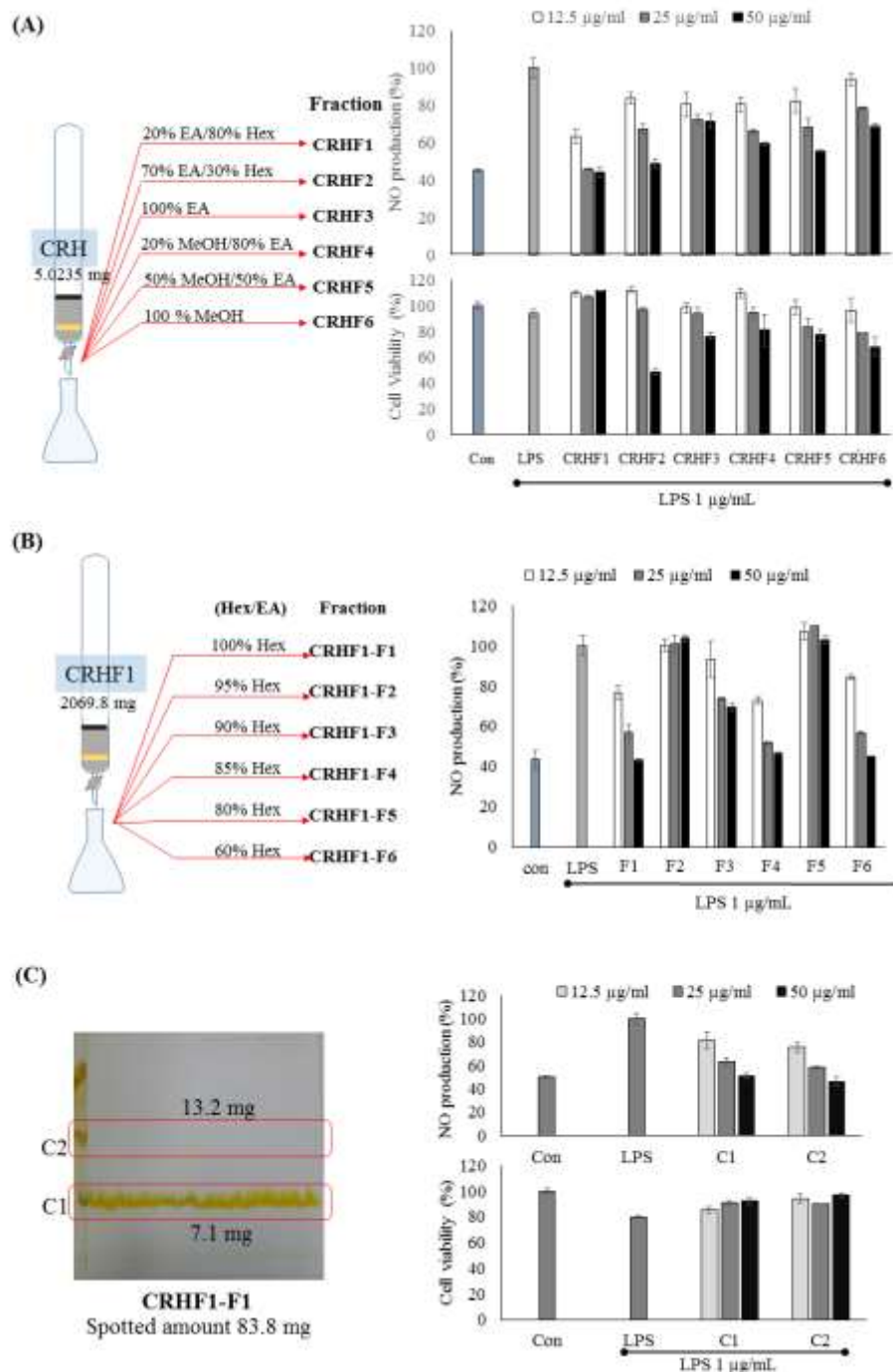
Fig. 31 Bioassay-guided purification of CRH. (A) First open column purification and anti-inflammatory activity of the column eluates, (B) Second open column purification and anti-inflammatory activity of the column eluates and (C) Isolation of compounds by PTLC.

124

3.12. Structural characterization of the isolated compounds by GC-MS/MS and NMR analysis

The molecular mass of the compound was evaluated using GC-MS/MS spectrum. Fig 32 represent the obtained GC chromatogram and the fragmentation pattern corresponding to the peak observed at 8.0 min. Based on the database search the compound was identified to be squalene with a similarity of 91%. Further, no other band was detected other than the peak corresponding to squalene in the GC spectrum confirming its purity.

Structural properties of the C1 and C2 were analyzed by NMR spectroscopy. Fig. 33 indicate the proton NMR of C1 and C2. The intense peak at 7.24 ppm represents chloroform. Accordingly, C2 resembles peak pattern of squalene. The Proton NMR signal of C1 is relatively weak (compared with the peak intensity of the solvent peak) when comparing with that of C2.

Fig. 34 represent the ^{13}C, DEPT, COSY and HMBC spectra of C2 all spectra indicate the characteristics that describe squalene.
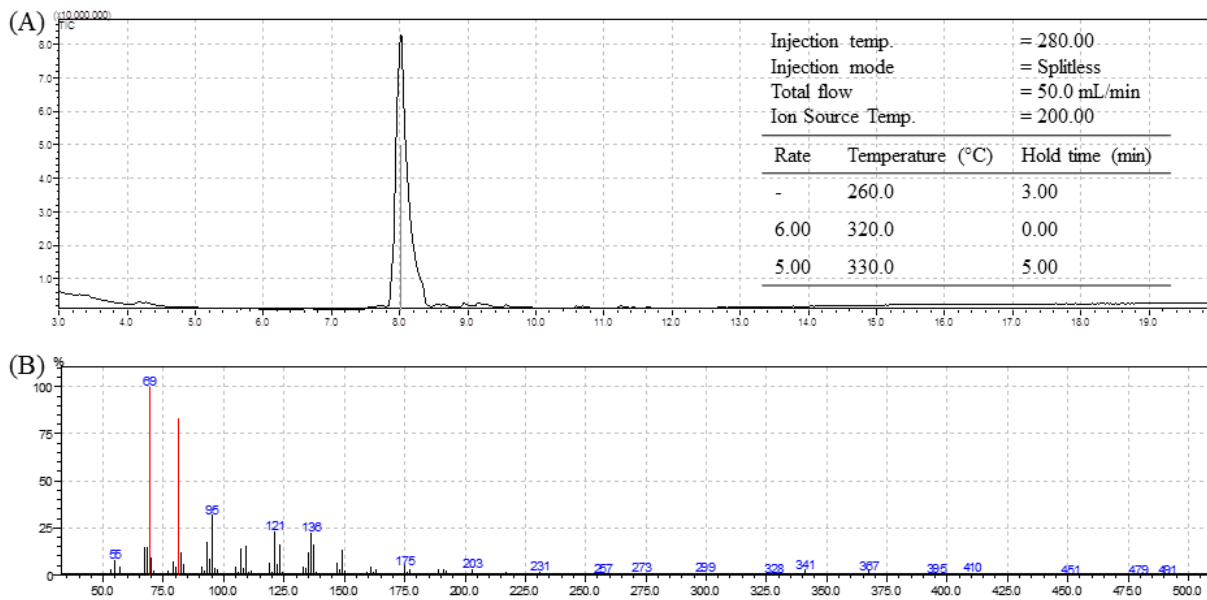
Fig. 32 GC-MS/MS analysis of the isolated compound C2
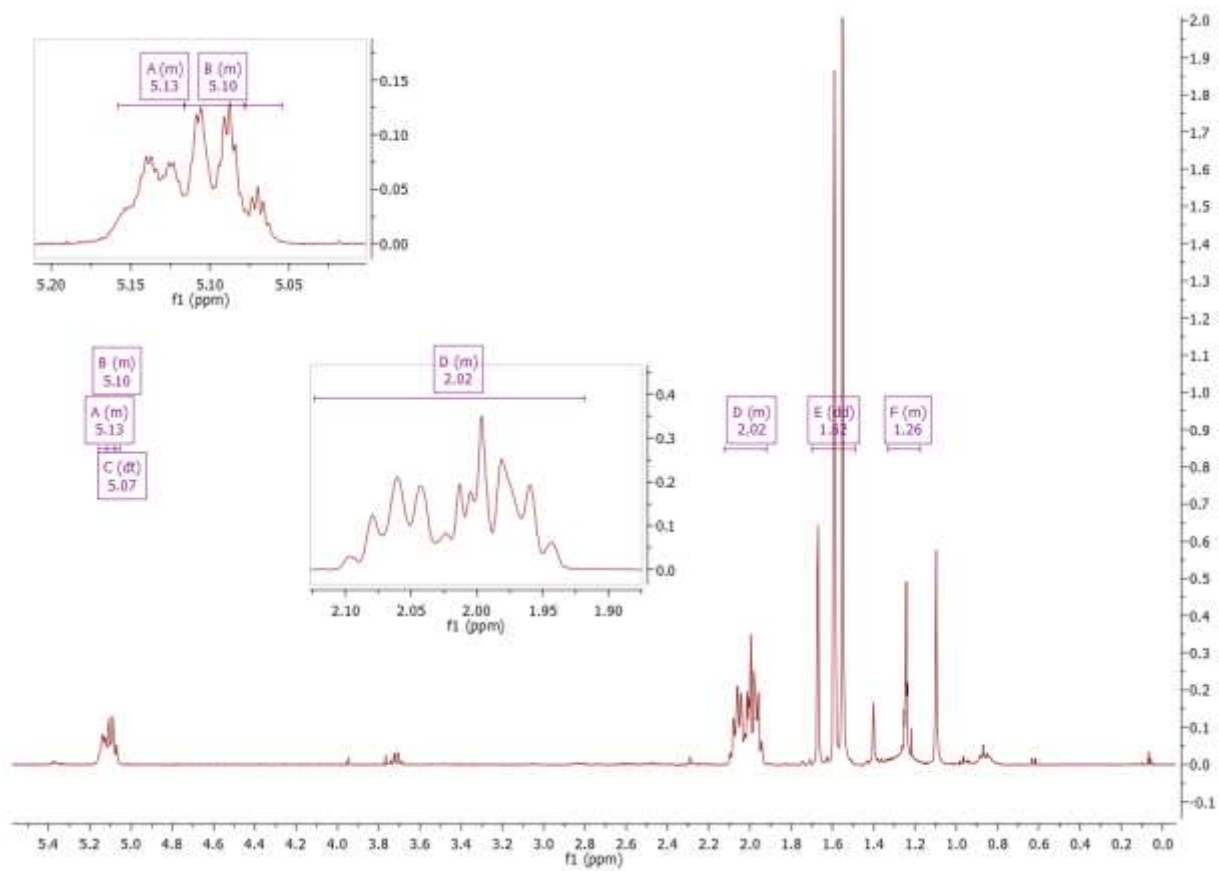
Fig. 33 Proton NMR spectra of C2.

(A)

(B)
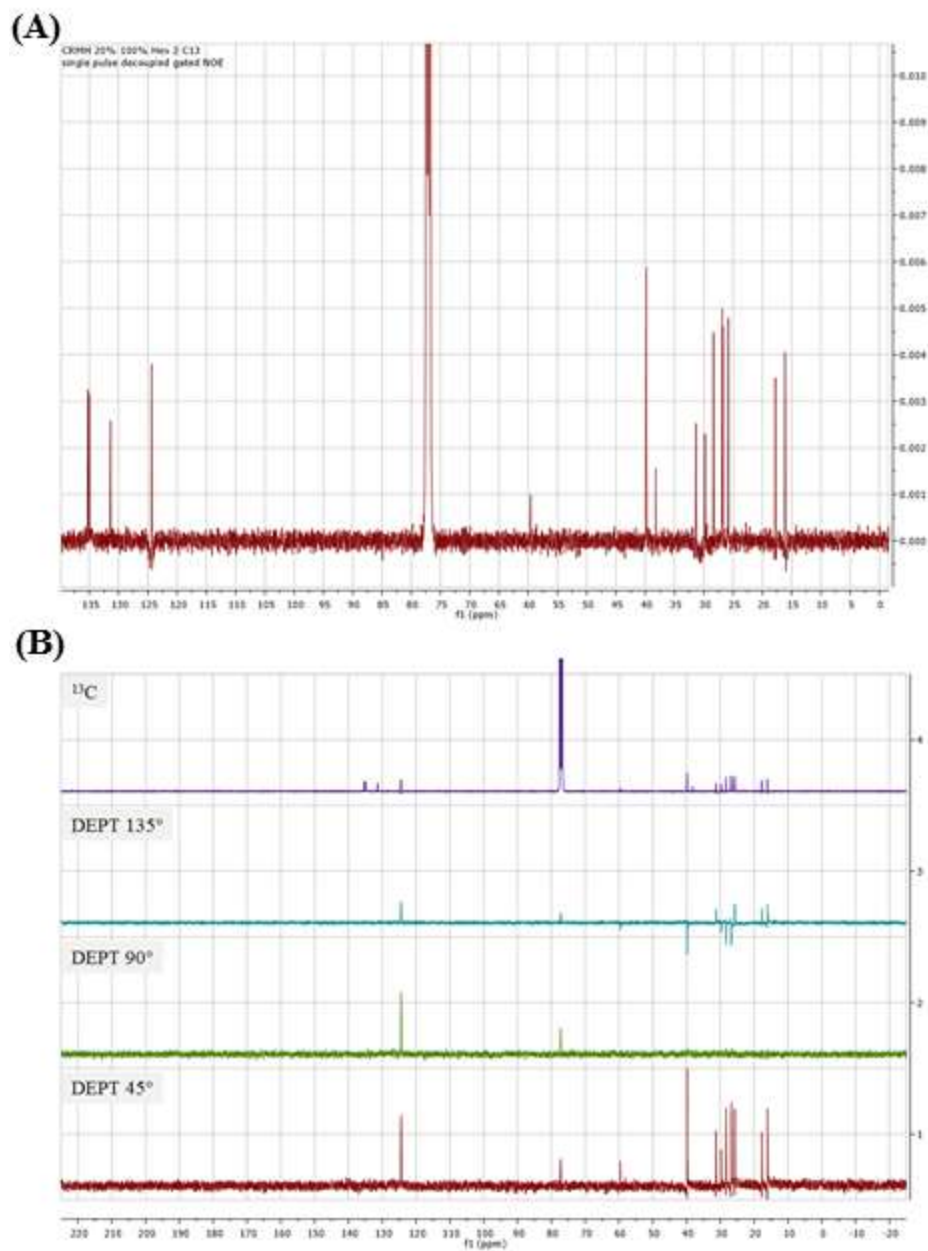
Fig. 34 1D NMR spectra of C2 (A) ^{13}C NMR spectrum and (B) DEPT spectrum

(A)

(B)
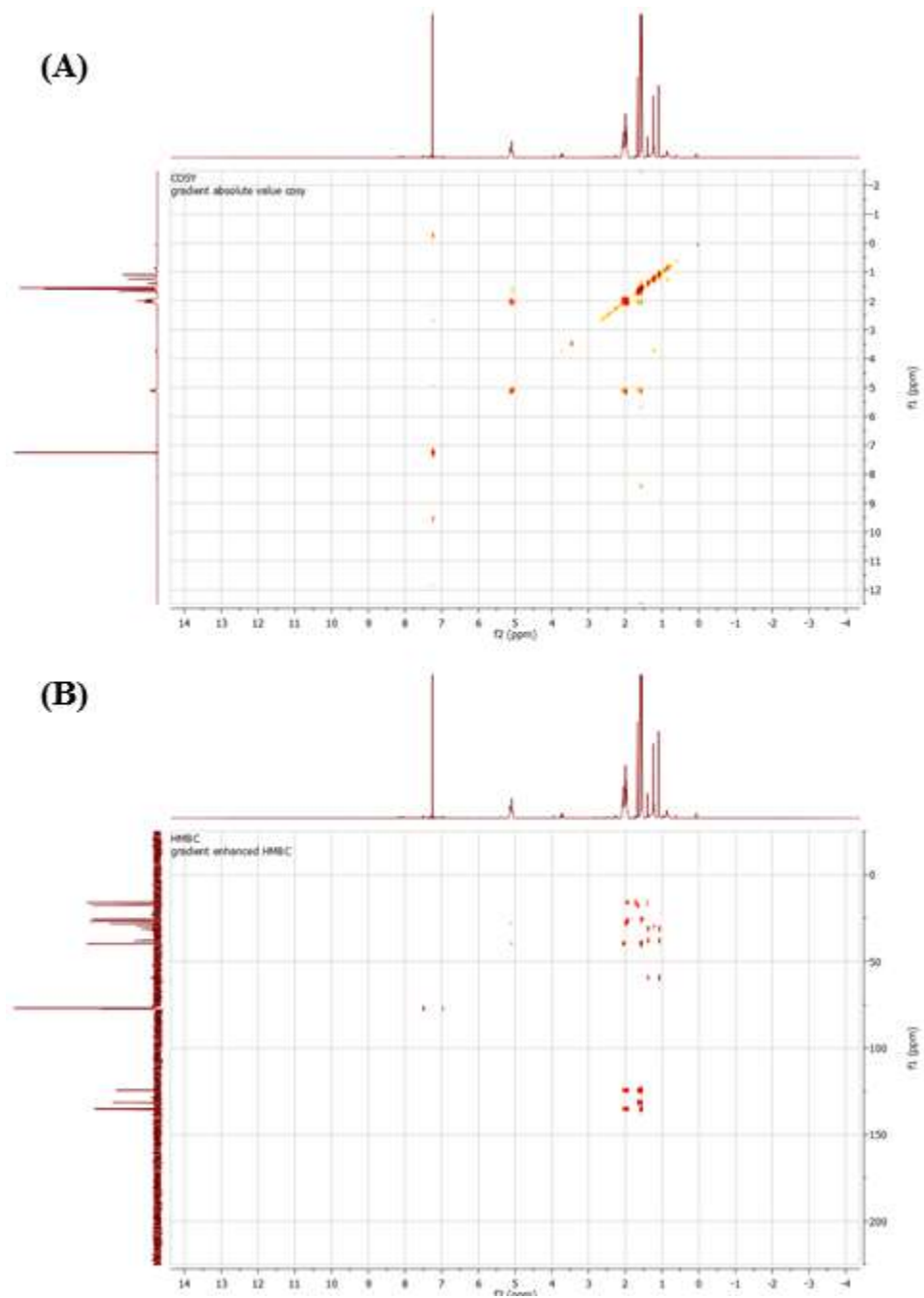
Fig. 35 2D NMR spectra of C2 (A) COSY spectrum and (B) HMBC spectrum

제주대학교 중앙도서관
JEJU NATIONAL UNIVERSITY LIBRARY

3.13. Squalene isolated from *C. racemose* could inhibit the inflammatory responses in RAW 264.7 murine macrophages via mediating protein expression.

Chronic inflammation is a detrimental pathological condition characterized by the upregulation of pro-inflammatory mediators that cause tissue destruction. Some immune cells including neutrophils, macrophages, and eosinophils are involved in the pathogenesis of inflammation through the production of inflammatory cytokines [53]. These inflammatory responses are mediated through a complex system of signaling pathways that regulate cellular responses [68, 69]. iNOS, COX-2, PGE_2 and proinflammatory cytokines such as TNF-α, IL1-β, and IL-6 are some of the key inflammatory mediators, which could be used to evaluate cellular responses and thereby anti-inflammatory activity of phytochemicals[68]. As evident from western blot analysis, (Fig. 36) treatment of squalene downregulated the LPS induced expression of iNOS and COX-2 in a dose-dependent manner. The down-regulation of iNOS expression successively results in the inhibition of NO production in RAW 264.7 macrophages. Prostaglandins, which are involved in causing a host of detrimental inflammatory responses eventually leads to tissue destruction [69]. Squalene could significantly reduce the PGE_2 production in LPS stimulated cells indicating a promising anti-inflammatory activity.
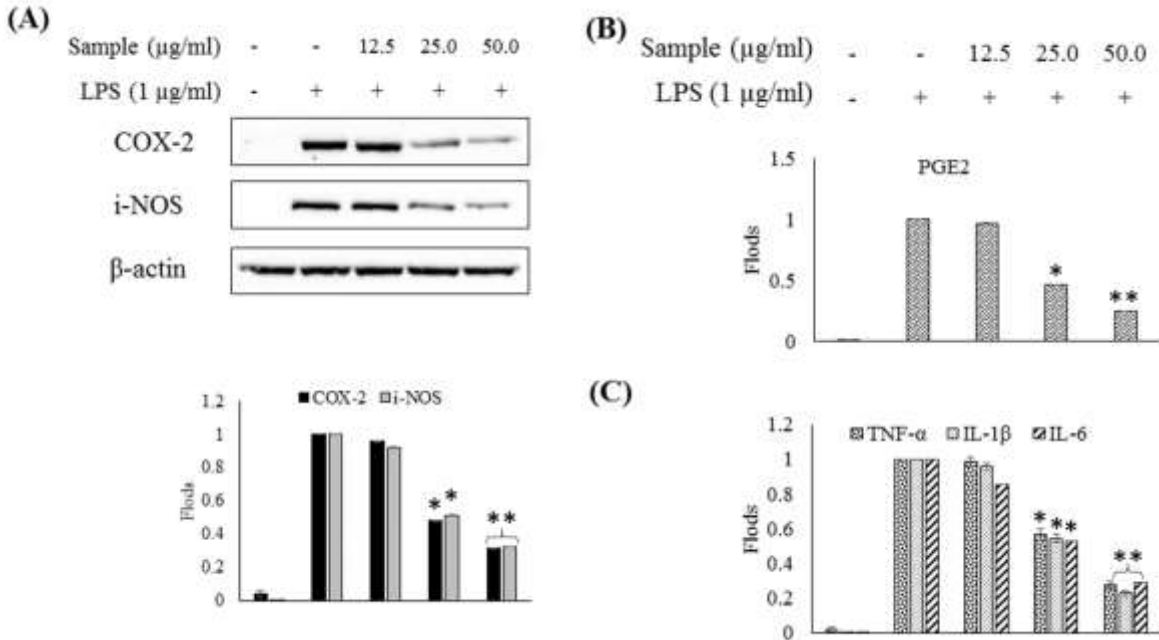
Fig. 36 Analysis of the expression levels of inflammatory regulators and pro-inflammatory cytokines. (A) Western blot analysis of the expression levels of iNOS and COX-2. Analysis of the downregulation of (B) PGE_2 and pro-inflammatory mediators including (C) TNF-α, IL1-β and IL-6 in LPS stimulated RAW 264.7 macrophages. RAW cells were pretreated with different concentrations of isolated squalene and co-treated with LPS (1 µg/ml). After 24h, culture media was retrieved for the analysis of PGE_2, TNF-α, IL1-β, and IL-6. Simultaneously the cells were harvested for the analysis of iNOS and COX-2 expression using western blot analysis. Experiments were carried out in triplicate, and the results are represented as means ± SD. Values are significantly different from the positive control (LPS treated group) at *P < 0.05 and **P < 0.001.

4. CONCLUSIONS

Investigating Marine natural products have received a special interest in recent years due to their fascinating structural diversity and functional properties. Marine algae represent one of the major organism in marine ecosystem (primary producers) that contribute to sustaining life in many marine organisms. Algae have extensively been studied for identifying bioactive natural products and have provided many important compounds with a broad range of biofunctional properties. Among them are the polyphenols, poly-unsaturated fatty acids, sterol derivatives, alkaloids, sulfated polysaccharides, and peptides. Current study reported the evaluation of biofunctional properties including, anti-oxidant, anti-inflammatory, and anti-cancer effects of 70% ethanol extracts of four different algae species including, *Ahnfeltiopsis pygmaea*, *Gracilaria corticata var. ramalinoides*, *Chnoospora minima* and *Caulerpa racemose*. Among the algae, extract of *C. minima* indicated better DPPH and Alkyl radical scavenging activity with comparatively higher polyphenolic content. The hydroxyl radical scavenging was higher in *C. racemose* ethanol extract. Based on the analysis of chemical composition ethanol extract of *C. racemose* indicated a higher sterol content.

Anti-inflammatory functionality evaluated via monitoring the inhibition of NO production in RAW 264.7 macrophages indicated that 70% ethanol extracts of C. racemose and C minima could strongly inhibit the NO production levels in a dose-dependent manner. Initially, the viability of RAW 264.7 macrophages increased with increasing concentrations of the samples. However higher concentrations of *C. racemose* indicated toxic effects on the cell viability. The same two extracts indicated potential anticancer activity on HL-60 and MCF-7 cells. Hence, these ethanol extracts were further purified by solvent/solvent fractionation. Evaluation of anti-inflammatory activity indicated that the hexane and ethyl ace fractions of the two algae ethanol extracts (CRH,

제주대학교 중앙도서관
JEJU NATIONAL UNIVERSITY LIBRARY

CRE, CMH, and CME) exhibit potential activity. Anti-cancer properties upon HL-60 and MCF-7 cells were prominent in the hexane and chloroform fractions. The selected CRH was further purified using open column chromatography and PTLC. The active constituent was identified as Squalene. Evaluation of their anti-inflammatory properties suggested that Squalene isolated from *C. racemose* could inhibit the inflammatory responses in RAW 264.7 murine macrophages via mediating protein expression. Squalene isolated from *C. racemose* have a broad range of anti-inflammatory potential expressing via suppressing the expression of iNOS, COX-2, PGE_2 and pro-inflammatory cytokines including TNF-α, IL-1β, and IL-6. These observations highlight the importance of exploring untapped marine algae bioresources in Sri Lanka.

Part II;

Natural products from Jeju soft corals

제주대학교 중앙도서관
JEJU NATIONAL UNIVERSITY LIBRARY

PART II;

NATURAL PRODUCTS FROM JEJU SOFT CORALS

SECTION 4

EXTRACTION, SCREENING, AND IDENTIFICATION OF ANTI-INFLAMMATORY ACTIVE PRINCIPALS.

ABSTRACT

Exploration of anti-inflammatory phytochemicals has received a tremendous importance worldwide with the rapid increases in inflammatory diseases. The current study reveals the identification of eight 3β-hydroxy-Δ5-steroidal congeners from a nonpolar column fraction of the ethanol solubles from the soft coral Dendronephthya gigantea collected from Jeju Island South Korea, using GC-MS/MS analysis. The sterol-rich fraction (DGEH21) indicated a prominent synergistic anti-inflammatory activity via inhibiting NO production (IC50 4.33 ± 0.50 µg/ml) and PGE$_2$ production in LPS-stimulated RAW 264.7 macrophages and dose-dependently suppressed the expression levels of proinflammatory cytokines, TNF-α, IL-1β, and IL-6. Further DGEH21 effectively reduced NO and ROS production as well as cell death in LPS-stimulated in-vivo zebrafish embryo model. However, DGEH21 indicated cytotoxicity at relatively high concentrations on both RAW cells and zebrafish embryos (RAW cell viability was nearly 80% at 25 µg/ml). This disclosure highlights the synergistic significance of several steroids from the soft coral D. gigantea that possess the potential to develop cosmeceuticals, pharmaceutical agents, and functional ingredients to counteract inflammation in consumer products.

1. INTRODUCTION

Corals (Anthozoans) are the most dominant benthic invertebrates that inhabit tropical seas accounting for over 6100 species diversity with distribution throughout the world [86]. They are amongst the marine organisms enriched with a unique set of bioactive secondary metabolites. A variety of terpenoid metabolites, some with novel structural properties, oxylipin derivatives, and fatty acids have been discovered from soft corals [6, 87]. However, much of these steroids have shown cytotoxic properties and have identified as potential tumor-inhibitory agents [88]. Soft corals belong to the genus *Dendronephthya* encompasses nearly 248 species and are highly prolific and widely distributed throughout the Indian Ocean, the Red Sea, Pacific Ocean and Southeast Asia [6]. They have the ability to synthesize and store toxic secondary metabolites as a defensive strategy. These metabolites function as antipredatory, allelopathy, antimicrobial and antifouling agents [89]. Some studies reveal the identification of anti-inflammatory sterols from soft corals which could reduce the expression levels of iNOS and COX-2 proteins involved in manifesting inflammatory responses in LPS stimulated RAW 264.7 macrophage cells [90-92]. A comprehensive review about marine sterols published in 1993 claims the discovery of more than 200 different types of monohydroxysterols from marine organisms [7]. Steroids, in particularly glucocorticosteroids are highly efficient in controlling cytokine- mediated inflammation through inhibiting the transcription of cytokines related to chronic inflammation, including inter-leukin-1 (IL-1), IL-3, IL-4, IL-5, IL-6, IL-8 TNF-α, and granulocyte-macrophage-colony-stimulating factor (GM-CSF) [93]. Moreover, the inhibitory effects of steroids on inflammatory mediators such as leukotrienes, prostaglandins, and plate- let-activating factor may also contribute to their anti-inflammatory effects [94]. In an era where inflammatory diseases have become one of the major

concern throughout the world, identification of natural biofunctional metabolites could provide a solution and broaden research perspectives for the development of potential pharmaceuticals.

2. MATERIALS AND METHODS

RAW 264.7 macrophages were purchased from the Korean Cell Line Bank (KCLB, Seoul, Korea). Adult experimental zebrafish were purchased from a commercial fish trader South Korea. Dulbecco's modified Eagle's medium (DMEM), fetal bovine serum (FBS) and penicillin/streptomycin mixture were purchased from GIBCO INC. (NY, USA). 2′,7′-2′ 7′-dichlorodihydrofluorescein diacetate (DCFH2-DA), acridine orange, and 3-(4,5-dimethylthiazol-2-yl)-2,5-diphenyltetrazolium bromide (MTT) were purchased from Sigma, Aldrich, USA. iNOS, COX-2, and β-actin antibodies were purchased from Santa Cruz Biotechnology (USA). Commercial ELISA kits including Mouse IL-1beta, Mouse IL-6, TNF-α, and PGE$_2$ were purchased from eBioscience, Inc. (USA), BD Biosciences (USA), and R&D Systems, Inc. All the organic solvents used in extraction and fractionation were of analytical grade.

2.1. Sample collection, identification, and extraction

Soft coral samples, *Dendronephthya gigantea*, *Dendronephthya spinulosa*, *Dendronephthya puetteri*, *Dendronephthya castanea*, *Dendronephthya aurea*, *Dendronephthya suensoni*, *Scleronephthya gracillimum*, *Chromonephthea hirotai*, *Dendronephthya SP1* and *Dendronephthya SP2* were harvested at a depth of 10-15 m from Jeju sea, South Korea. The samples were identified at the Jeju Biodiversity Research Institute based on their morphological characteristics and the repositories were kept at the Laboratory of Marine Bioresource Technology

제주대학교 중앙도서관
JEJU NATIONAL UNIVERSITY LIBRARY

at Jeju National University. Collected samples were surface sterilized using 70% ethanol, washed carefully with tap water to remove attached debris and other organisms. Then the specimens were cut into small pieces and frozen under -40°C. The samples were then lyophilized and powdered. Each 20.00 g of the sample powder was separately extracted using 70% ethanol at 25°C under continuous agitation for 24h. The extract was obtained by filtration under vacuum. Extraction was performed for three times. The sample extracts were concentrated using a rotary evaporator under 35°C to obtain the crude extract. During the second phase of sample extraction, 6.00 kg of the selected *Dendronephthya gigantea* dry powder was used to obtain the 70% ethanol extract following the same method as mentioned above.

2.2. Solvent/solvent fractionation and further purification

The crude extract was homogenized in distilled water and respectively fractionated between hexane, chloroform, and ethyl acetate. The solvents were removed under vacuum. The selected hexane fraction indicating anti-inflammatory activity was further purified using a silica open column eluting with a gradient of hexane and ethyl acetate in order 100% H, 80% H + 20 % EA, 50% H + 50% EA, 100% EA. The solvent in each eluate was removed under vacuum. The selected fraction 80% H +20% EA was further purified using a silica open column using a gradient of hexane and ethyl acetate in order 95% H + 5% EA, 85% H + 15% EA and 80% H + 20% EA respectively. Again the solvents were removed under vacuum. Each step of purification was monitored using TLC, observing under UV and with 10% H_2SO_4 in ethanol staining. The extraction and purification methods are summarized in Fig. 40 with the relevant abbreviations.

2.3. GC-MS/MS analysis

The selected column eluate (DGEH21') which indicated the best anti-inflammatory properties was subjected to GC-MS/MS analysis using a Shimadzu GCMS-TQ8040 system (Japan) equipped with a Rtx-5MS fused-silica capillary column (30.0mx0.25mm i.d. 0.25µm). The iron source temperature 200°C, scan range 50-500 m/z, GC oven program; 260°C, 3 min, 6°C/min to 320°C, 5°C/min to 330°C, 2 min. Helium was used as the carrier gas at a constant flow rate of 0.73 ml/min. The sample was injected by splitless mode.

2.4. Analysis of the Proximate composition

Analysis of the Proximate composition of the constituents of the samples was performed adhering to the AOAC 2005 specifications [27]. This includes the evaluation of polysaccharide, protein and polyphenol content. Accordingly, the ash content was evaluated by dry ashing in a muffle furnace at 550°C for 6h, the levels of polysaccharide were evaluated according to the phenol-sulfuric method, protein content by the Kjeldahl method, and lipid content by soxhlet extraction. The mineral content of the specimens was examined using an Optima 7300 DV inductively coupled plasma atomic emission spectroscopy (ICP-OES) system (PerkinElmer, USA) [60]. The sterol content was measured by the Liebermann-Burchard method as described by Xiong et al. [95]. Cholesterol was used as the calibration standard.

2.5. Cell culture

RAW 264.7 mouse macrophage cells were maintained in DMEM supplemented with 10% FBS and 1% antibiotic (100 µg mL-1 penicillin, 100 µg mL-1 of streptomycin) at 37°C under a humidified atmosphere with 5% CO_2 with the periodical subculture. Cells under exponential

growth were seeded for experiments at 1×10^4 cells/ml concentration in 24 well culture plates. Sample treatment was done at different sample concentrations, 24h after the cell seeding. After 1h LPS was introduced into each well (1 µg/ml). Griess assay was used to evaluate the LPS induced NO production, and MTT assay was adopted to assess the cell viability [96].

2.6. Western blot analysis

Seeded RAW cells 24h after sample treatment were harvested, lysed using lysis buffer and centrifuged at 16000 rpm to clear up the cellular debris. SDSPAGE was done with a sample loading of 30µg of proteins. The protein bands were blotted onto a nitrocellulose membrane. The nonspecific binding sites were blocked using skim milk. The membranes were incubated with respective 1^{ry} (4°C for 8h) and 2^{ry} (room temperature for 2h) antibodies. Excess nonbound antibodies were removed by washing with Tris-buffered saline with Tween 20. Signals were developed by adding chemiluminescent substrate (Cyanagen Srl, Bologna, Italy) [84]. Fluoresce images were taken using a FUSION SOLO Vilber Lourmat system (Paris, France). The band intensities were quantified using Image J program.

2.7. Evaluation of PGE₂ and pro-inflammatory cytokine production

Culture media from RAW cells were separately collected 24h after the sample treatment. They were then used to measure the PGE₂ level and proinflammatory cytokine (TNF-α, IL-1β, IL-6) production. Experiments were done using commercial enzyme immunoassay kits, following manufacturer's instructions.

제주대학교 중앙도서관
JEJU NATIONAL UNIVERSITY LIBRARY

2.8. Statistical analysis

All the data values are expressed as mean ± SD based on at least three independent experiments. Statistical analysis for comparing the data was performed using IBM SPSS Statistics 20 software using one-way ANOVA by Duncan's multiple range test (DMRT). P-values less than 0.05 ($P < 0.05$) were considered as significant.

3. RESULTS AND DISCUSSION

3.1. Proximate chemical composition of the specimens

Table 14 represent the proximate composition of the samples. Accordingly, all samples contained a comparatively higher amount of ash than other constituents. This relates to the fact that soft corals have a calcified structure. Highest ash content was seen in *D. puetteri* and *D. castanea* samples. Next, to its ash content, samples were rich in proteins. Low levels of lipids were also present in the extracts.

3.2. Mineral composition indicated high levels of Ca^{2+}

Table 15 reports the mineral content of the soft coral specimens. The samples indicated a higher amount of Ca^{2+} with the presence of Na^+ and Mg^{2+}. The highest Ca^{2+} amount was recorded from *D. spinulosa*. These observations relate to the large amount of ash content observed during the compositional analysis.

Table 14. Proximate chemical composition of the soft coral specimens

No.	Species	Ash (%)	Lipids (%)	Protein (%)
SC1	*Dendronephthya gigantea*	69.04 ± 0.63	1.21±0.01	15.87 ± 0.51
SC2	*Dendronephthya spinulosa*	66.41 ± 0.33	0.89±0.00	17.92 ± 0.82
SC3	*Dendronephthya puetteri*	78.74 ± 0.71	1.08±0.02	12.54 ± 0.82
SC4	*Dendronephthya castanea*	78.14 ± 0.18	1.20±0.00	11.84 ± 1.35
SC5	*Dendronephthya aurea*	66.11 ± 0.83	1.07±0.00	27.75 ± 2.45
SC6	*Dendronephthya suensoni*	66.58 ± 0.04	1.27±0.03	17.05 ± 1.23
SC7	*Scleronephthya gracillimum*	69.17 ± 0.26	1.13±0.09	22.44 ± 1.23
SC8	*Chromonephthea hirotai*	68.71 ± 0.80	1.26±0.08	22.37 ± 0.00
SC9	*Dendronephthya SP1*	67.29 ± 0.36	0.80±0.02	21.04 ± 0.47
SC10	*Dendronephthya SP2*	64.82 ± 0.18	0.93±0.05	16.18 ± 0.00

Results represent mean ± standard deviation of at least triplicate determinations.

Table 15. Mineral composition of the soft coral specimens

Sample	Mineral composition (ppm)													
	Ca	Na	Mg	As	K	Sr	Al	Ni	Cr	Mn	V	Ba	Cd	Fe
SC1	255503.40	34843.47	31389.26	4129.49	3616.32	2987.32	1072.08	348.00	236.63	52.00	44.45	27.40	18.00	0.00
SC2	330417.20	39215.94	40398.54	1602.64	4439.26	4083.56	1995.19	722.31	137.57	32.23	44.59	99.16	73.48	0.00
SC3	302933.10	35566.63	38134.62	3587.90	6824.68	3788.19	1866.98	820.08	232.64	73.22	157.94	57.52	40.47	20727.16
SC4	234294.60	65557.98	36729.06	4015.98	6001.60	2932.95	1083.36	497.97	192.39	14.72	348.11	203.73	63.23	0.00
SC5	237805.00	54534.21	34792.20	2352.85	5954.20	3062.33	1016.71	588.40	560.88	58.53	0.00	121.74	73.60	4188.85
SC6	297374.50	37192.56	35911.08	2005.11	4843.84	3868.06	1689.36	652.37	295.00	37.28	99.98	45.91	117.64	0.00
SC7	291630.40	43895.15	36677.10	2705.08	4671.20	3767.91	2187.46	776.37	245.31	85.12	264.30	608.41	0.00	0.00
SC8	216832.30	15544.28	26136.73	0.00	2428.31	1507.68	600.35	0.00	27.35	6.48	5.53	7.98	0.00	229.53
SC9	214712.99	20247.26	27528.85	0.00	1917.50	1427.93	625.07	2.01	18.67	4.97	0.00	15.10	2.54	162.70
SC10	188847.89	25916.01	25470.92	0.00	2322.89	1341.60	567.88	0.41	14.54	6.49	3.64	5.20	0.19	191.16

3.3. Extraction yields and chemical composition of the soft coral ethanolic extracts

Table 16 shows the extraction yields and sterol composition of the soft coral ethanolic extracts. Accordingly, *D. gigantea* gave a higher yield (38.70±1.54 %) compared to the others.

3.4. Anti-inflammatory activity of soft coral ethanol extracts

Anti-inflammatory activity of 70% ethanol extracts of the ten soft coral samples is shown in Fig. 37. Accordingly, SC1E, SC3E, SC5E, SC7E, and SC8E were selected to be active for anti-inflammatory functionality.

Table 16. Extraction yields and chemical composition of the soft coral ethanolic extracts

Ethanol extract	Yield (%)	Sterol (%)
SC1E	38.70±1.54	0.22 ± 0.00
SC2E	17.35±0.92	0.37 ± 0.00
SC3E	12.35±1.82	0.37 ± 0.10
SC4E	22.14±0.75	0.37 ± 0.10
SC5E	11.32±1.58	0.22 ± 0.00
SC6E	11.23±0.68	0.22 ± 0.00
SC7E	14.54±1.60	0.68 ± 0.15
SC8E	15.29±0.98	0.47 ± 0.05
SC9E	8.68±2.06	0.30 ± 0.10
SC10E	18.25±1.63	0.30 ± 0.00

Results represent the mean ± standard deviation of at least triplicate determinations.
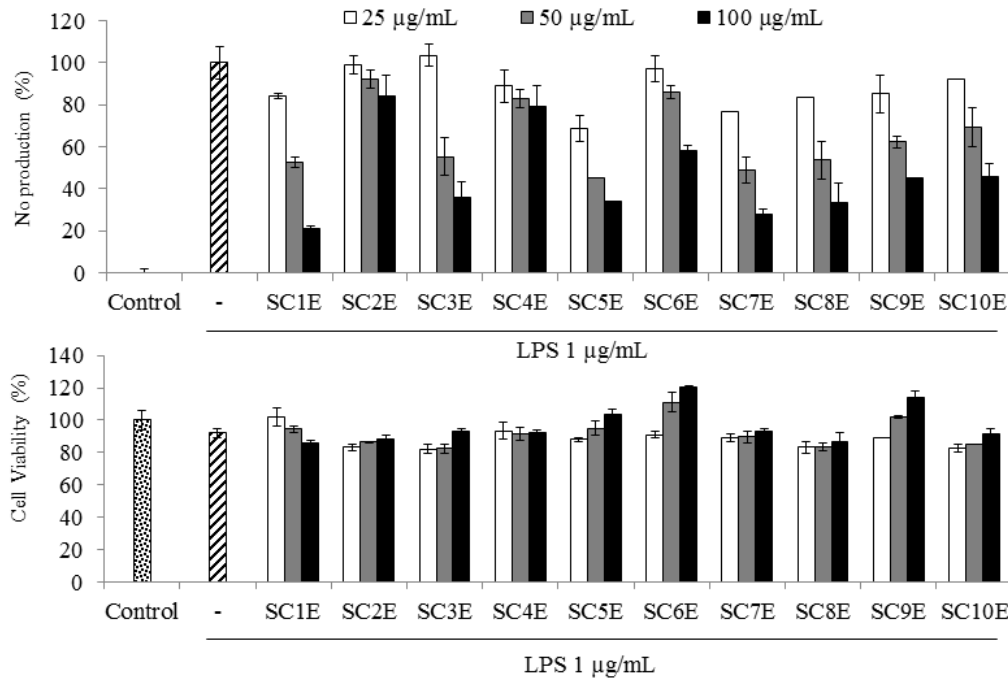
Fig. 37 Anti-inflammatory activity of soft coral ethanol extracts. Evaluations were done on the inhibition of NO production in LPS-stimulated RAW macrophages. RAW cells were pretreated with different sample concentrations and co-treated with LPS (1 µg/ml). After 24h, culture media was retrieved for the analysis of NO levels using Griess assay and MTT assay was adopted for the determination of cell viability. Experiments were carried out in triplicate, and the results are represented as means ± SD. Values are significantly different from the positive control (LPS treated group) at *P < 0.05 and **P < 0.001.

제주대학교 중앙도서관
JEJU NATIONAL UNIVERSITY LIBRARY

3.5. Mediation of anti-inflammatory activity in LPS-stimulated RAW macrophages

The selected fractions were further analyzed for their anti-inflammatory functionality by evaluating the expression levels of iNOS and COX-2 expression levels by western blot analysis and PGE_2 level by cytokine kit (Fig. 38). All three inflammatory mediators indicated downregulation of their expression levels with increasing sample concentrations. Moreover, the expression levels of pro-inflammatory cytokines, including TNF-α, IL-1β, and IL-6 indicated to be downregulated with increasing sample concentrations. These effects indicated a desirable and a broad range of anti-inflammatory functionality in RAW cells.
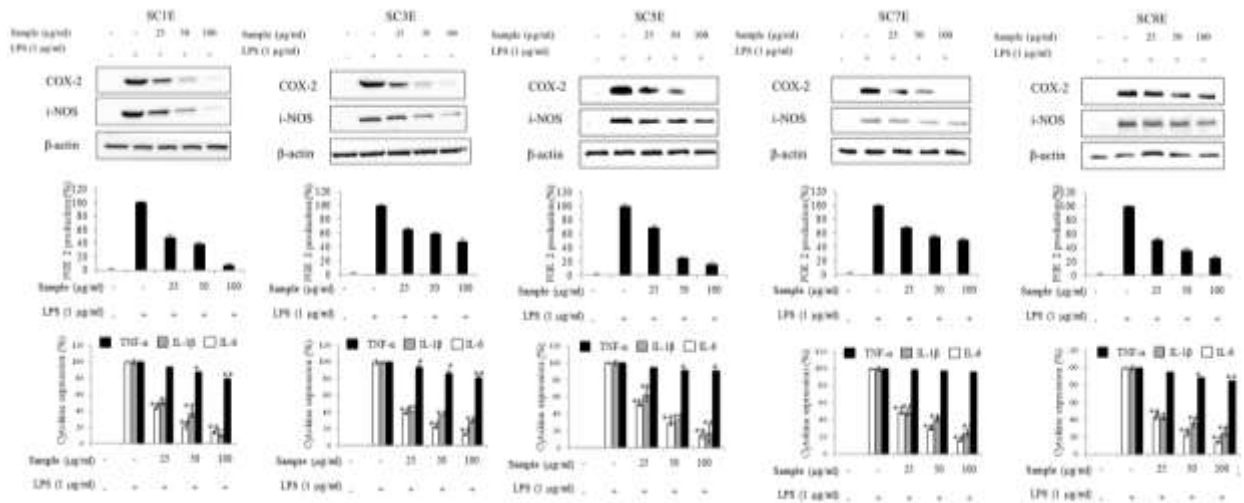
Fig. 38 The ability of the soft coral extracts to reduce the inflammatory responses in RAW cytokines. RAW cells were pretreated with different sample concentrations and co-treated with LPS (1 µg/ml). After 24h, culture media was retrieved for the analysis of cytokine levels and the cells were harvested for the analysis of the expression levels of proteins. Experiments were carried out in triplicate, and the results are represented as means ± SD. Values are significantly different from the positive control (LPS treated group) at *P < 0.05 and **P < 0.001.

3.6. Large-scale extraction, solvent/solvent fractionation, and chromatographic purification processes

Fig. 39 graphically represents the extraction and initial purification processes that include solvent/solvent fractionation and first open column chromatographic process with respective yield percentage obtained at each step. Yields of the solvent/solvent fractionation indicated the accumulation of a higher yield of constituents in the aqueous fraction. The constituents accumulated in the aqueous fraction could be mainly minerals and other polar substituents. However, the hexane solvent fraction (DGEH) was selected for further purification based on its anti-inflammatory activity. Accordingly, the 1st open column purification yielded in 4 column eluates with the targeted activity centered in the 80% hexane/20% ethyl acetate eluate (DGEH2).
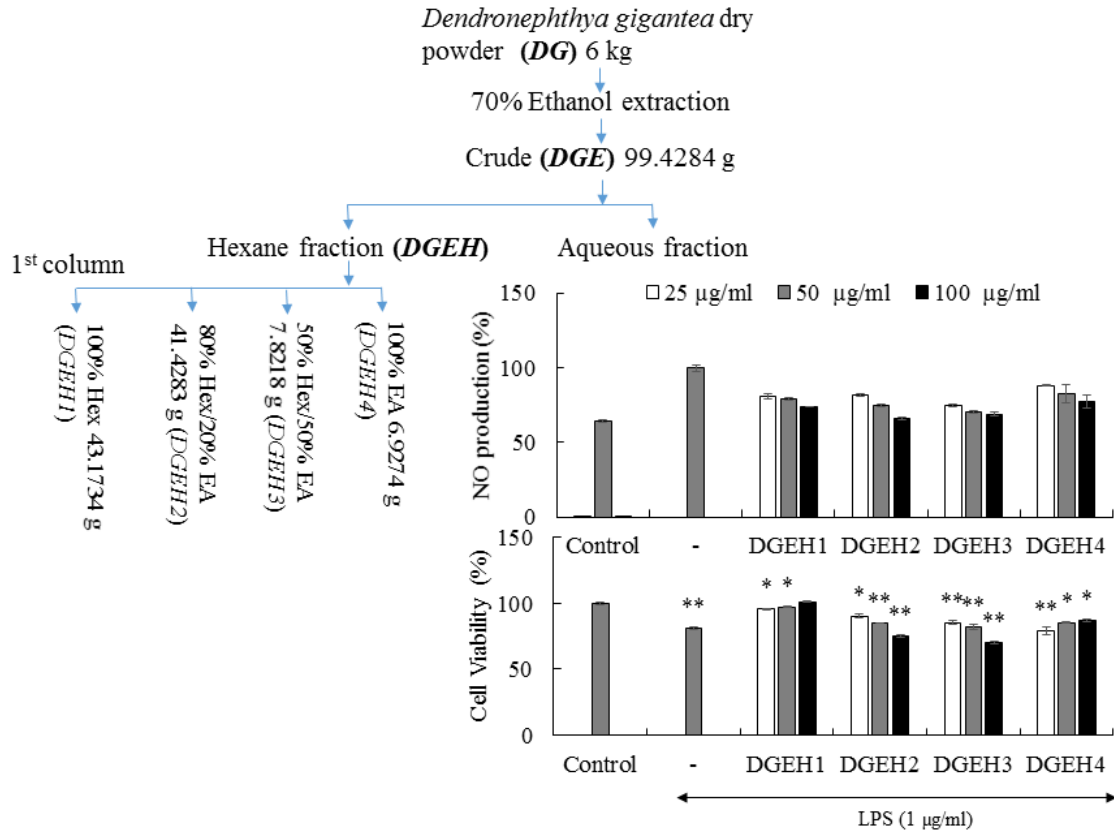
Fig. 39 The purification procedure for the 70% ethanol solubles of the soft coral *D. gigantea*. Illustrating the solvent/solvent fractionation and the first silica open column purification step. The eluates of the first open column were analyzed for its anti-inflammatory activity as a measure of reduction of NO levels in LPS-induced RAW macrophages.

As shown in Fig. 40, the consecutive 2nd open column purification of DGEH2 yielded in 3 eluates with the targeted active column fraction centered in the 95% hexane /5% ethyl acetate eluate (DGEH21'). TLC visualization of DGEH2 before and after the purification by 2nd open column comparatively clarifies the separation processes. The dark maroon (almost black) color spot observed after heating the TLC plate stained with 10% H_2SO_4 in ethanol indicates steroids. These features are evident in DGEH21'suggesting the presence of steroids.
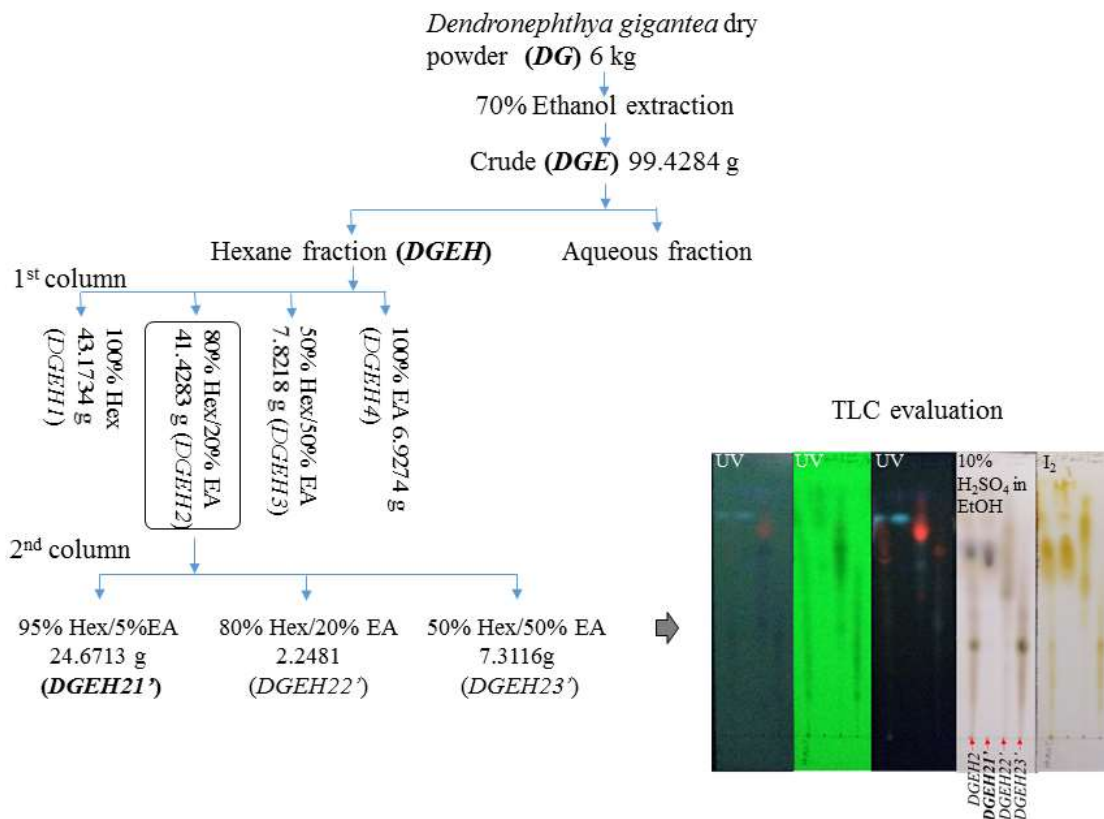
Fig. 40 The purification procedure for the 70% ethanol solubles of the soft coral *D. gigantea*. Illustrating the solvent/solvent fractionation and the first silica open column purification step. The eluates obtained from the second open column was evaluated for its separation efficiency using TLC visualization methods respectively by using UV, 10% H2SO4 in ethanol and by Iodine vapor.

3.7. Characterization of chemical constituents in DGEH21'

Chemical constituents in DGEH21', DGEH22' and DGEH23' responsible for the observed anti-inflammatory activity was determined using GC-MS/MS analysis (Fig. 41-43). Accordingly, DGEH21' consist a mixture of 8 3β-hydroxy-Δ^5-steroidal congeners including, 26,27-Dinorergosta-5,22-dien-3-ol (Fig. 41), Cholesta-5,22-dien-3-ol (Fig. 41), Cholest-5-en-3-ol (Fig. 41), Ergosta-5,22-dien-3-ol (Fig. 41), Stigmasta-5,24(28)-dien-3-ol (Fig. 41), Stigmasta-5,22-dien-3-ol (Fig. 41), Stigmasta-5-en-3-ol (Fig. 41), and 22,23-Methylenecholesterol (Fig. 41) respectively. Peaks designated as 2/3 was found to represent the same compound. All of the above compounds have the Δ^5-sterol backbone depicting the metabolic similarities between the structures. Literature reports the presence of 26,27-Dinorergosta-5,22-dien-3-ol in marine organisms [97]. Cholesta-5,22-dien-3-ol have previously been identified from the deep-sea scallop *Placopecten magellanicus* [98]. Barnatha et al. report the identification of several Cholesta-5,22-dien-3-ol derivatives from the marine sponges belongs to the genus *Cinachyreila* [99]. Ergosta-5,22-dien-3-ol with moderate anticancer effects on Dalton's lymphoma ascites cells has been reported from the soft coral *Subergorgia reticulate* [100]. Stigmasta-5,24(28)-dien-3-ol commonly known as Fucosterol is found in some organisms including fungi [101], sponges [102, 103] and brown algae [104]. Ribeiro et al. report the identification of eight different sterols from sponges *Tethya rubra and Tethya maza* whereas six of them matches with the once identified during the current study which includes cholesterol, cholesta-5,22-dien-ol, ergosta-5,22-dien-3-ol, stigmasta-5,22-dien-3-ol, stigmast-5-en-3-ol, and stigmasta-5,24(28)-dien-3-ol [103].
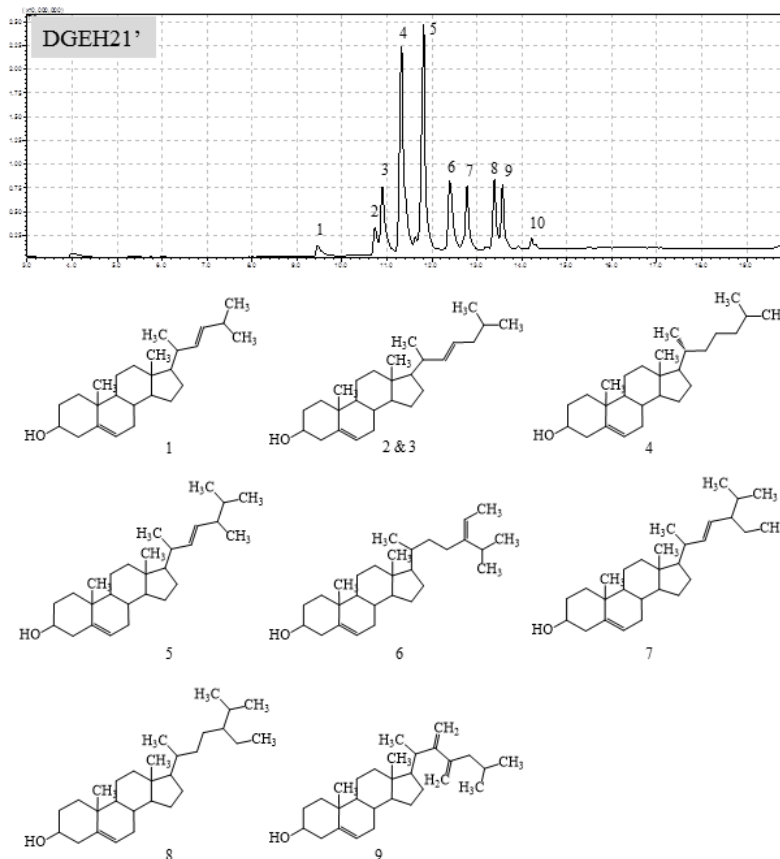
Fig. 41 GC-MS/MS analysis of the nonpolar fraction DGEH21' purified from the hexane solvent fraction of the 70% ethanol solubles of the soft coral *D. gigantea* through silica open column purification. (A) The chromatographic separation of the eight native 3β-hydroxy-Δ5-steroidal congeners. (B) Molecular structures of (1) 26,27-Dinorergosta-5,22-dien-3-ol, (2 and 3) Cholesta-5,22-dien-3-ol, (4) Cholest-5-en-3-ol, (5) Ergosta-5,22-dien-3-ol, (6) Stigmasta-5,24(28)-dien-3-ol, (7) Stigmasta-5,22-dien-3-ol, (8) Stigmasta-5-en-3-ol, and (9) 22,23-Methylenecholesterol.

155
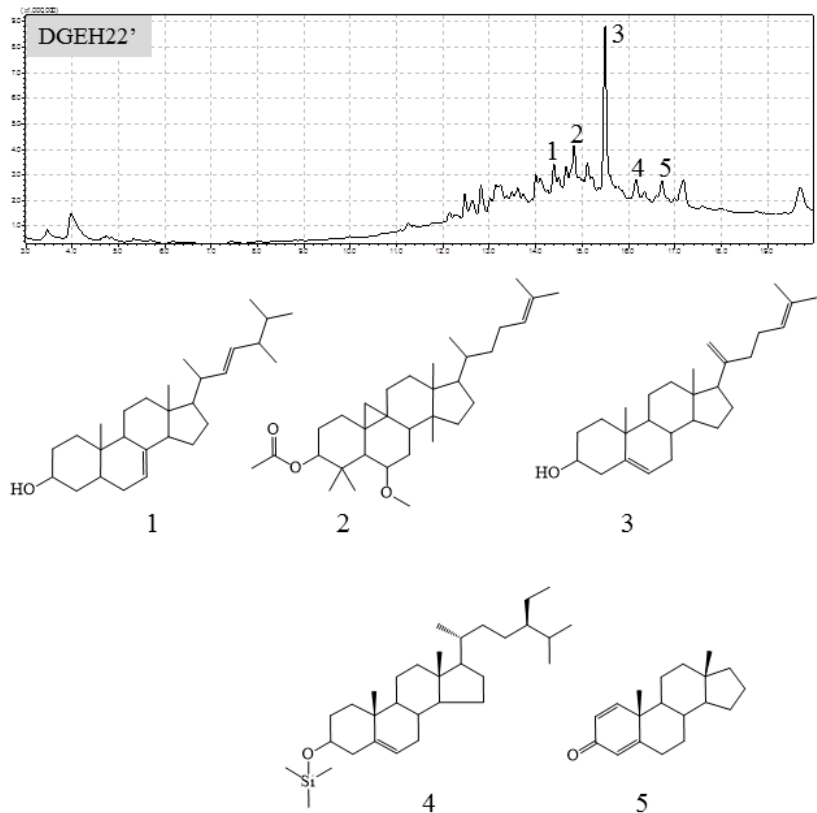
Fig. 42 GC-MS/MS analysis of the nonpolar fraction DGEH22' purified from the hexane solvent fraction of the 70% ethanol solubles of the soft coral *D. gigantea* through silica open column purification. (A) The chromatographic separation of the five native 3β-hydroxy-Δ5-steroidal congeners. (B) Molecular structures of (1) Ergosta-7,22-dien-3-ol, (2) 3-O-Acetyl-6-methoxy-cycloartenol, (3) Cholesta-5,20,24-trien-3-ol, (4) (20R,24R)-3-[(Trimethylsilyl)oxy]stigmast-5-ene, and (5) Androsta-1,4-dien-3-one.

제주대학교 중앙도서관
JEJU NATIONAL UNIVERSITY LIBRARY
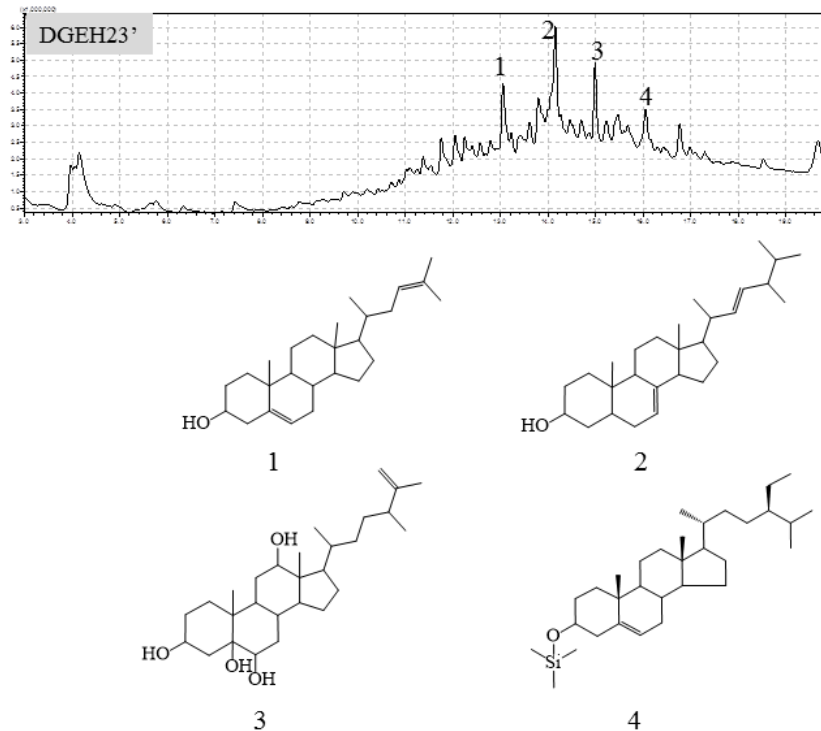
Fig. 43 GC-MS/MS analysis of the nonpolar fraction DGEH21' purified from the hexane solvent fraction of the 70% ethanol solubles of the soft coral *D. gigantea* through silica open column purification. (A) The chromatographic separation of the eight native 3β-hydroxy-Δ5-steroidal congeners. (B) Molecular structures of (1) 26,27-Dinorergosta-5,23-dien-3-ol, (2) Ergosta-7,22-dien-3-ol, (3) Ergost-25-ene-3,5,6,12-tetrol, and (4) Ergosta-5,22-dien-3-ol. (20R,24R)-3-[(Trimethylsilyl)oxy]stigmast-5-ene

157

3.8. Anti-inflammatory potential against NO production in LPS stimulated RAW 264.7 macrophages.

The anti-inflammatory activity of the extract/fractions were evaluated as a function of inhibition of the NO production in LPS stimulated RAW 264.7 macrophages. Each separation and purification step were performed following the selection of best anti-inflammatory fraction (bioassay guided). Initially, the hexane solvent fraction (DGEH) of the *D. gigantea* extract which indicated the best anti-inflammatory activity with an IC_{50} value of 31.58 mg/mL accounting for a 100% Raw cell viability (results not shown) was selected for further open column purification. From the 4 column fractions obtained, the 80% hexane/20% ethyl acetate eluate (DGEH2) indicated the best anti-inflammatory activity with an IC_{50} value of 25.25 mg/mL accounting for >90% Raw cell viability (results not shown). With further column purification, 95% hexane /5% ethyl acetate fraction (DGEH21') indicated the best anti-inflammatory activity against the LPS induced NO production in RAW cells (Fig. 44). The calculated IC_{50} value was 13.27 ± 1.19 µg/ml. The RAW cell viability at the IC_{50} was over 80% which suggest that the compounds in DGEH21' possess rather interesting anti-inflammatory activity against the LPS induced NO production in RAW 264.7 macrophages. At 100 µg/ml, the NO production almost went to a level similar to the control. However, the respective cell viability at 100 µg/ml was 55% which is toxic and inappropriate for the cells. These observations could agree with the cytotoxic properties of steroidal metabolites at higher concentrations as previously been reported in several studies which rather highlight their anti-cancer properties [105]. Although several studies report anti-inflammatory steroids isolated from soft corals [5, 90, 106], there is a lack of information regarding the anti-inflammatory properties of steroids from *D, gigantea*. Current observations reveal the potent anti-inflammatory activity of a steroid rich fraction from *D, gigantea*.
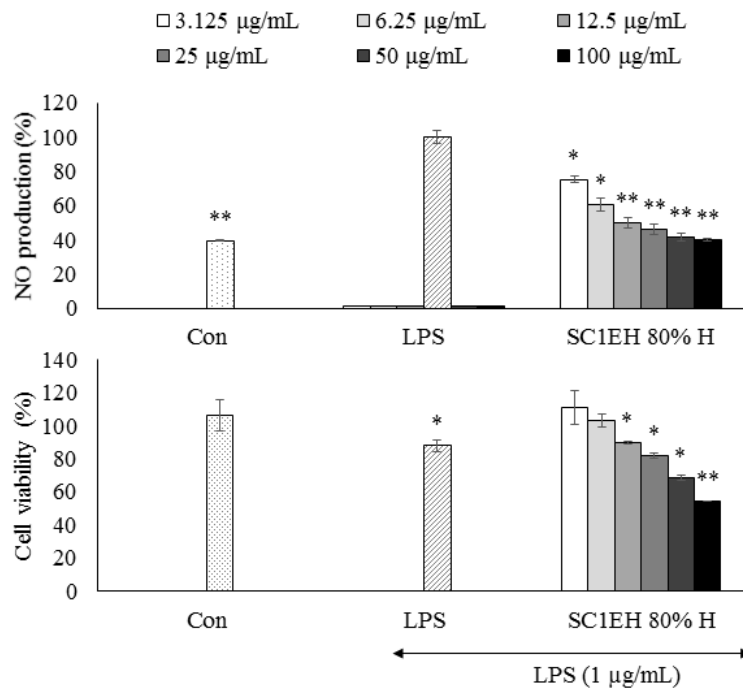
Fig. 44 Anti-inflammatory activity of DGEH21' against the NO production in RAW 264.7 macrophages and cell viability. RAW 264.7 macrophages were pretreated with different DGEH21' concentrations and co-treated with LPS (1 µg/ml). Following 24h the NO production was evaluated by Griess assay, and the cell viability was measured by MTT assay. Results were obtained by three independent experiments and represented as means ± SD. * $p < 0.05$, ** $p < 0.001$ were considered as significant compared to the positive control (LPS).

3.9. Regulation of inflammatory mediators

Regulation of inflammatory responses is mediated by some different signaling pathways which involves several of the key mediators such as iNOS, COX-2, and PGE_2. They regulate the production of NO and prostaglandins which in turn regulate some different cellular responses [53, 68]. Proinflammatory cytokines such as TNF-α, IL-β, and IL-6 are involved in alleviating inflammatory responses overwhelmingly causing harmful effects such as tissue destruction resulting inflammatory disease conditions such as inflammatory bowel disease and rheumatoid arthritis. Therefore downregulation of proinflammatory cytokine production is an utmost necessity in treating inflammation. According to Western blot analysis co-treatment of DGEH21' and LPS effectively suppressed the expression levels of iNOS and COX-2 in a dose-dependent manner (Fig. 45 (A)). Further, it reduced the expression levels of PGE_2, and proinflammatory cytokines including TNF-α, IL1-β and IL-6 in a dose-dependent manner (Fig. 45 (B-D)). Downregulation of iNOS expression explain the ability of DGEH21' to reduce the NO production in LPS stimulated RAW 264.7 macrophages. Further, these results suggest that DGEH21' could effectively reduce the production of COX-2 under experimented sample concentrations which in turn could suppress the production of prostaglandin E2 and downstream signaling molecules reducing the number of detrimental inflammatory responses including redness, heat, swelling, and pain [107].
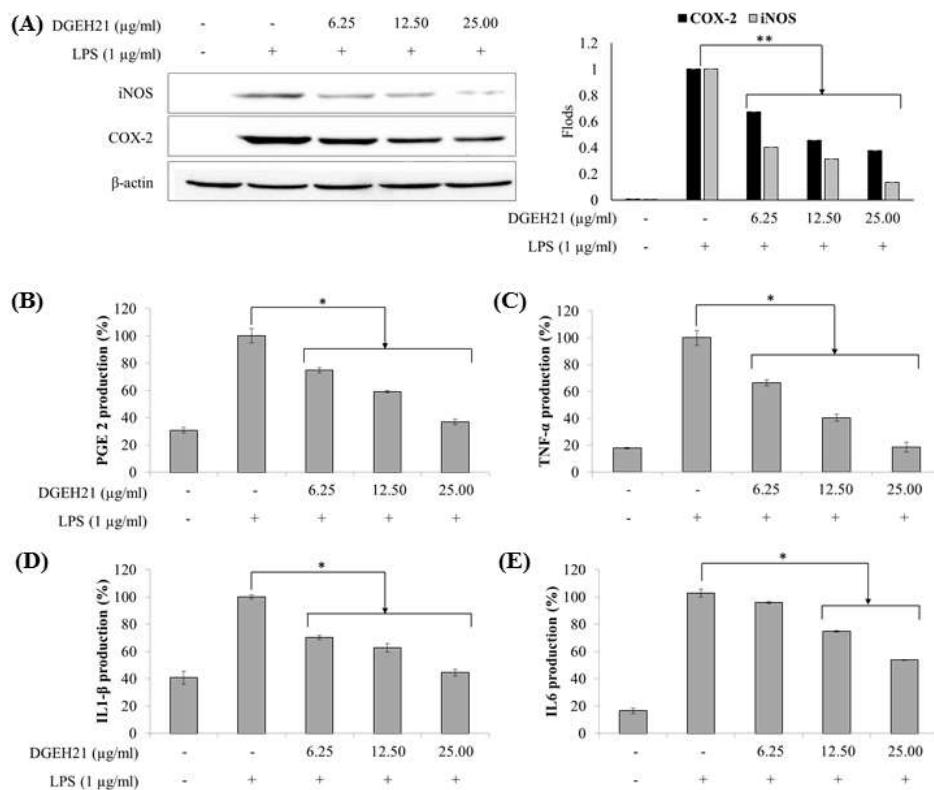
Fig. 45 Effects of DGEH21' upon the mediation of inflammatory regulators. (A) Western blot analysis of the expression levels of iNOS and COX-2. Downregulation of (B) PGE_2 production, (C) TNF-α, (D) IL1-β and (E) IL-6 in LPS stimulated RAW 264.7 macrophages. RAW 264.7 macrophages were pretreated with different DGEH21' concentrations and co-treated with LPS (1 µg/ml). Following 24h, the culture media was retrieved for the analysis of PGE_2, TNF-α, IL1-β, and IL-6. The cells were harvested, lysed and used for the analysis of iNOS and COX-2 expression levels using western blot. Results were obtained from three independent experiments, and the graphs are represented as means ± SD. * $p < 0.05$, ** $p < 0.001$ were considered significant compared to the positive control (LPS).

3.10. *In vivo* anti-inflammatory effects of DGEH21' as a measure of inhibiting NO production, ROS production, and cell death in LPS stimulated zebrafish embryos.

Evaluation of anti-inflammatory effects under in vivo conditions could provide a better understanding of the functional and detrimental effects of compounds. Based on recent findings zebrafish model is gaining popularity over the conventional mouse model in mimicking human disease conditions [108]. As shown in Fig. 46, the sudden increase in the fluorescence intensity of the Zebrafish embryos treated with LPS suggest the increased production of NO and ROS along with increased cell damage due to ROS. However, co-treatment of LPS and DGEH21' effectively inhibited the NO and ROS levels and reduced the cell death in a dose-dependent manner. These results indicate that DGEH21' could significantly attenuate the inflammatory responses in LPS induced zebrafish model.
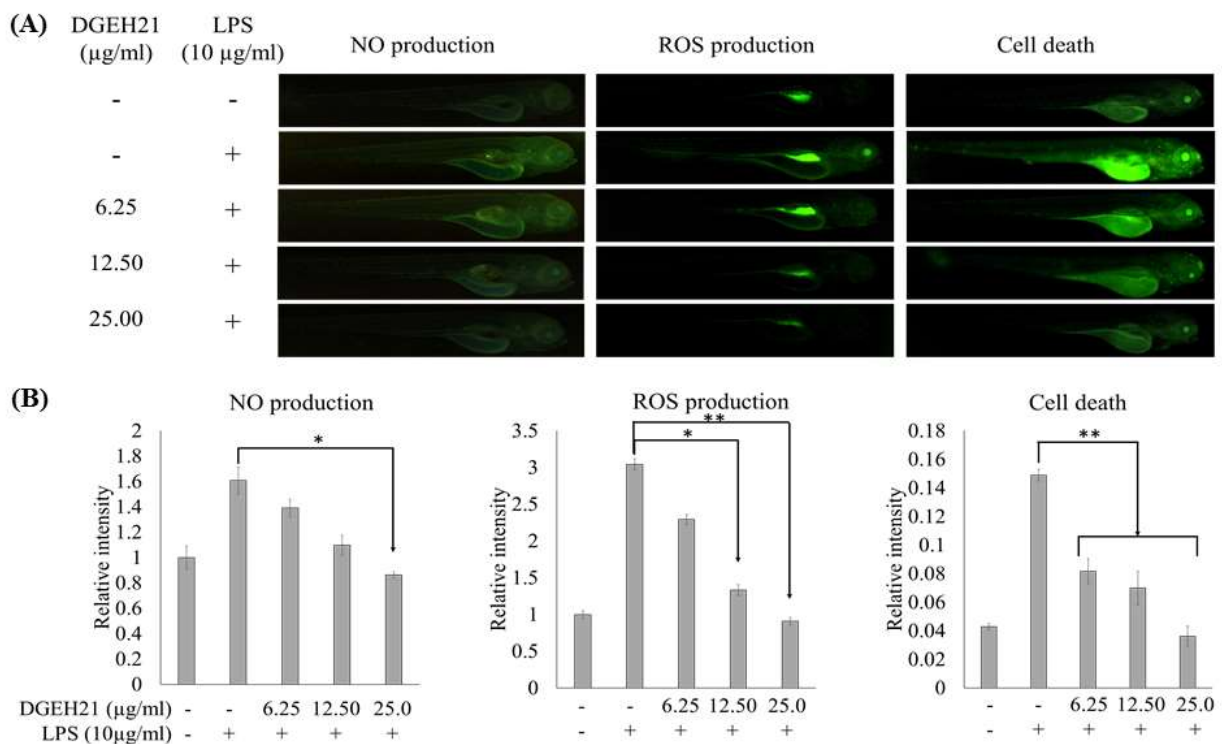
Fig. 46 Effects of DGEH21' upon the inhibition of LPS induced NO production, ROS production and cell death in zebrafish embryo model. (A) Fluorescence microscopic images of the NO production, ROS production, and cell death in LPS induced zebrafish embryo model. (B) Densitometry analysis of the fluorescence intensities corresponding to NO production, ROS production and cell death in LPS induced zebrafish. Zebrafish embryos were co-treated with different concentrations of DGEH21' and LPS (1μg/ml). Fluorescence image analysis was done at 3 dpf after staining with suitable fluorescence staining dyes. Results were obtained from three independent experiments and represented as means $\pm$ SD. * $p < 0.05$, ** $p < 0.001$ were considered as significant compared to the positive control (LPS).

4. CONCLUSIONS

Soft corals are considered as a rich source of bioactive terpenoides that indicate desirable functionalities as anti-inflammatory and anticancer agents. During the current study five of the ethanol extracts obtained from the soft corals indicated anti-inflammatory activity on RAW macrophages by downregulating the NO production and expression levels of i-NOS, COX-2 PGE$_2$ and other inflammatory cytokines including TNF-α, IL-β, and IL-6. Among the screened soft corals, the ethanol extract of *Dendronephthya gigantea* was selected for further studies. Sesqui- and diterpenes among other known compounds represent a major group of secondary metabolites produced by soft corals. Over 200 different kinds of steroids with their common cholestane nucleus 3β-hydroxy-Δ^5- (or Δ^0-) moiety and a C$_8$-C$_{10}$ side chain [50] have been discovered from marine organisms by GC-MS methods following liquid chromatographic purification. Many of these compounds have found to possess potential pathological, physiological, or pharmacological significance as bioactive agents against cancer, inflammation, and pathogenesis of some disease conditions [109]. Current findings elaborate the utility of gas chromatography-tandem mass spectrometry for the identification of sterols in a nonpolar column eluate obtained from the hexane fraction of the 70% ethanol solubles of the soft coral *D. gigantea* following bioassay guided fractionation and purification. The purified sterol-rich fraction (DGEH21') indicated a synergistic effect of reducing inflammation induced by LPS in *in vitro* RAW 264.7 macrophages with an IC$_{50}$ of 13.27 ± 1.19 µg/ml and in *in vivo* zebrafish embryo model. The inhibition of NO production in RAW 264.7 macrophages was associated with the downregulation of iNOS expression. Moreover, DGEH21' could effectively suppress the expression of PGE2 and proinflammatory cytokines. The next attempt of ours would be to isolate the targeted bioactive compounds and to explore their biological significance.

SECTION 5;

SCREENING OF ANTI-CANCER ACTIVITIES, PURIFICATION AND ISOLATION OF BIOACTIVE STEROLS WITH ANTI-CANCER PROPERTIES FROM THE SOFT CORAL *Dendronephthya gigantea.*

ABSTRACT

Cancer is listed as the second most leading factor that contributes to death globally. Hence, the search for anti-cancer drug leads receives an exceptional attention. The focus of the current study was to screen the anti-proliferative properties of extracts obtained by soft corals harvested from Jeju Island. Further, this reports the identification, evaluation, and purification of functional ingredients from the selected soft coral *Dendronephthya gigantea* that have the potential to inhibit the proliferation of HL-60 (leukemia) and MCF-7 (breast cancer) cells. The study reports the synergistic significance and possible anti-cancer activity of a fraction containing eight 3β-hydroxy-Δ5-steroidal congeners (DGEHF21'). The results indicate that the steroid mixture could potentially increase the formation of apoptotic bodies and increase the proportion of sub-G1 cells in both cancer cell lines. Western blot analysis revealed that DGEHF21' indicates the ability to control apoptosis via mitochondrial-mediated apoptosis pathway. However, further purified constituents obtained by purification of DGEHF21' did not demonstrate anti-proliferative potential effective as DGEHF21'. Nonetheless, a fraction rich in Stigmasta-5-en-3-ol indicated a considerable anti-proliferative potential. Hence, this highlights the importance of studying synergistic anti-proliferative effects of steroidal congeners from *D. gigantea.*

1. INTRODUCTION

Natural products have long been investigated as the source of bioactive secondary metabolites for the discovery of potential pharmaceutical agents. Marine organisms have immensely contributed to enrich and extend the boundaries of natural product drug discovery to a whole new level of research with the discovery of a structurally diverse set of secondary metabolites with a broad range of biological functionality [14, 53]. Soft corals have proven to possess a large number of biofunctional secondary metabolites mainly encompassing sesquiterpenes and diterpenes derivatives [110]. According to the comprehensive review by Valeria et al. by 1993, more than 200 different types of monohydroxysterols have been discovered from marine organisms [7]. Triterpenoids are at the center of some ongoing drug evaluations. A range of potentially beneficial biological effects including anticancer, anti-inflammatory, antimicrobial, analgesic, antiviral, antiplasmodial, antimycotic, antiulcerogenic, vascular protective, immunomodulatory, antiobesity, and tonic effects have been reported for triterpenoids [111]. Much of these compounds are proven to be cytotoxic at elevated concentration and are effective against cancer. Examples of these are, antitumorigenic properties of a monohydroxycembratetraene, Sarcophytol A isolated from the soft coral *Sarcophyton glaucum* [112], discovery of five eunicellin diterpenes, pachycladins A-E from the soft coral *Cladiella pachyclados* with potential anti-proliferative activity against PC-3 prostate cancer cells [113], isolation of hydroperoxysterol, (22R,23R,24R)-5R,8R-epidioxy-22,23-methylene-24-methylcholest-6-en-3â-ol with potential anti-cancer effects on P-388 and KB carcinoma cells from a soft coral belongs to *Sinularia sp.* [114].

The physiological balance between cell proliferation and apoptosis is essential for the homeostasis of biological functions in an organism. However, some stochastic effects could influence genetic aberrations which could alter the balance above causing tumor progression [115]. Cancer is a major

public issue in many countries around the globe accounting for an increased mortality rate. Though, natural products have done an enormous endeavor for the discovery of anticancer drugs. Anticancer effects of natural products could proceed through some direct and indirect pathways including induction of apoptosis, slowing down / arresting cell cycle phases, and inhibition of tumor metastasis. Moreover, indirectly by boosting immune recognition, downregulating the hormonal dependent proliferation of endocrine tumors, and affecting sterol biosynthesis [116]. Finding the mechanisms responsible of exerting anti-cancer effects of these natural products could expand the research perspectives of developing anticancer therapeutics. Much of the anticancer drugs in use are so far have recognized to cause detrimental side effects on normal cells. Since continuing efforts on the discovery of novel anticancer agents could expand the possibilities of finding treatment methods for cancer.

2. MATERIALS AND METHODS

HL-60 human leukemia, MCF-7 human breast cancer and "Chang" human liver cell lines were purchased from the Korean Cell Line Bank (KCLB, Seoul, Korea). Dulbecco's modified Eagle's medium (DMEM), Roswell Park Memorial Institute medium (RPMI), fetal bovine serum (FBS) and penicillin/streptomycin mixture were purchased from GIBCO INC. 3-(4,5-dimethylthiazol-2-yl)-2,5-diphenyltetrazolium bromide (MTT), Hoechst, ethidium bromide and acridine orange were purchased from Sigma (USA). All organic solvents used in extraction and fractionation were of analytical grade.

SCREENING OF ANTI-CANCER ACTIVITIES, PURIFICATION AND ISOLATION OF BIOACTIVE STEROLS WITH ANTI-CANCER PROPERTIES FROM SOFT CORALS.

2.1. Sample collection and extraction

Soft coral samples were collected from the Jeju Sea, Jeju Island South Korea during April 2016 at a depth of 10-15 m. The sample was identified with the aid of Jeju Biodiversity Research Institute (Jeju, Korea). Sample repositories were stored in the Laboratory of Marine Bioresource Technology at Jeju National University. The samples were dually washed, lyophilized, ground into a powder (6.00 kg) and extracted thrice using 70% ethanol in water and the solvent was removed under vacuum using a rotary evaporator to obtain the crude extract.

2.2. Fractionation and further purification

The crude obtained was dissolved in water and respectively fractioned between hexane, chloroform, and ethyl acetate. All solvents were evaporated under vacuum. Henceforth further purification was performed following bioassay guided fractionation and purification. Accordingly, the selected hexane solvent fraction was further purified by a silica open column eluted with a gradient of hexane and ethyl acetate in order of increasing polarity. The selected column fraction 80% H +20% EA was further purified following another silica open column. The 95% H + 5% EA fraction designated as DGEHF21' was selected for further investigations.

2.3. GC-MS/MS analysis

GC-MS/MS analysis of DGEHF2 column fractions was done using a Shimadzu GCMS-TQ8040 tandem GC/MS system (Japan). Chromatographic separation was done using a Rtx-5MS fused-silica capillary column with an internal diameter of 0.25µm and column length 30.0 m. The detection limits were set to 50-500 m/z range. The samples were injected by splitless mode. The ions were generated at 200°C, and the GC oven was programmed as 260°C, 3 min, 6°C/min to 320°C, 5°C/min to 330°C, 2 min. The carrier gas (Helium) flow was kept constant at a rate of 0.73 ml/min.

2.4. Cell culture

MCF-7 and Chang cells were cultured in DMEM media and HL-60 was cultured in RPMI media. Both media were supplemented with 10% FBS and 1% penicillin, streptomycin mixture. The cells were maintained under a humidified atmosphere at 37°C with 5% CO_2. Periodical subcultures were done until the cells attain the exponential growth phase. The cells were then seeded for experiments at a $1x10^4$ cells/ml concentration in 96 well plates. Sample treatment was done after 24 hours. Following another 24h period, MTT assay was done to evaluate the anticancer effect of samples as a measure of the percentage of cell viability compared to the control.

2.5 Apoptotic and necrotic body formation

Nuclear staining with Hoechst 33342 was used to characterize the apoptotic cells represented by chromatin condensation and nuclear fragmentation [117]. Acridine orange/ethidium bromide double staining method was used to characterize apoptotic and necrotic cells. HL-60 and MCF-7

cells were seeded in 24 well culture plates and after 24h, treated with different concentrations of DGEHF21'. Following 24h 5 µl of cell-permeable DNA dye Hoechst 33342 (10 µg/mL,) or 10 µl of acridine orange/ethidium bromide (100 µg mL-1) was treated into each well. After 10 min incubation, cells stained with Hoechst 33342 were observed under a fluorescence microscope equipped with a CoolSNAP-Pro color digital camera [82]. Cells stained with acridine orange/ethidium bromide mixed stain was dually washed using PBS and observed by the fluorescence microscope [83].

2.6. Cell cycle analysis

The proportion of apoptotic hypodiploid cells in sub-G1 were analyzed by flow cytometry [84]. The cells were seeded in six-well plates, and sample treatment was done after 24h. Again after 24h the cells were harvested, fixed in 70% ethanol at 4 °C for 30 min and washed with 2 mM Sodium Ethylenediaminetetraacetate (EDTA) in PBS. The cells were prepared for the flow cytometric analysis by suspending in a solvent containing PI (100 µg/ml) and RNase (µg/ml) for 30 min. The analysis was done using an FACSCalibur flow cytometer (Becton Dickinson, San Jose, USA).

2.7. Western blot analysis

The cells were seeded in six-well plates ($2x10^5$) and harvested 24h after the sample treatment. Cells were homogenized in lysis buffer, centrifuged (12000 x g for 20 min) to remove debris and the protein content in the supernatants were analyzed by BCA protein assay kit. Lysates containing 50 µg of proteins were loaded onto 12% polyacrylamide gels. Sodium dodecyl sulfate-polyacrylamide gel electrophoresis was carried out to resolve the protein bands based on their

molecular weight and electrophoretically transferred onto polyvinylidene difluoride membranes. The membranes were blocked with skim milk and incubated with specific primary antibodies followed by secondary antibodies. Signals were developed using a chemiluminescent substrate (Cyanagen Srl, Bologna, Italy) and the fluorescence images were taken by a FUSION SOLO Vilber Lourmat system (Paris, France) [118]. Densitometry analysis of the protein expression was done using Image J program.

2.8. NMR analysis

The purified compounds that indicated considerable purity was analyzed using a JNM-ECX400 NMR system (JEOL, Japan) with a 40TH5AT/FG Probe. Gradient shim was automatically executed to obtain better NMR resolution. Experiments were done for proton and ^{13}C.

2.9. Statistical analysis

All data are expressed as means $\pm$ SD based on at least three independent determinations. Significant differences among the data sets were determined using IBM SPSS Statistics 20 software using one-way ANOVA by Duncan's multiple range test (DMRT). ** P-values less than 0.05 (P < 0.05) were considered significant.

3. RESULTS AND DISCUSSION

3.1. Cytotoxicity of the soft coral extracts

Based on the results (Fig. 47) none of the samples indicated a considerable level of toxicity on normal cells (Vero) within the used concentration range after incubating for 24h. Hence, the concentrations of 25 – 100 µg/ml could be selected for the further evaluation of their biofunctional properties.
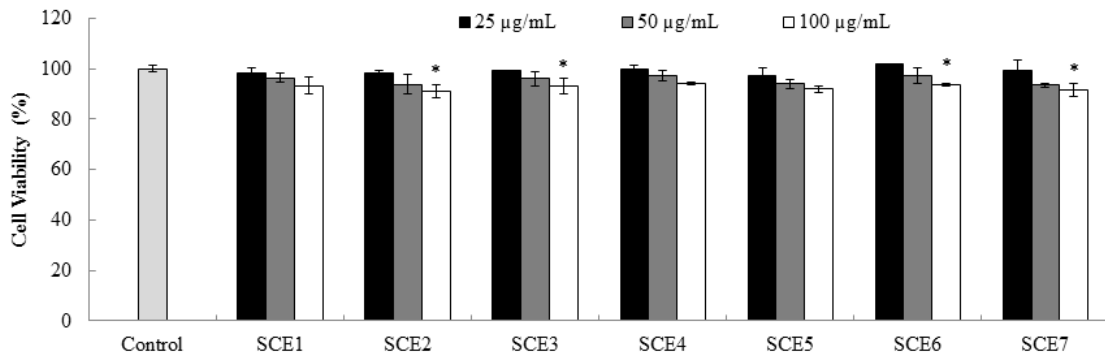
Fig. 47 Cytotoxicity of the soft coral extracts on normal cells. Measurements were taken as the proportion of viable cells after 24 h incubation period. Vero cells were treated with different sample concentrations and incubated for a 24h period. MTT assay was adopted for the determination of cell viability. Experiments were carried out in triplicate, and the results are represented as means ± SD. Values are significantly different from the control at *P < 0.05 and **P < 0.001.

3.2. Anti-proliferative Effects of the soft coral ethanol extracts on HL-60 cells

Anticancer effects of the soft corals were evaluated on HL-60 cell line (Fig. 48). The results indicate that the viabilities of HL-60 cells are reducing with increasing concentrations of sample extracts. Among the extracts, SC1E indicated the best anti-proliferative effects. Hence, SC1 was selected for the further evaluation of its bioactive principals responsible for its functional properties.

3.3. Evaluation of nuclear morphology

Analysis of nuclear morphology of the cells provides a better understanding of the anti-proliferative effects of samples. Hoechst 33342 is a DNA-specific fluorescent dye that stains nuclear matter in cells allowing the clarification of nuclear morphology to identify the formation of apoptotic bodies (Fig. 49). Based on the results increased the frequency of nuclear condensation and fragmentation was observed with increasing sample concentrations. These observations mark the formation of apoptotic bodies.
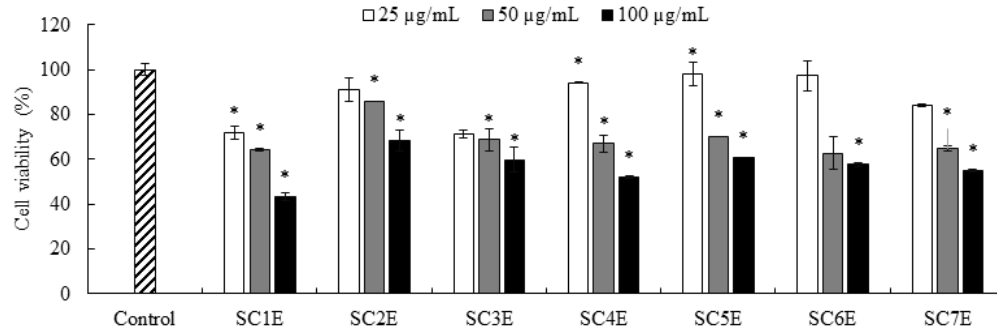
Fig. 48 Anti-proliferative effects of the ethanolic extracts of soft corals on HL-60 cells. HL-60 cells were treated with different sample concentrations and incubated for a 24h period. MTT assay was adopted for the determination of cell viability. Experiments were carried out in triplicate, and the results are represented as means ± SD. Values are significantly different from the control at *P < 0.05 and **P < 0.001.
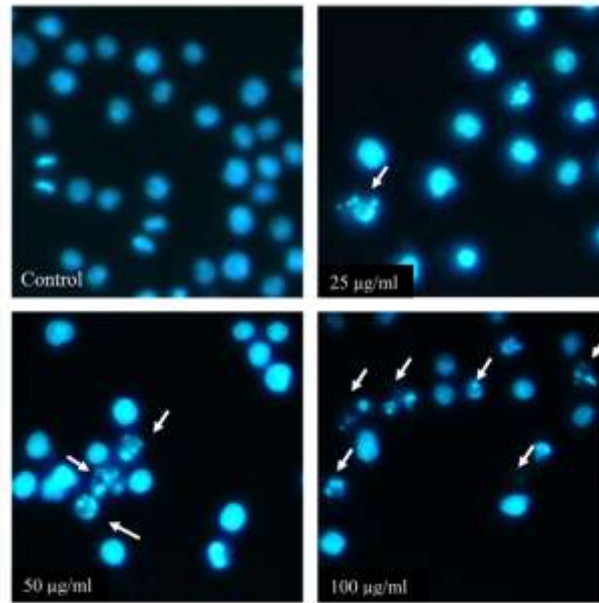
Fig. 49 Evaluating nuclear morphology of HL-60 cells. HL-60 cells were treated with different sample concentrations and incubated for a 24h period. Hoechst 33342 was used to stain the nuclear material. Fluorescence images were taken after 15 min of incubation. Experiments were carried out in triplicate.

3.4. Anti-cancer activity of the solvent extracts of selected soft corals on HL-60 and MCF-7 cells.

The selected ethanol extracts of the soft coral samples were fractionated between hexane, chloroform and ethyl acetate as the first step towards their purification. Based on the results (Fig. 50), the hexane fractions of the both soft coral samples indicated anti-cancer effects compared to other solvent fractions by markedly inhibiting the cell viability of the cancer cell lines with increasing sample concentrations.
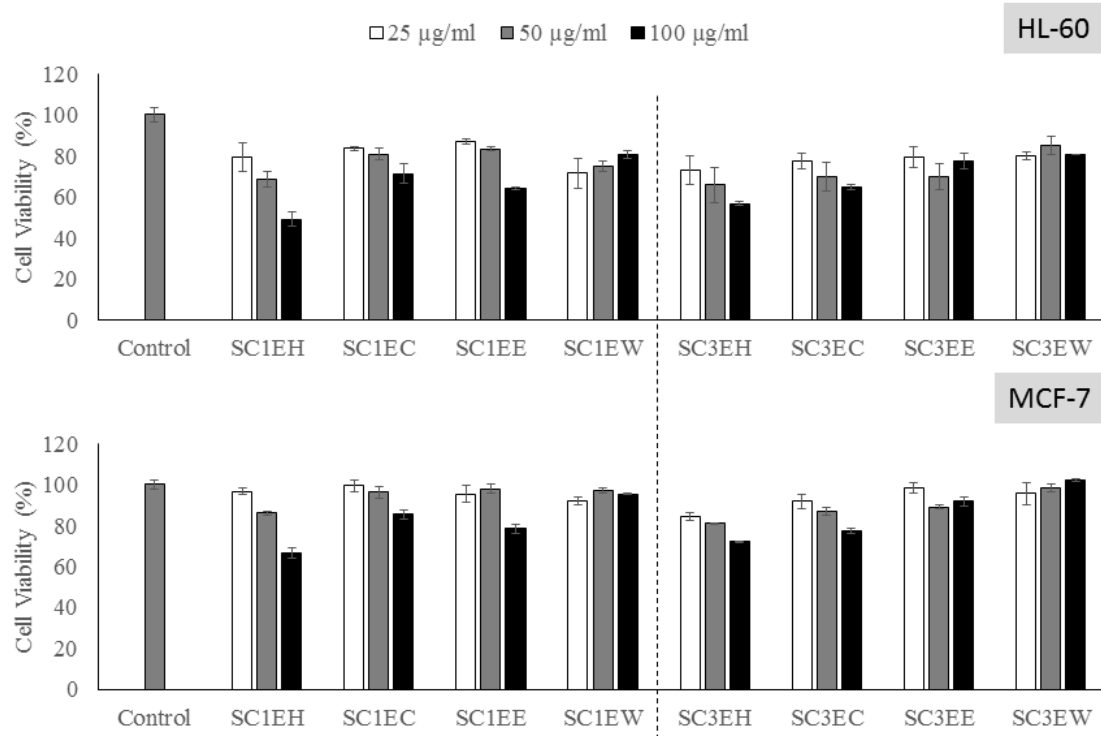
Fig. 50 Anti-cancer activity of the solvent extracts of *D. gigantea* and *D. spinulosa* on HL-60 and MCF-7 cells. HL-60 and MCF-7 cells were treated with different sample concentrations and incubated for a 24h period. MTT assay was adopted for the determination of cell viability. Experiments were carried out in triplicate, and the results are represented as means ± SD.

3.5. Cytotoxicity and anti-cancer activity of DGEHF2 column fractions on Vero, MCF-7, and HL-60 cell lines.

MTT colorimetric cell viability assay was used to measure the cytotoxicity of DGEHF21' DGEHF22' and DGEHF23' on HL-60, a human leukemia cell line and MCF-7 human breast adenocarcinoma cell line (Fig. 51). Same time, Vero cells, a monkey kidney epithelial cell line more commonly used as a normal cell line was used in the comparison. The cytotoxic effects of DGEHF21' and DGEHF22' were not much strong on Vero cells. Both DGEHF21' and DGEHF22' indicated strong inhibitory effects on cell viability in all cell lines with increasing concentrations. The normal cell line, "Vero" was able to withstand the toxic effects of the samples compared to the two carcinoma cells at each concentration. Among the tested samples, DGEHF21' had the highest antiproliferative effects against all cell lines. The IC_{50} value for the anti-proliferative effect of DGEHF21' was calculated as 13.59 ± 1.40 µg/ml and 29.41 ± 0.87 µg/ml respectively for HL-60 and MCF-7 cell lines. Correspondingly, the Vero cells indicated a cell viability of 93% and 87% at aforementioned IC_{50} concentrations. Rationally DGEHF21' at 50.00 µg/ml concentration could be further investigated as a potential substance with anti-proliferative effects on human leukemia and breast adenocarcinoma. The anti-proliferative effects of DGEHF22' was comparatively higher compared to DGEHF21' accounting for IC_{50} values of 23.37 ± 0.75 µg/ml µg/ml against HL-60 cells and 41.88 ± 0.15 against MCF-7. Hence, DGEHF21' that indicated better anti-proliferative effects was selected for further investigation.
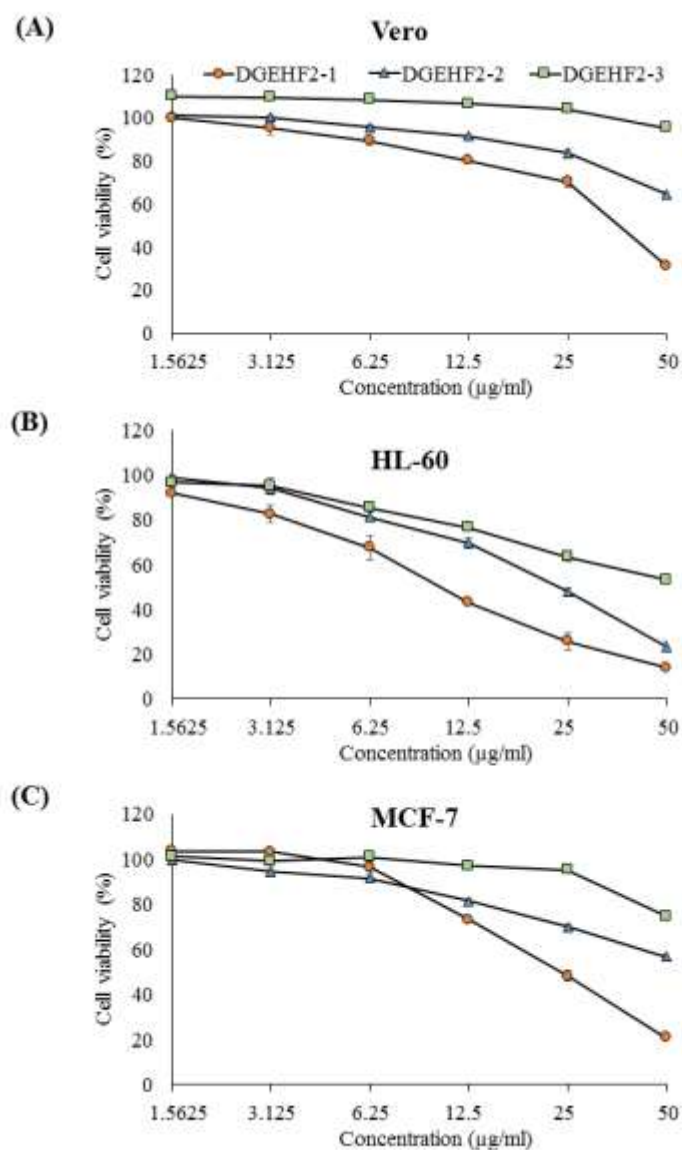
Fig. 51 The percentage of cell viability as a measure of cell proliferation by different concentrations of DGEHF2 sub-fractions. (A) Vero cell represents a normal cell line, (B) HL-60 and (C) MCF-7 represent two carcinoma cell lines. Percentage of cell viability represent the proportion of viable cells compared to the control (100%). All experiments were performed in triplicate, and each value represents the mean ± SD.

180

3.6. Chemical composition of the eluates from the second open column

Chemical constituents in the column eluates were analyzed using a triple quadrupole GC-MS/MS system. As shown in Fig. 52 the constituents were mainly a mixture of 8 3β-hydroxy-Δ5-steroidal congeners. The two peaks designated as 2 in (Fig. 52, A) was arising from the same compound. Soft corals are renounced for their bioactive sesqui- and diterpene metabolites among the other various classes of secondary metabolites. Many of these sterols exist as complex inseparable mixtures whereas their identification is usually made using GC-MS or much recent, more accurate GC-tandem MS methods
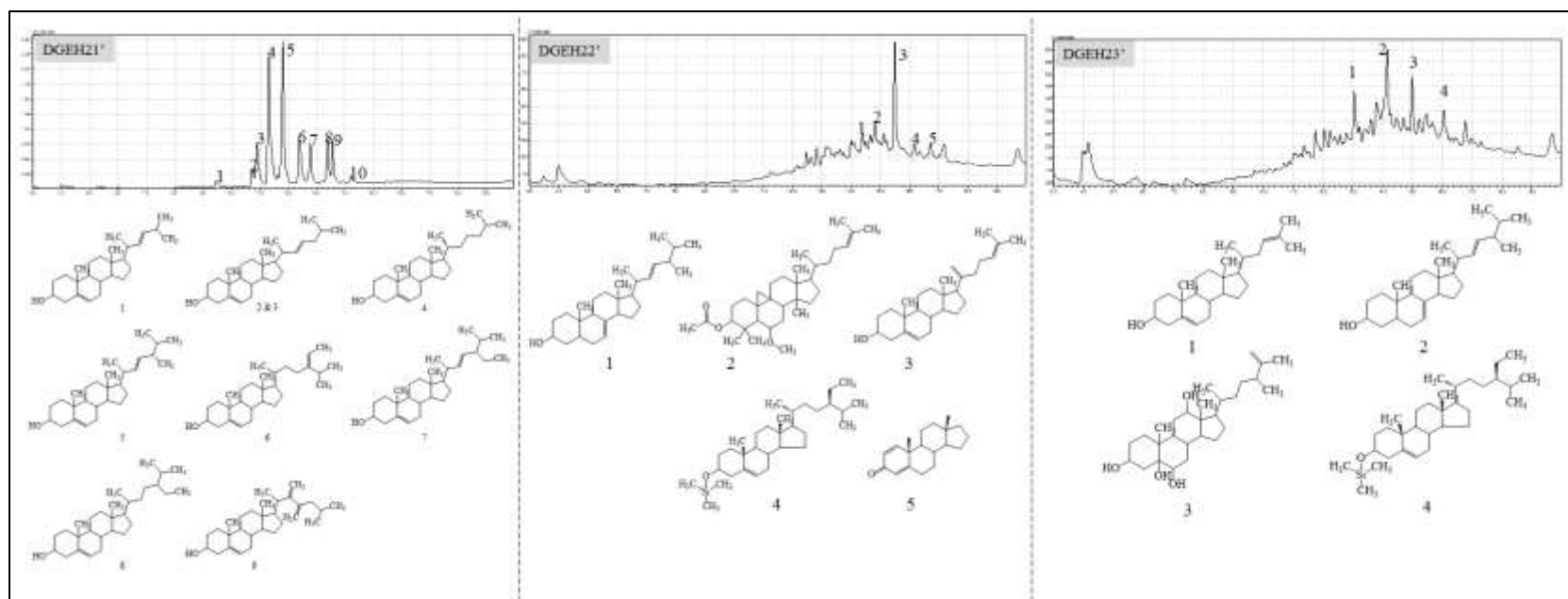
Fig. 52 GC-MS/MS evaluation of the constituents in the column eluates, DGEHF22' and DGEHF23'. Samples were dissolved in hexane and analyzed using GC-MS/MS. (A) DGEHF21' and its constituents (A) 1. 26,27-Dinorergosta-5,22-dien-3-ol, (A) 2 and 3. Cholesta-5,22-dien-3-ol, (A) 4. Cholest-5-en-3-ol, (A) 5. Ergosta-5,22-dien-3-ol, (A) 6. Stigmasta-5,24(28)-dien-3-ol, (A) 7. Stigmasta-5,22-dien-3-ol, (A) 8. Stigmasta-5-en-3-ol, and (A) 9. 22,23-Methylenecholesterol. (B) DGEHF22' and its constituents (B) 1. Ergosta-7,22-dien-3-ol, (B) 2. 3-O-Acetyl-6-methoxy-cycloartenol, (B) 3. Cholesta-5,20,24-trien-3-ol, (B) 4. (20R,24R)-3-[(Trimethylsilyl)oxy]stigmast-5-ene, and (B) 5. Androsta-1,4-dien-3-one. (C) DGEHF22' and its constituents (C) 1. 26,27-Dinorergosta-5,23-dien-3-ol, (C) 2. Ergosta-7,22-dien-3-ol, (C) 3. Ergost-25-ene-3,5,6,12-tetrol and (C) 4. (20R,24R)-3-[(Trimethylsilyl)oxy]stigmast-5-

182

3.7. Nuclear morphology of cells indicating apoptotic body formation induced by DGEHF21'

in MCF-7 and HL-60 cell lines.

Hoechst 33342 is a DNA-specific fluorescent dye that stains nuclear matter in cells allowing the clarification of nuclear morphology to identify the formation of apoptotic bodies. Cells with homogeneously stained nuclei are indicative of viable cells. Fragmented nuclear morphology is indicative of chromatin condensation and/or nuclear fragmentation which is indicative of apoptosis [119]. Acridine orange/ethidium bromide double staining allow characterizing the nuclear morphology in more detail. Acridine orange being taken up by both viable and nonviable cells stains double stranded nucleic acids in green and single-stranded nucleic acid in orangish red color. Ethidium bromide been absorbed only by nonviable cells, stains the nuclear matter with red fluorescence. This method facilitates the evaluation of cells with four different nuclear morphologies. Viable cells are indicative of a green homogeneous nucleus, early apoptotic cells are observed with fragmented green patches, late apoptotic cells are seen with both green and orange or orange particulate matter and necrotic cells with a damaged cytoplasmic membrane in homogenous red color [120]. Fig. 53 represents microscopic fluorescence images of cell populations taken randomly from different wells with different sample concentrations. Based on our observations, both HL-60 and MCF-7 cells indicated a dose-dependent increase of apoptotic body formation. Several early apoptotic cells were observed in both cell lines at 12.5 µg/ml DGEHF21' concentration after 24h whereas none was in late apoptosis nor necrosis. At 50 µg/ml concentration, an increased number of cells were found to be in late apoptosis, but none were necrotic. Moreover, a marked cell shrinkage was visible at 50 µg/ml concentration compared to the control. Unlike necrosis that occurs due to loss of osmoregulation, that involve the rupture of cell membrane and dissolution of cellular organelles, apoptosis occurs with chromatin

condensation while maintaining the normal organelle structure. Apoptotic events include DNA fragmentation, chromatin condensation, membrane blebbing, cell shrinkage, and disassembly into membrane-enclosed vesicles (apoptotic bodies) [121]. By contrast, apoptosis has been implicated as the best strategy for achieving anti-cancer activity on therapeutic grounds [122]. Present observations indicate that DGEHF21' can dose-dependently induce apoptosis in MCF-7 and HL-60 cancer cell lines.
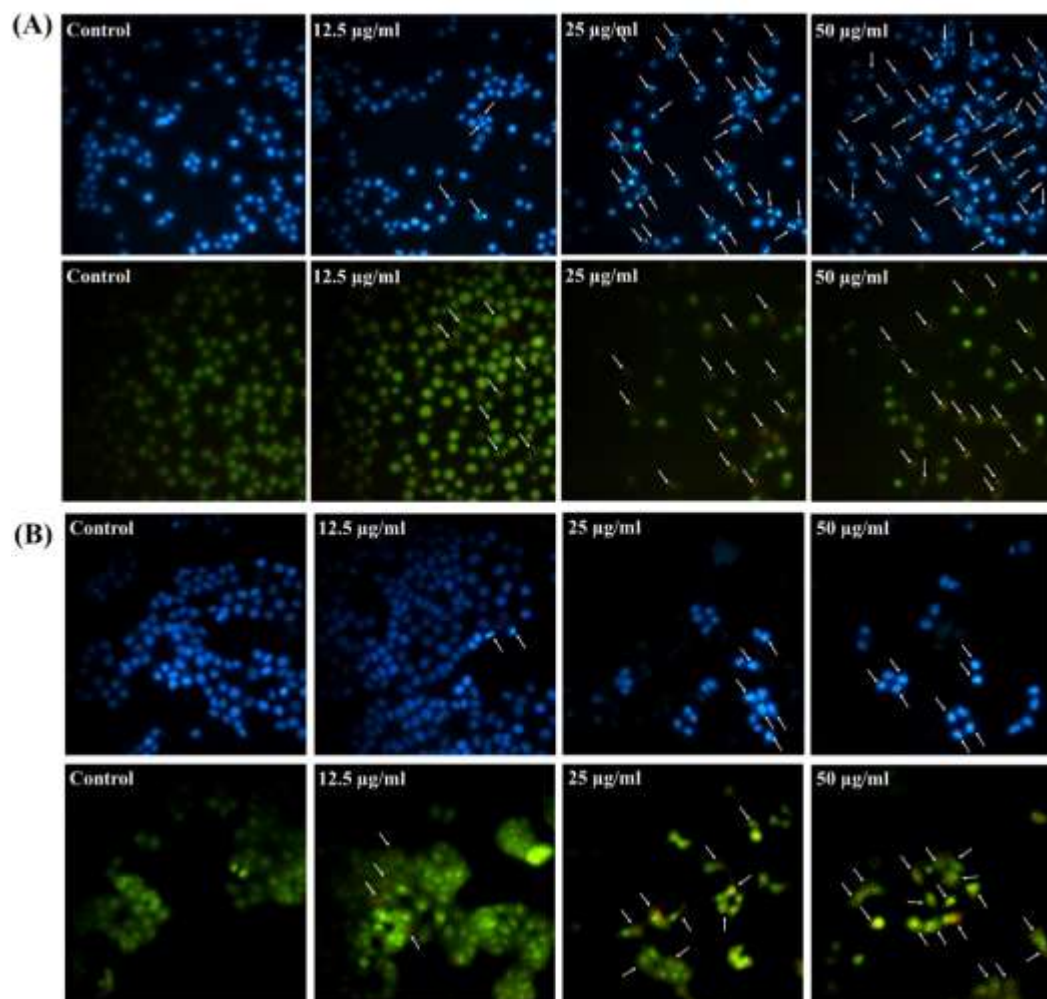
Fig. 53 Fluorescence microscopic evaluation of the effects of the nuclear morphology of cancer cells upon DGEHF21' treatment. (A) HL-60 and (B) MCF-7. DGEHF21' treatment was carried out at 12.5, 25 and 50 µg/ml sample concentrations. The observations were done after 24h by Hoechst 33342 and by acridine orange/ethidium bromide double staining method. Nuclear condensation/fragmentation with bright green color patches are indicative of early apoptosis. The appearance of discrete orange color nuclear fragments is indicative of late apoptosis. Experiments were done in triplicate, and a set of random cell populations under the microscope were taken into account during each experiment.

3.8. Flow-cytometric analysis of the proportion of apoptotic cells in Sub-G1

The anti-proliferative effects of DGEHF21' could be resulting from the induction of apoptosis, cell cycle arrest or through the combination of both effects. As shown in Fig. 54, DGEHF21' treatment dysregulates cell cycle progression causing a dose-dependent increase of the sub-G1 apoptotic cell population both in HL-60 and MCF-7 cells. DGEHF21' at 50 µg/ml concentration resulted in a sub-G1 apoptotic cell population of 48.44% in HL-60 cells while 63.86% in MCF-7 cells. These results are slightly controversial to the results of cell viability assay, which indicated a comparatively lower IC_{50} value of DGEHF21' towards HL-60 cells. These results further clarify that DGEHF21' induced antiproliferative effects are causing primarily through the induction of apoptosis. These findings are consistent with the results observed for nuclear morphology evaluation.
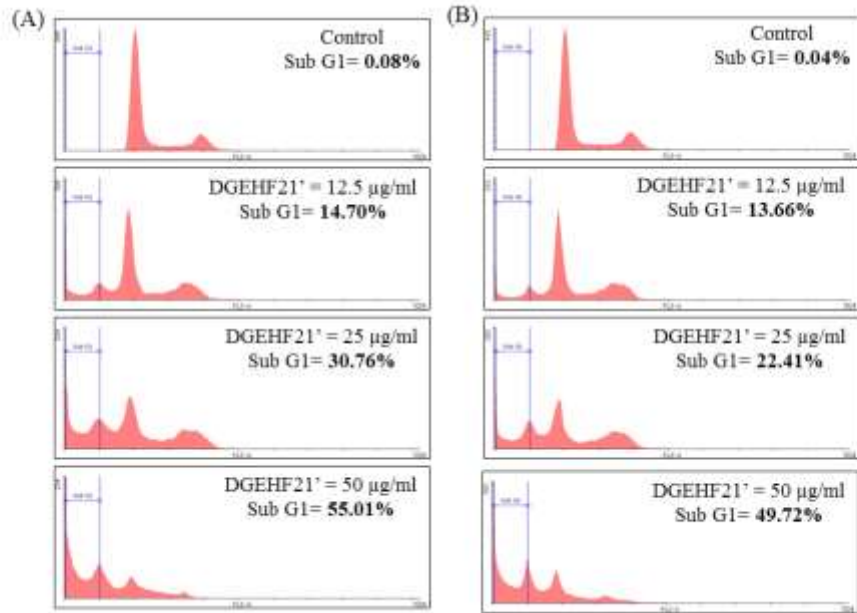
Fig. 54 DGEHF21' treated HL-60 and MCF-7 cells exhibit dysregulated cell cycle progression. Flow cytometric analysis of the apoptotic sub-G1 cell population with propidium iodide staining. (A) HL-60 and (B) MCF-7 cells were treated with different concentrations of DGEHF21' and evaluated after 24h.

3.9. DGEHF21' could regulate the expression of apoptosis-related proteins.

Carcinogenesis is a complex multistep process followed by molecular alterations that result in the transformation of normal cells into mutated highly malignant derivatives. Apoptosis the normal and controlled cellular degradation process seen during differentiation, metamorphosis and physiological cell turnover. An active process controlled by cellular mediators involving the synthesis and cleavage of proteins and initiation of a signaling cascade that ultimately cause cellular apoptosis. Under physiological conditions, the suicidal genes responsible for apoptosis stay dormant [122]. Compounds that could bring about the activation of these genes are at the center of anti-cancer research. Hence the understanding the inhibitory effects of compounds on apoptosis signaling pathways in different cancer cells is an essential strategy to investigate their therapeutic potential. Caspases and Bcl-2 family of proteins are the major regulators of apoptosis. Bcl-2 family includes pro-(Bax, Bid, Bad) and anti- (Bcl-xL, Bcl-2, Mcl-1) apoptotic proteins [123]. Among them, BAX disrupts the voltage dependent anion channels in mitochondria resulting in the release of cytochrome c and pro-apoptotic factors. This process further causes the activation of caspases [124]. Hence, the expression of BAX is a hallmark of apoptosis common to most of the eukaryotic cells. On the other hand, Bcl-xL, an anti-apoptotic Bcl-2 family protein, reduces the release of mitochondrial material such as cytochrome C that causes apoptosis by associating with Apaf-1 and pro-caspase-9 that initiate the mitochondrially mediated apoptosis [125]. The upregulation of pro-apoptotic regulator, BAX, and down-regulation of anti-apoptotic protein, Bcl-xL is considered as an indication of apoptosis. Hence, the ratio of Bax/Bcl-xL is an important prognostic factor of apoptosis [126]. According to current observations, an increase of Bax/Bcl-xL ratio in both cell lines with increasing DGEHF21' concentrations mark the induction of apoptosis in both cell lines via the mitochondrial-mediated pathway.

Caspases reside in cells in their inactive pro-enzyme form, which becomes activated by cytochrome c, auto-catalytic process or initiator caspases such as caspases-8 and -9. This, in turn, activates 'effector' caspases such as caspases-3, -6 and -7 which contribute to biochemical and morphological changes of apoptosis via disabling/proteolysing key regulatory and structural proteins within the cell. PARP or the poly (ADP-ribose) polymerase are such a family of proteins involved in mediating DNA repair processes. They initiate some mechanisms involved in the single-strand damage repair [123]. According to Fig 55, the upregulation of caspases-9 could be explained by the increased Bax/Bcl-xL ratio that causes the release of cytochrome C. This further agrees with the cleavage of PARP observed by western blot analysis. However much variation is observed in apoptotic events based on the cell type and stimulating drugs. Caspase-3 has been found to play a central role in mediating apoptosis (cleavage of PARP) compared to other caspases. However, MCF-7 cells lack the ability to synthesize caspase-3. Nevertheless, it indicated cleavage of PARP suggesting that another caspase might remain dominant in MCF-7 responding to the PARP cleavage. This confirms that sterol derivatives in DGEHF21' indicate the ability to control apoptosis via mitochondrial-mediated apoptosis pathway.
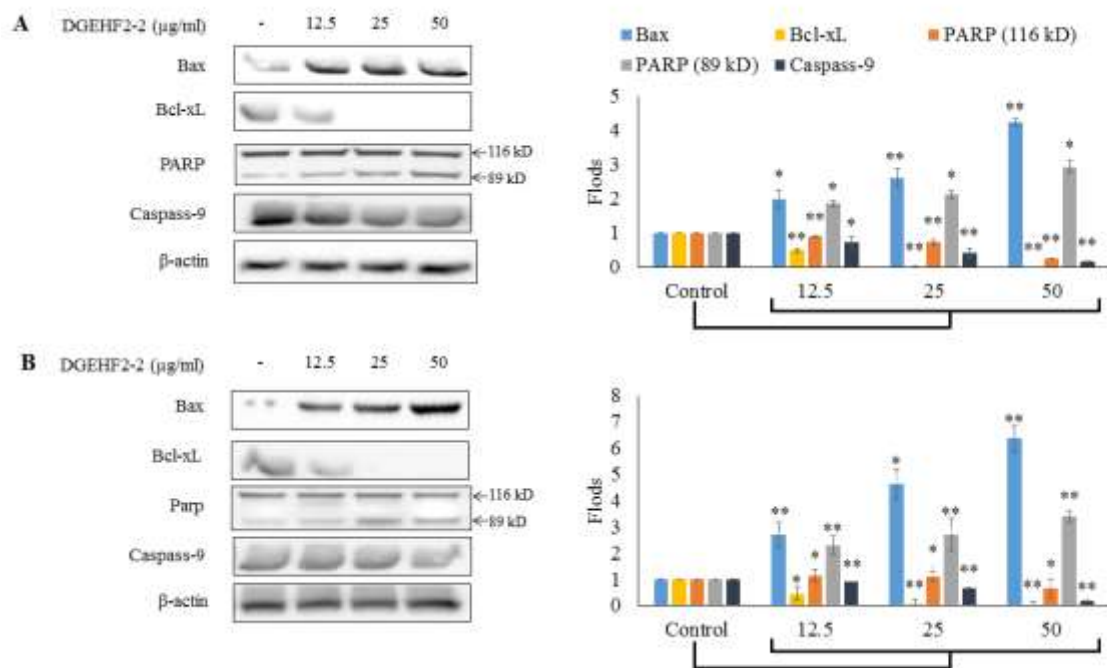
Fig. 55 DGEHF21' exhibit anticancer effects by regulating the expression levels of apoptosis-related proteins. Western blot analysis indicated A. HL-60 and B. MCF-7 cells could upregulate expression levels of Bax, Cleaved caspase 3 and P53 while downregulating Bcl-xL expression. Pre-seeded cancer cells were treated with 12.5, 25 and 50 µg/ml sample concentrations and harvested after 24h for western blot analysis.

3.10. Further purification and isolation of bioactive constituents from DGEHF21'

Further purification of the DGEHF21' was done using a long normal phase open column to achieve a better resolution. The column was eluted with a mixture of hexane and ethyl acetate, and the eluates were collected into test tubes. Test tubes were pooled according to TLC analysis. The pooled fractions were resolved on preparative thin layer chromatographic plates, and the individual bands were scrapped and dissolved in a mixture of hexane and ethyl acetate. Fig. 56 indicate the isolated fractions and their identification by GC-MS/MS analysis. Based on the results DGEH21'-3-1 contained Stigmasta-5-en-3-ol, DGEH21'-3-2 contained 26,27-Dinorergosta-5,22-dien-3-ol, Stigmasta-5,24(28)-dien-3-ol and a large amount of Stigmasta-5-en-3-ol, DGEH21'-4-1 contained Stigmasta-5,22-dien-3-ol and DGEH21'-5-1 contained Cholest-5-en-3-ol. However, some of the fractions including DGEH21'-3-3, DGEH21'-4-2 and DGEH21'-5-2 were failed to identify.
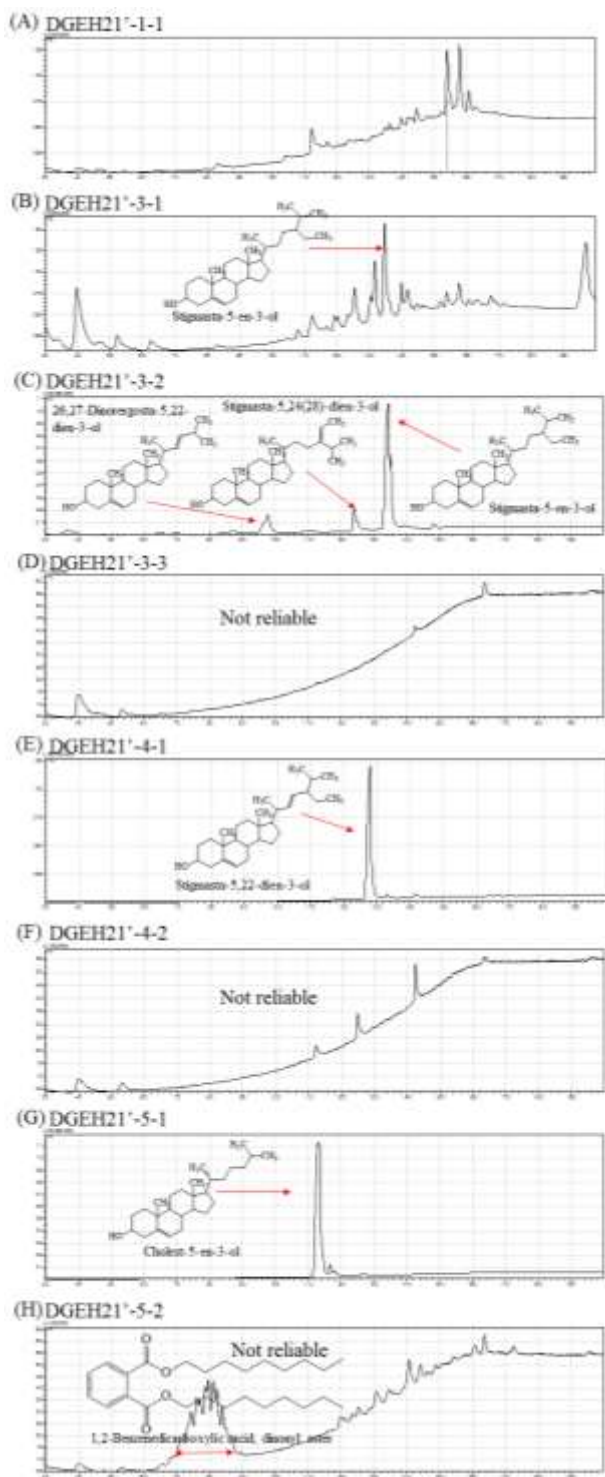
Fig. 56 GC-MS/MS analysis of the purified and isolated compounds. (A) DGEH21'-1-1, (B) DGEH21'-3-1, (C) DGEH21'-3-2, (D) DGEH21'-3-3, (E) DGEH21'-4-1, (F) DGEH21'-4-2, (G) DGEH21'-5-1 and (H) DGEH21'-5-2

192

3.11. Characterization of purified and isolated compounds

The purified compounds that indicated a considerable purity was analyzed for proton and ^{13}C NMR. Fig. 57 represent the structure of Stigmasta-5-en-3-ol with the general notation of its structural backbone. Based on Fig. 57 (A and B), in the purified fraction DGEH21'-1-1 the NMR signals indicate the peaks corresponding to 26,27-Dinorergosta-5,22-dien-3-ol, Stigmasta-5,24(28)-dien-3-ol and Stigmasta-5-en-3-ol. All these compounds share the basic 3β-hydroxy-Δ5-steroid skeleton. Hence, the overlapping peaks in the proton NMR make it difficult to determine the splitting pattern and couplings. However, considering the major compound Stigmasta-5-en-3-ol, the triplet observed at 5.5 ppm could be representing the vinylic H atoms at B-ring of the sterol skeleton. Hydrogen attached to the C3 (bearing the OH group) is represented by the quintet at 3.5. The methyl hydrogens are represented by peaks at 0.7 – 1.0 ppm. Peaks at 2.25 and 1.97 could be representing the allylic H atoms consecutively located at C4 and C7. Considering the compound DGEH21'-4-1, Fig 57 (C and D) the proton and ^{13}C NMR peaks represent peaks corresponding to Stigmasta-5,22-dien-3-ol. Considering the compound DGEH21'-4-1, Fig 57 (E and F) the proton and ^{13}C NMR peaks represent peaks corresponding to Cholest-5-en-3-ol.
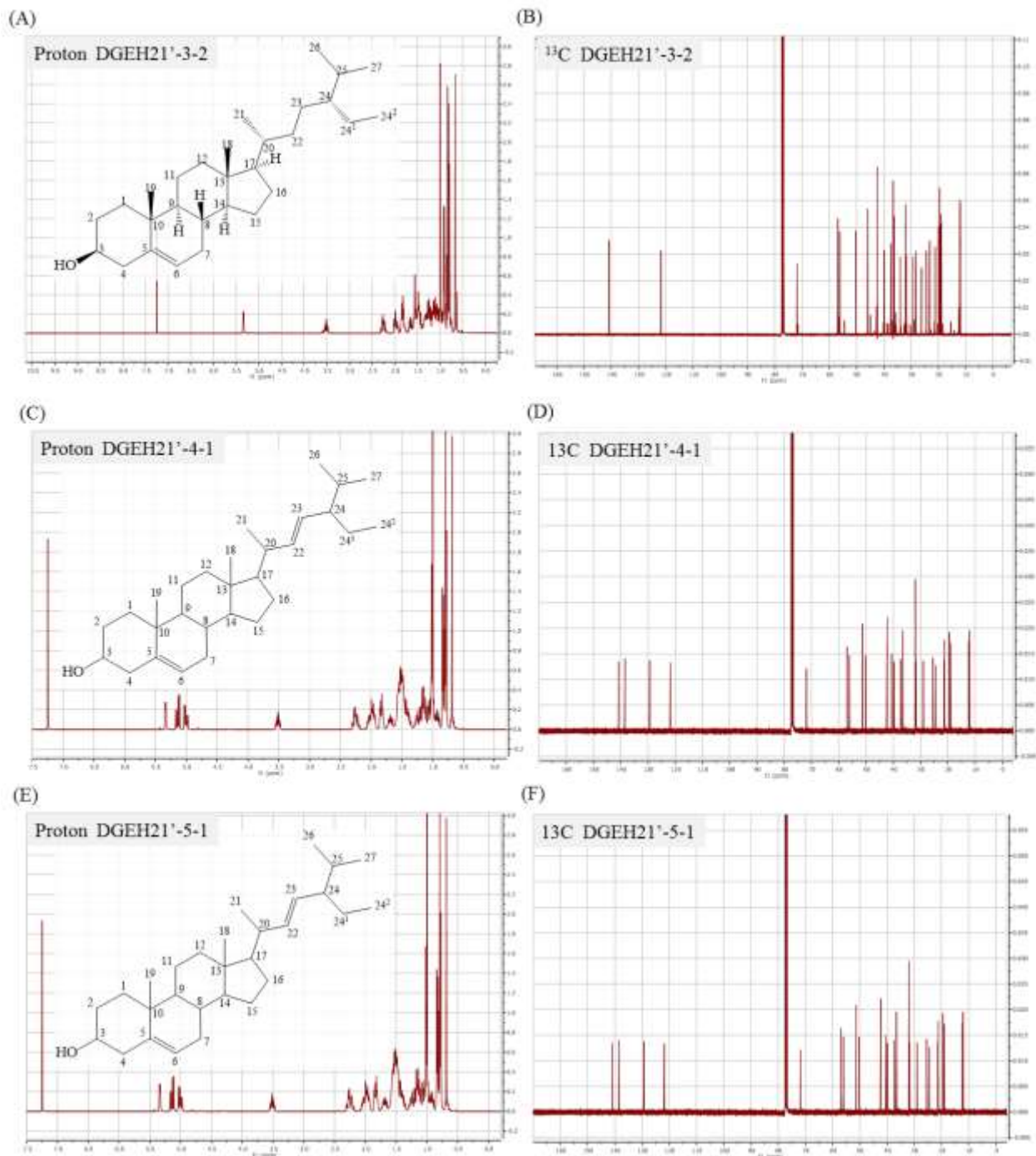
Fig. 57 NMR analysis of purified compounds. (A) Proton NMR of DGEH21'-1-1, and (B) ^{13}C NMR of DGEH21'-1-1, (D) Proton NMR of DGEH21'-4-1, (E) ^{13}C NMR of DGEH21'-4-1, (F) Proton NMR of DGEH21'-5-1, and (G) ^{13}C NMR of DGEH21'-5-1

3.12. Evaluating anti-cancer activities of purified fractions by PTLC separation

Anti-cancer effects of the fractions obtained after the PTLC purification were evaluated for their anticancer activity on HL-60 and MCF-7 cell lines. Among the fractions, DGEH21'-3-2 and DGEH21'-5-2 indicated desirable anti-proliferative effects on both evaluated cell lines. However based on the GC-MS/MS analysis, DGEH21'-3-2 was found to contain three sterol metabolites including 26,27-Dinorergosta-5,22-dien-3-ol, Stigmasta-5,24(28)-dien-3-ol and Stigmasta-5-en-3-ol. Among the compounds, the peak corresponding to Stigmasta-5-en-3-ol indicated an intense value suggesting its abundance in the selected fraction.
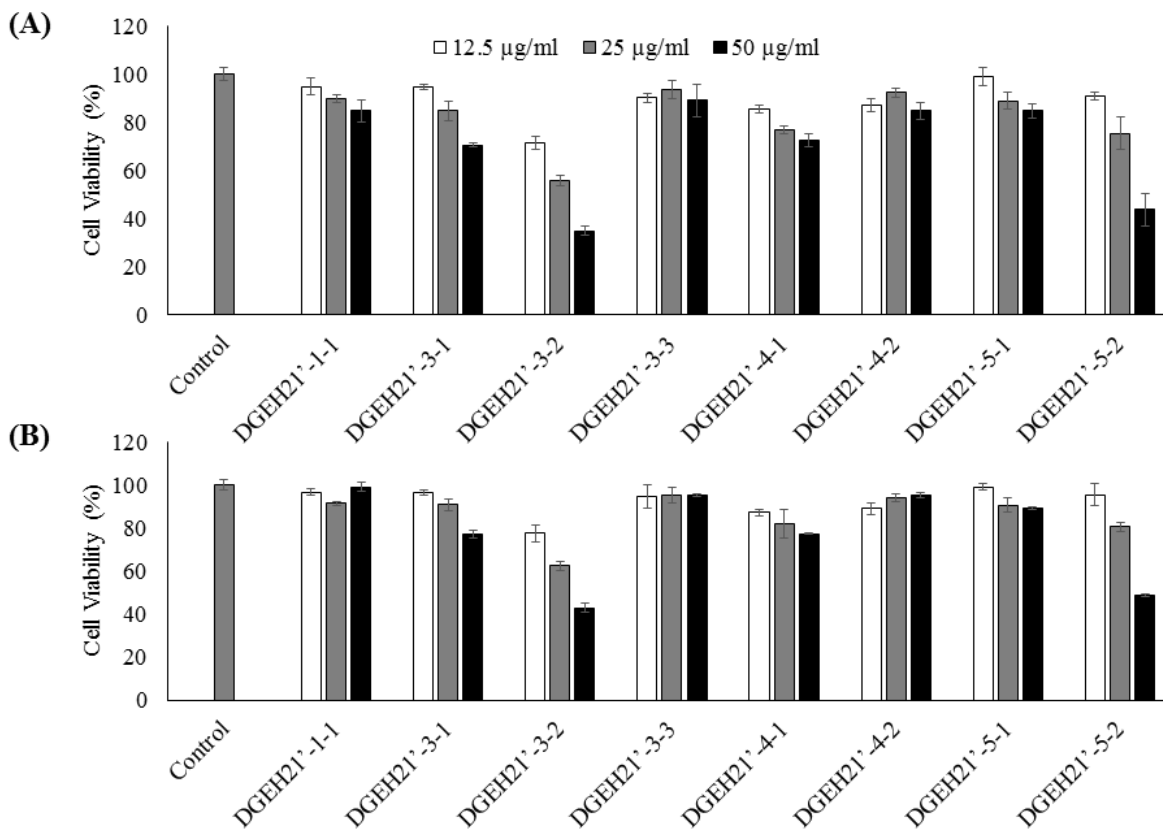
Fig. 58 The percentage of cell viability as a measure of cell proliferation by different concentrations of purified fractions. (A) HL-60 and (B) MCF-7 cells representing two carcinoma cell lines. Percentage of cell viability represent the proportion of viable cells compared to the control (100%). All experiments were performed in triplicate, and each value represents the mean ± SD.

196

3.13. Evaluating Nuclear morphology of HL-60 and MCF-7 cells for the determination of apoptotic body formation.

Analysis of nuclear morphology of the cells provides a better understanding of the anti-proliferative effects of samples. Hoechst 33342 is a DNA-specific fluorescent dye that stains nuclear matter in cells allowing the clarification of nuclear morphology to identify the formation of apoptotic bodies. Based on the results (Fig. 59) increased the frequency of nuclear condensation and fragmentation was observed with increasing sample concentrations. These observations mark the formation of apoptotic bodies. Moreover, the ethidium bromide and acridine orange double staining method allow the ability to identify the stage of apoptosis. Based on the results in control all the cells indicated a homogenous green color nucleus whereas with sample treatment we were able to observe early apoptotic events under the low sample concentrations and late apoptotic cells were observed at high concentrations. None of the cells were in necrosis even at the highest sample concentration of 50 µg/ml. These results clearly suggest the observed anti-proliferative activity of the cancer cells are proceeding through the induction off apoptosis.
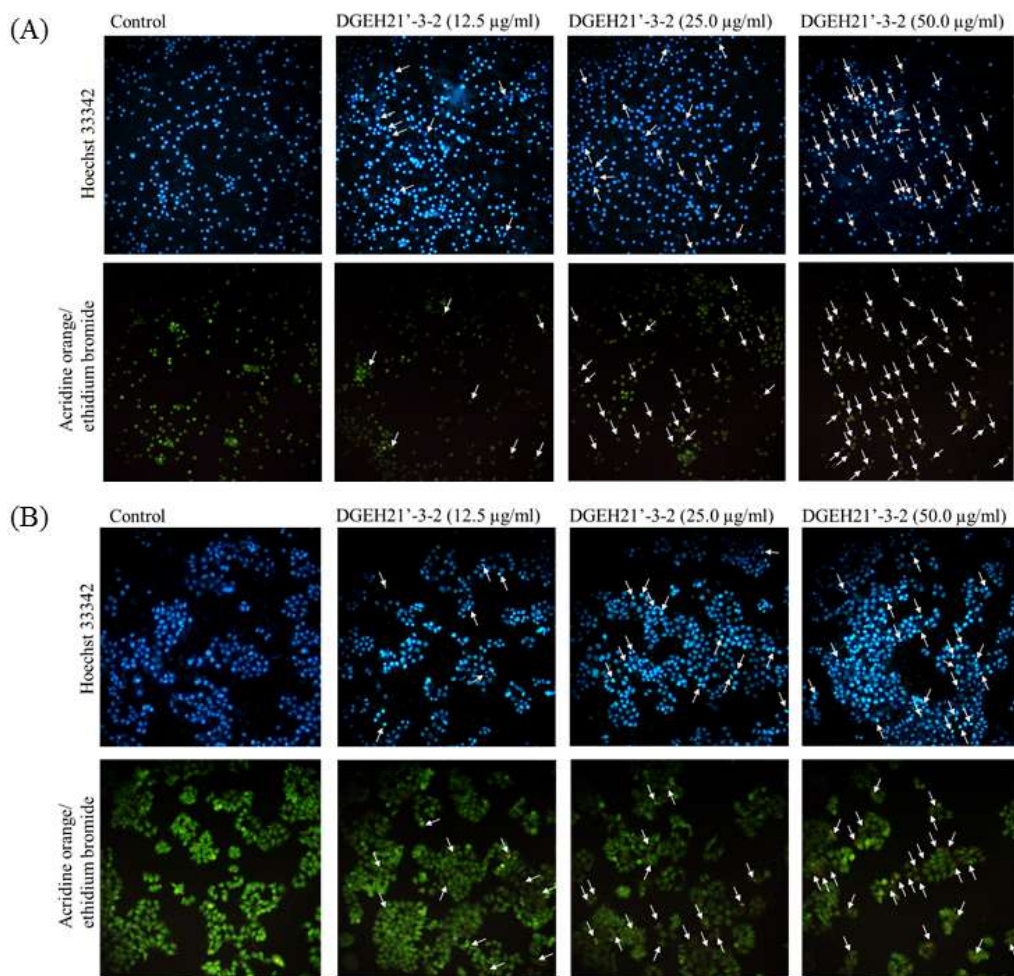
Fig. 59 Fluorescence microscopic evaluation of the effects of the nuclear morphology of cancer cells upon DGEHF21' treatment. (A) HL-60 and (B) MCF-7. Treatment of purified samples was carried out at 12.5, 25 and 50 µg/ml sample concentrations. The observations were done after 24h by Hoechst 33342 and by acridine orange/ethidium bromide double staining method. Nuclear condensation/fragmentation with intense green color patches are indicative of early apoptosis. The appearance of discrete orange color nuclear fragments is indicative of late apoptosis. Experiments were done in triplicate, and a set of random cell populations under the microscope were taken into account during each experiment.

198

3.14. Flow-cytometric analysis of the proportion of apoptotic cells in Sub-G1

The anti-proliferative effects of DGEHF21'3-2 could be resulting from the induction of apoptosis, cell cycle arrest or through the combination of both effects. As shown in Fig. 60, DGEHF21'3-2 treatment dysregulates cell cycle progression causing a dose-dependent increase of the sub-G1 apoptotic cell population both in HL-60 and MCF-7 cells. DGEHF21'3-2 at 50 µg/ml concentration resulted in a sub-G1 apoptotic cell population of 66.30% in HL-60 cells while 60.05% in MCF-7 cells. These results further clarify that DGEHF21'3-2 induced antiproliferative effects are causing primarily through the induction of apoptosis. These findings are consistent with the results observed for nuclear morphology evaluation.
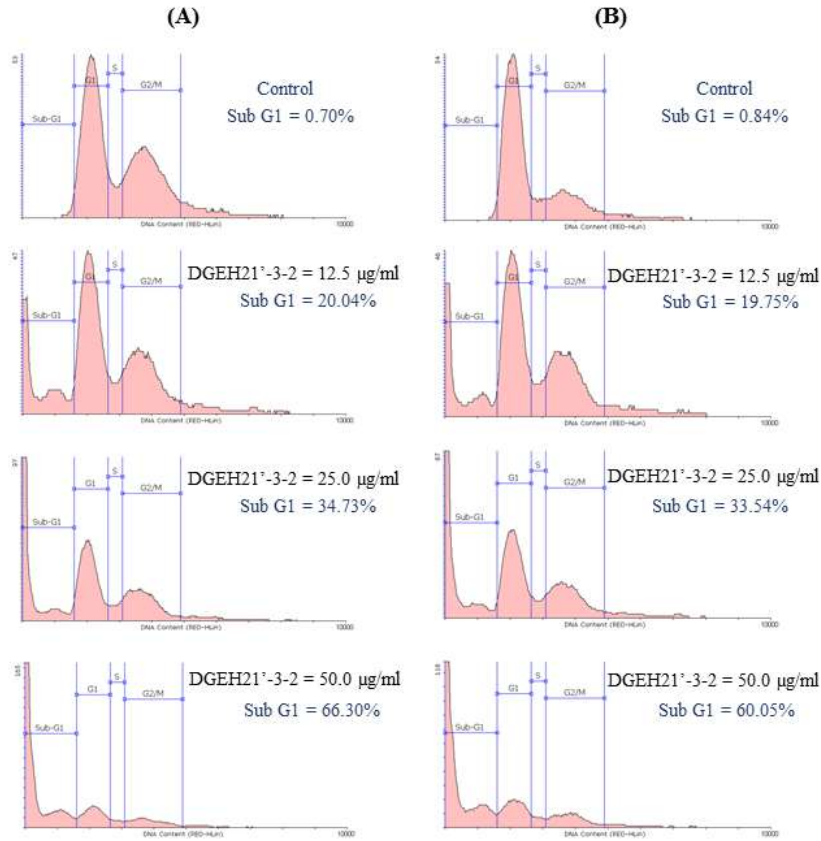
Fig. 60 Flow cytometric analysis of the apoptotic sub-G1 cell population with propidium iodide staining. (A) HL-60 and (B) MCF-7 cells were treated with different concentrations of DGEHF21'-3-2 and evaluated after 24h.

4. CONCLUSIONS

Cancer is a global catastrophe, one of the leading cause contributing to mortality. Numerous chemotherapeutic agents have been developed to treat cancer. While some of these drugs are efficient for the cancer treatment, they cause severe side effects. Several methods are used to selectively target cancer cells. These include but not limited to 1) Exploiting the rapid uptake of materials and metabolism in cancer cells whereas the cancer cells will acquire more materials and reach toxic concentrations than the normal cells do (e.g. cisplatin) [127]. 2) Block cancer-specific pathways. 3) Blocking cancer-specific membrane receptors. This approach is becoming increasingly popular, for example in cancer immunotherapies, and in some nanoparticle-mediated drug delivery systems [128]. 4) Use of prodrugs that activates once they are inside cancer cells [129]. 5) Use of minimally soluble drugs. These drugs will not cause a wide systemic availability, other than the area around the application. However, this technique is not recommended. Unlike targeting bacteria or fungi, still, there is no perfect, totally selective way to treat cancer due to the similarities between cancer cells and normal cells.

Hence continuing the search for anticancer drug leads are of utmost necessity. Recently consumption of phytochemicals has also gained increased attention as preventive precautions for reducing the incidence of cancer. Previous studies have shown the protective and therapeutic effects of triterpenoid derivatives including vitamin D, oleanolic acid and ursolic acid against cancer [130]. Some previous studies also have reported the potential anti-tumor effects of sterols and other secondary metabolites purified from *Dendronephthya sp*. An example of this is the anti-cancer effect of a monoalkyl glycerol ether, (±)-1-nonadecyloxy-2,3-propanediol purified from *Dendronephthya gigantea* upon A549, HT-1080, HT-29, and SNU-638 cancer cell lines [131]. The findings of the current study elaborate the anticancer activity of steroidal derivatives in

201

DGEHF21' against the proliferation of HL-60 and MCF-7 carcinoma cells and its cytotoxic dose limitations on normal cells. Present study report for the first time the anticancer activity of triterpenoids from Jeju soft coral *D. gigantea*. Moreover, these results explain the role of steroidal derivatives in regulating apoptosis. Marie organisms are found to contain the most unusual types of secondary metabolites with interesting structural and functional features. Therefore, further exploration of marine natural products will provide a new insight for the discovery of an array of bifunctional compounds.

ACKNOWLEDGEMENTS

It is a pleasure to thank all the academic and non-academic staff of the Dept. of Marine Bio-Medical Sciences, College of Ocean Sciences, Jeju National University, the Republic of Korea for the great support they lend me during the entire period.

I would also like to thank my parents and my brother for their support and motivation throughout this time.

Further, I would like to extend my thanks to all the Sri Lankan friends that were with me at Jeju National University.

I wish all the very best to all the people who helped me in many ways during this project even if I have not mentioned their names in here.

REFERENCES

1.   Blunt, J.W., et al., *Marine natural products.* Natural product reports, 2007. **24**(1): p. 31-86.

2.   Blunt, J.W., et al., *Marine natural products.* Natural product reports, 2008. **25**(1): p. 35-94.

3.   Blunt, J.W., et al., *Marine natural products.* Natural product reports, 2013. **30**(2): p. 237-323.

4.   Wei, W.-C., et al., *Anti-inflammatory activities of natural products isolated from soft corals of Taiwan between 2008 and 2012.* Marine drugs, 2013. **11**(10): p. 4083-4126.

5.   Fenical, W., *Marine soft corals of the genus Pseudopterogorgia: a resource for novel anti-inflammatory diterpenoids.* Journal of natural products, 1987. **50**(6): p. 1001-1008.

6.   Ma, A., et al., *Dendronpholides A− R, Cembranoid Diterpenes from the Chinese Soft Coral Dendronephthya sp.* Journal of natural products, 2008. **71**(7): p. 1152-1160.

7.   D'Auria, M.V., L. Minale, and R. Riccio, *Polyoxygenated steroids of marine origin.* Chemical Reviews, 1993. **93**(5): p. 1839-1895.

8.   Dias, D.A., S. Urban, and U. Roessner, *A Historical Overview of Natural Products in Drug Discovery.* Metabolites, 2012. **2**(2): p. 303-336.

9.   Harvey, A.L., *Natural products in drug discovery.* Drug Discovery Today, 2008. **13**(19–20): p. 894-901.

10.   Taylor, T.N. and E.L. Taylor, *The biology and evolution of fossil plants*. 1993: New Jersey, USA.: Prentice Hall.

11.   Li, Y.-X., et al., *Phlorotannins as bioactive agents from brown algae.* Process Biochemistry, 2011. **46**(12): p. 2219-2224.

12. Mobi, T., *Seaweed Polysaccharides*, in *Advances in Carbohydrate Chemistry*, S.H. Claude and L.W. Melville, Editors. 1953, Academic Press. p. 315-350.

13. Plaza, M., et al., *Screening for bioactive compounds from algae.* Journal of pharmaceutical and biomedical analysis, 2010. **51**(2): p. 450-455.

14. Fernando, I.P.S., et al., *Antioxidant Activity of Marine Algal Polyphenolic Compounds: A Mechanistic Approach.* Journal of Medicinal Food, 2016. **19**(7): p. 1-14.

15. Kraan, S., *Algal polysaccharides, novel applications and outlook*. 2012: INTECH Open Access Publisher.

16. Agatonovic-Kustrin, S. and D. Morton, *Cosmeceuticals derived from bioactive substances found in marine algae.* Oceanography: Open Access, 2013. **2013**.

17. Wijesinghe, W. and Y.J. Jeon, *Biological activities and potential industrial applications of fucose rich sulfated polysaccharides and fucoidans isolated from brown seaweeds: A review.* Carbohydrate Polymers, 2012. **88**(1): p. 13-20.

18. Kim, E.-A., et al., *Protective effect of fucoidan against AAPH-induced oxidative stress in zebrafish model.* Carbohydrate Polymers, 2014. **102**: p. 185-191.

19. Illangasinghe, W., K. Fujiwara, and H. Saito, *A Preliminary Study of Forests in Sri Lnaka.* 1999.

20. Trimen, H., *Hermann's Ceylon Herbarium and Linnæus's 'Flora Zeylanica'.* Journal of the Linnean Society of London, Botany, 1887. **24**(160): p. 129-155.

21. Sigmond, G.G. and F.J. Farre, *The Ceylon moss : communications read to the Royal Medico-Botanical Society of London, and published with its permission* Royal College of Surgeons of England, 1840: p. 87.

22.   Durairatnam, M., *Contribution to the study of the marine algae of Ceylon*. 1961: Fisheries Research Station.

23.   Mahendran, M., et al., *Sterols of some Sri Lankan marine algae.* Journal of the National Science Council of Sri Lanka, 1980.

24.   Chae, T., et al., *Novel biomimetic hydroxyapatite/alginate nanocomposite fibrous scaffolds for bone tissue regeneration.* Journal of Materials Science: Materials in Medicine, 2013. **24**(8): p. 1885-1894.

25.   Papageorgiou, S.K., et al., *Metal–carboxylate interactions in metal–alginate complexes studied with FTIR spectroscopy.* Carbohydrate Research, 2010. **345**(4): p. 469-473.

26.   DuBois, M., et al., *Colorimetric Method for Determination of Sugars and Related Substances.* Analytical Chemistry, 1956. **28**(3): p. 350-356.

27.   International, A., *Official methods of analysis of AOAC International*. 2005: AOAC International.

28.   Chandler, S.F. and J.H. Dodds, *The effect of phosphate, nitrogen and sucrose on the production of phenolics and solasodine in callus cultures of solanum laciniatum.* Plant Cell Rep, 1983. **2**(4): p. 205-8.

29.   Nanjo, F., et al., *Scavenging effects of tea catechins and their derivatives on 1,1-diphenyl-2-picrylhydrazyl radical.* Free Radic Biol Med, 1996. **21**(6): p. 895-902.

30.   Hiramoto, K., et al., *DNA breaking activity of the carbon-centered radical generated from 2,2'-azobis(2-amidinopropane) hydrochloride (AAPH).* Free Radic Res Commun, 1993. **19**(5): p. 323-32.

31. Finkelstein, E., G.M. Rosen, and E.J. Rauckman, *Spin trapping of superoxide and hydroxyl radical: Practical aspects.* Archives of Biochemistry and Biophysics, 1980. **200**(1): p. 1-16.

32. Wijesinghe, W., et al., *5 [Beta]-Hydroxypalisadin B isolated from red alga Laurencia snackeyi attenuates inflammatory response in lipopolysaccharide-stimulated RAW 264.7 macrophages.* Algae, 2014. **29**(4): p. 333.

33. Cardenas-Jiron, G., et al., *Vibrational spectroscopy and density functional theory calculations of poly-D-mannuronate and heteropolymeric fractions from sodium alginate.* Journal of Raman Spectroscopy, 2011. **42**(4): p. 870-878.

34. Alves, A., et al., *Extraction and physico-chemical characterization of a versatile biodegradable polysaccharide obtained from green algae.* Carbohydrate Research, 2010. **345**(15): p. 2194-2200.

35. Mollet, J.-C., A. Rahaoui, and Y. Lemoine, *Yield, chemical composition and gel strength of agarocolloids of Gracilaria gracilis, Gracilariopsis longissima and the newly reported Gracilaria cf. vermiculophylla from Roscoff (Brittany, France).* Journal of Applied Phycology, 1998. **10**(1): p. 59-66.

36. Pereira, L., S.F. Gheda, and P.J.A. Ribeiro-Claro, *Analysis by Vibrational Spectroscopy of Seaweed Polysaccharides with Potential Use in Food, Pharmaceutical, and Cosmetic Industries.* International Journal of Carbohydrate Chemistry, 2013. **2013**: p. 7.

37. Mathlouthi, M. and J.L. Koenig, *Vibrational Spectra of Carbohydrates*, in *Advances in Carbohydrate Chemistry and Biochemistry*, R.S. Tipson and H. Derek, Editors. 1987, Academic Press. p. 7-89.

38.   Pereira, L., et al., *Use of FTIR, FT-Raman and 13C-NMR spectroscopy for identification of some seaweed phycocolloids.* Biomol Eng, 2003. **20**(4-6): p. 223-8.

39.   Xia, S., et al., *Preliminary Characterization, Antioxidant Properties and Production of Chrysolaminarin from Marine Diatom Odontella aurita.* Marine Drugs, 2014. **12**(9): p. 4883.

40.   Matsuhiro, B., *Vibrational spectroscopy of seaweed galactans.* Hydrobiologia, 1996. **326**(1): p. 481-489.

41.   Fenoradosoa, T.A., et al., *Highly sulphated galactan from Halymenia durvillei (Halymeniales, Rhodophyta), a red seaweed of Madagascar marine coasts.* International Journal of Biological Macromolecules, 2009. **45**(2): p. 140-145.

42.   Dunn, E.K., et al., *Spectroscopic and biochemical analysis of regions of the cell wall of the unicellular 'mannan weed', Acetabularia acetabulum.* Plant and cell physiology, 2007. **48**(1): p. 122-133.

43.   Roberts, M.A. and B. Quemener, *Measurement of carrageenans in food: challenges, progress, and trends in analysis.* Trends in Food Science & Technology, 1999. **10**(4–5): p. 169-181.

44.   Bhakuni, D.S. and D.S. Rawat, *Bioactive marine natural products*. 2006: Springer Science & Business Media.

45.   Li, J.W. and J.C. Vederas, *Drug discovery and natural products: end of an era or an endless frontier?* Science, 2009. **325**(5937): p. 161-5.

46.   Wijesinghe, W.A.J.P. and Y.J. Jeon, *Enzyme-assistant extraction (EAE) of bioactive components: A useful approach for recovery of industrially important metabolites from seaweeds: A review.* Fitoterapia, 2012. **83**(1): p. 6-12.

47. Hehemann, J.-H., et al., *Transfer of carbohydrate-active enzymes from marine bacteria to Japanese gut microbiota.* Nature, 2010. **464**(7290): p. 908-912.

48. Lee, W.-W., et al., *Enzyme-assisted extraction of Ecklonia cava fermented with Lactobacillus brevis and isolation of an anti-inflammatory polysaccharide.* Algae, 2011. **26**(4): p. 343-350.

49. Pham-Huy, L.A., H. He, and C. Pham-Huy, *Free Radicals, Antioxidants in Disease and Health.* International Journal of Biomedical Science : IJBS, 2008. **4**(2): p. 89-96.

50. Scheuer, P.J., *Marine natural products: chemical and biological perspectives*. 2013: Academic Press.

51. Lee, S.H., et al., *Anti-inflammatory effect of fucoidan extracted from Ecklonia cava in zebrafish model.* Carbohydrate polymers, 2013. **92**(1): p. 84-89.

52. Hansson, G.K., *Inflammation, Atherosclerosis, and Coronary Artery Disease.* New England Journal of Medicine, 2005. **352**(16): p. 1685-1695.

53. Fernando, I.P.S., J.W. Nah, and Y.J. Jeon, *Potential anti-inflammatory natural products from marine algae.* Environmental Toxicology and Pharmacology, 2016. **48**: p. 22-30.

54. Wang, C.Y. and Y.C. Chen, *Extraction and characterization of fucoidan from six brown microalgae.* Journal of Marine Science and Technology, 2016. **24**(2): p. 319-328.

55. Li, B., et al., *Fucoidan: Structure and Bioactivity.* Molecules, 2008. **13**(8): p. 1671-1695.

56. Oh, J.Y., I.S. Fernando, and Y.J. Jeon, *Potential applications of radioprotective phytochemicals from marine algae.* Algae, 2016. **31**(4): p. 403-414.

57. Mulloy, B., *The specificity of interactions between proteins and sulfated polysaccharides.* Anais da Academia Brasileira de Ciências, 2005. **77**: p. 651-664.

58. Costa, L.S., et al., *Biological activities of sulfated polysaccharides from tropical seaweeds.* Biomedicine & Pharmacotherapy, 2010. **64**(1): p. 21-28.

59. Wang, J., et al., *Antioxidant activity of sulfated polysaccharide fractions extracted from Laminaria japonica.* Int J Biol Macromol, 2008. **42**(2): p. 127-32.

60. Pasławski, P. and Z. Migaszewski, *The quality of element determinations in plant materials by instrumental methods.* Pol. J. Environ. Stud, 2006. **15**(2a): p. 154-164.

61. Ngo, D.H. and S.K. Kim, *Sulfated polysaccharides as bioactive agents from marine algae.* International Journal of Biological Macromolecules, 2013. **62**: p. 70-75.

62. Percival, E. and R.H. McDowell, *Chemistry and enzymology of marine algal polysaccharides.* Science Progress 1968. **56**(222): p. 283-285.

63. Dzul, J.C., et al., *Hepatoprotective effect of the fucoidan from the brown seaweed Turbinaria tricostata.* Journal of Applied Phycology, 2015. **27**(5): p. 2123-2135.

64. Pielesz, A. and W. Biniaś, *Cellulose acetate membrane electrophoresis and FTIR spectroscopy as methods of identifying a fucoidan in Fucus vesiculosus Linnaeus.* Carbohydrate Research, 2010. **345**(18): p. 2676-2682.

65. Lim, S.J., et al., *Isolation and antioxidant capacity of fucoidan from selected Malaysian seaweeds.* Food Hydrocolloids, 2014. **42, Part 2**: p. 280-288.

66. Chevolot, L., et al., *Further data on the structure of brown seaweed fucans: Relationships with anticoagulant activity.* Carbohydrate Research, 1999. **319**(1-4): p. 154-165.

67. Patankar, M.S., et al., *A revised structure for fucoidan may explain some of its biological activities.* Journal of Biological Chemistry, 1993. **268**(29): p. 21770-21776.

68.   Kim, K.N., et al., *Fucoxanthin inhibits the inflammatory response by suppressing the activation of NF-kappaB and MAPKs in lipopolysaccharide-induced RAW 264.7 macrophages.* Eur J Pharmacol, 2010. **649**(1-3): p. 369-75.

69.   Dubois, R.N., et al., *Cyclooxygenase in biology and disease.* The FASEB journal, 1998. **12**(12): p. 1063-1073.

70.   Haefner, B., *Drugs from the deep: marine natural products as drug candidates.* Drug Discovery Today, 2003. **8**(12): p. 536 - 544.

71.   Croteau, R., T.M. Kutchan, and N.G. Lewis, *Natural products (secondary metabolites).* Biochemistry and molecular biology of plants, 2000. **24**: p. 1250-1319.

72.   Tomás-Barberan, F.A., F. Ferreres, and M.I. Gil, *Antioxidant phenolic metabolites from fruit and vegetables and changes during postharvest storage and processing*, in *Studies in Natural Products Chemistry*, R. Atta ur, Editor. 2000, Elsevier. p. 739-795.

73.   Clifford, M., *A nomenclature for phenols with special reference to tea.* Critical reviews in food science and nutrition, 2001. **41**(5): p. 393.

74.   Khoddami, A., M.A. Wilkes, and T.H. Roberts, *Techniques for analysis of plant phenolic compounds.* Molecules, 2013. **18**(2): p. 2328-75.

75.   Tsao, R., *Chemistry and biochemistry of dietary polyphenols.* Nutrients, 2010. **2**(12): p. 1231-46.

76.   Grigelmo-Miguel, N., et al., *Methods of Analysis of Antioxidant Capacity of Phytochemicals*, in *Fruit and Vegetable Phytochemicals*. 2009, Wiley-Blackwell. p. 271-307.

77. Fatland, B.L., et al., *Molecular characterization of a heteromeric ATP-citrate lyase that generates cytosolic acetyl-coenzyme A in Arabidopsis.* Plant Physiol, 2002. **130**(2): p. 740-56.

78. Kirke, D.A., et al., *The chemical and antioxidant stability of isolated low molecular weight phlorotannins.* Food Chemistry, 2017. **221**: p. 1104-1112.

79. Kumari, P., et al., *Algal lipids, fatty acids and sterols.* Functional Ingredients from Algae for Foods and Nutraceuticals; Domínguez, H., Ed, 2013: p. 87-134.

80. Mendis, E. and S.-K. Kim, *Present and future prospects of seaweeds in developing functional foods.* advances in food and nutrition research, 2011. **64**: p. 1-15.

81. Mizusawa, N. and H. Wada, *The role of lipids in photosystem II.* Biochimica et Biophysica Acta (BBA)-Bioenergetics, 2012. **1817**(1): p. 194-208.

82. Kim, K.-N., et al., *Fucoxanthin induces apoptosis in human leukemia HL-60 cells through a ROS-mediated Bcl-xL pathway.* Toxicology in Vitro, 2010. **24**(6): p. 1648-1654.

83. Ribble, D., et al., *A simple technique for quantifying apoptosis in 96-well plates.* BMC Biotechnology, 2005. **5**(1): p. 1-7.

84. Sanjeewa, K.K.A., et al., *Anti-inflammatory and anti-cancer activities of sterol rich fraction of cultured marine microalga Nannochloropsis oculata.* Algae, 2016. **31**(3): p. 277-287.

85. Lee, S.-H., et al., *Anti-inflammatory effect of fucoidan extracted from Ecklonia cava in zebrafish model.* Carbohydrate Polymers, 2013. **92**(1): p. 84-89.

86. Zhang, W., et al., *Chemical studies on sesquiterpenes in soft coral Lobophytum sp. from the South China Sea.* Natural Product Research and Development, 2005. **17**(6): p. 740.

87. Schmitz, F.J., K. Hollenbeak, and R. Prasad, *Marine natural products: Cytotoxic spermidine derivatives from the soft coral Sinularia brongersmai.* Tetrahedron Letters, 1979. **20**(36): p. 3387-3390.

88. Kaul, P.N. and C.J. Sindermann, *Drugs and food from the sea: myth or reality?* 1978.

89. Changyun, W., et al., *Chemical defensive substances of soft corals and gorgonians.* Acta Ecologica Sinica, 2008. **28**(5): p. 2320-2328.

90. Hu, J., et al., *Chemical and biological studies of soft corals of the Nephtheidae family.* Chemistry & biodiversity, 2011. **8**(6): p. 1011-1032.

91. Chang, C.-H., et al., *New anti-inflammatory steroids from the Formosan soft coral Clavularia viridis.* Steroids, 2008. **73**(5): p. 562-567.

92. Huang, Y.-C., et al., *New anti-inflammatory 4-methylated steroids from the Formosan soft coral Nephthea chabroli.* Steroids, 2008. **73**(11): p. 1181-1186.

93. Guyre, P.M., et al., *Glucocorticoid effects on the production and actions of immune cytokines.* Journal of Steroid Biochemistry, 1988. **30**(1): p. 89-93.

94. Barnes, P.J., et al., *Anti-inflammatory actions of steroids: molecular mechanisms.* Trends in pharmacological sciences, 1993. **14**(12): p. 436-441.

95. Xiong, Q., W.K. Wilson, and J. Pang, *The Liebermann–Burchard reaction: Sulfonation, desaturation, and rearrangment of cholesterol in acid.* Lipids, 2007. **42**(1): p. 87-96.

96. Wijesinghe, W.A.J.P., et al., *5β-Hydroxypalisadin B isolated from red alga Laurencia snackeyi attenuates inflammatory response in lipopolysaccharide-stimulated RAW 264.7 macrophages.* ALGAE, 2014. **29**(4): p. 333-341.

97. Smith, A.G. and L.J. Goad, *Sterol biosynthesis by the sea urchin Echinus esculentus.* Biochemical Journal, 1974. **142**(2): p. 421-427.

98.   Idler, D. and P. Wiseman, *Identification of 22-cis-cholesta-5, 22-dien-3β-ol and other scallop sterols by gas-liquid chromatography and mass spectrometry.* Comparative Biochemistry and Physiology Part A: Physiology, 1971. **38**(3): p. 581-590.

99.   Barnathan, G., et al., *Sterol composition of three marine sponge species from the genus Cinachyrella.* Comparative Biochemistry and Physiology Part B: Comparative Biochemistry, 1992. **103**(4): p. 1043-1047.

100.   Byju, K., et al., *In vitro and in silico studies on the anticancer and apoptosis-inducing activities of the sterols identified from the soft coral, subergorgia reticulata.* Pharmacognosy Magazine, 2014. **10**(Suppl 1): p. S65-S71.

101.   Goad, L.J., G.G. Holz, and D.H. Beach, *Sterols of Leishmania species, implications for biosynthesis.* Molecular and biochemical parasitology, 1984. **10**(2): p. 161-170.

102.   Sheikh, Y.M. and C. Djerassi, *Steroids from sponges.* Tetrahedron, 1974. **30**(23-24): p. 4095-4103.

103.   Ribeiro, S.M., et al., *Isolated and synergistic effects of chemical and structural defenses of two species of Tethya (Porifera: Demospongiae).* Journal of Sea Research, 2012. **68**: p. 57-62.

104.   Cattel, L., G. Balliano, and O. Caputo, *Stigmasta-7, E-24 (28)-dien-3β-ol from Bryonia dioica roots.* Phytochemistry, 1979. **18**(5): p. 861-862.

105.   Yoshikawa, K., et al., *Polyhydroxylated sterols from the octocoral Dendronephthya gigantea.* Journal of natural products, 2000. **63**(5): p. 670-672.

106.   Radhika, P., et al., *Anti-inflammatory activity of a new sphingosine derivative and cembrenoid diterpene (lobohedleolide) isolated from marine soft corals of Sinularia crassa*

Tixier-Durivault and Lobophytum species of the Andaman and Nicobar Islands. Biological and Pharmaceutical Bulletin, 2005. **28**(7): p. 1311-1313.

107.   Ricciotti, E. and G.A. FitzGerald, *Prostaglandins and Inflammation.* Arteriosclerosis, thrombosis, and vascular biology, 2011. **31**(5): p. 986-1000.

108.   Kim, E.A., et al., *A marine algal polyphenol, dieckol, attenuates blood glucose levels by Akt pathway in alloxan induced hyperglycemia zebrafish model.* RSC Advances, 2016. **6**(82): p. 78570-78575.

109.   Sarma, N.S., et al., *Marine Metabolites: The Sterols of Soft Coral.* Chemical Reviews, 2009. **109**(6): p. 2803-2828.

110.   Rashid, M.A., K.R. Gustafson, and M.R. Boyd, *HIV-Inhibitory Cembrane Derivatives from a Philippines Collection of the Soft Coral Lobophytum Species 1.* Journal of natural products, 2000. **63**(4): p. 531-533.

111.   Sales, P.M., et al., *alpha-Amylase inhibitors: a review of raw material and isolated compounds from plant source.* J Pharm Pharm Sci, 2012. **15**(1): p. 141-83.

112.   Narisawa, T., et al., *Inhibition of methylnitrosourea-induced large bowel cancer development in rats by sarcophytol A, a product from a marine soft coral Sarcophyton glaucum.* Cancer research, 1989. **49**(12): p. 3287-3289.

113.   Hassan, H.M., et al., *Pachycladins A− E, prostate cancer invasion and migration inhibitory eunicellin-based diterpenoids from the Red Sea soft coral Cladiella pachyclados.* Journal of natural products, 2010. **73**(5): p. 848-853.

114.   Sheu, J.-H., K.-C. Chang, and C.-Y. Duh, *A cytotoxic 5α, 8α-epidioxysterol from a soft coral Sinularia species.* Journal of natural products, 2000. **63**(1): p. 149-151.

115.   Heng, H.H.Q., et al., *Stochastic cancer progression driven by non-clonal chromosome aberrations.* Journal of Cellular Physiology, 2006. **208**(2): p. 461-472.

116.   Bradford, P.G. and A.B. Awad, *Phytosterols as anticancer compounds.* Molecular nutrition & food research, 2007. **51**(2): p. 161-170.

117.   Athukorala, Y., K.-N. Kim, and Y.-J. Jeon, *Antiproliferative and antioxidant properties of an enzymatic hydrolysate from brown alga, Ecklonia cava.* Food and Chemical Toxicology, 2006. **44**(7): p. 1065-1074.

118.   *Cellular activities and docking studies of eckol isolated from Ecklonia cava (Laminariales, Phaeophyceae) as potential tyrosinase inhibitor.* ALGAE, 2015. **30**(2): p. 163-170.

119.   Ahn, G., et al., *A sulfated polysaccharide of Ecklonia cava inhibits the growth of colon cancer cells by inducing apoptosis.* EXCLI Journal, 2015. **14**: p. 294-306.

120.   Baskić, D., et al., *Analysis of cycloheximide-induced apoptosis in human leukocytes: Fluorescence microscopy using annexin V/propidium iodide versus acridin orange/ethidium bromide.* Cell Biology International, 2006. **30**(11): p. 924-932.

121.   Thornberry, N.A. and Y. Lazebnik, *Caspases: Enemies Within.* Science, 1998. **281**(5381): p. 1312-1316.

122.   Barry, M.A., C.A. Behnke, and A. Eastman, *Activation of programmed cell death (apoptosis) by cisplatin, other anticancer drugs, toxins and hyperthermia.* Biochemical Pharmacology, 1990. **40**(10): p. 2353-2362.

123.   Mooney, L.M., et al., *Apoptotic mechanisms in T47D and MCF-7 human breast cancer cells.* Br J Cancer, 0000. **87**(8): p. 909-917.

124.   Weng, C., et al., *Specific cleavage of Mcl-1 by caspase-3 in tumor necrosis factor-related apoptosis-inducing ligand (TRAIL)-induced apoptosis in Jurkat leukemia T cells.* Journal of Biological Chemistry, 2005. **280**(11): p. 10491-10500.

125.   Bertini, I., et al., *The anti-apoptotic Bcl-x L protein, a new piece in the puzzle of cytochrome c interactome.* PLoS One, 2011. **6**(4): p. e18329.

126.   Salakou, S., et al., *Increased Bax/Bcl-2 ratio up-regulates caspase-3 and increases apoptosis in the thymus of patients with myasthenia gravis.* In Vivo, 2007. **21**(1): p. 123-32.

127.   Wang, D. and S.J. Lippard, *Cellular processing of platinum anticancer drugs.* Nature reviews Drug discovery, 2005. **4**(4): p. 307-320.

128.   Allen, T.M., *Ligand-targeted therapeutics in anticancer therapy.* Nature Reviews Cancer, 2002. **2**(10): p. 750-763.

129.   Rooseboom, M., J.N. Commandeur, and N.P. Vermeulen, *Enzyme-catalyzed activation of anticancer prodrugs.* Pharmacological reviews, 2004. **56**(1): p. 53-102.

130.   Ovesná, Z., K. Kozics, and D. Slameňová, *Protective effects of ursolic acid and oleanolic acid in leukemic cells.* Mutation Research/Fundamental and Molecular Mechanisms of Mutagenesis, 2006. **600**(1–2): p. 131-137.

131.   Han, A.-R., et al., *Cytotoxic constituents of the octocoralDendronephthya gigantea.* Archives of Pharmacal Research, 2005. **28**(3): p. 290-293.